

# Dark matter in compact stars

Joseph Bramante

*Department of Physics, Engineering Physics, and Astronomy, Queen's University, Kingston, Ontario, K7N 3N6, Canada*

*The Arthur B. McDonald Canadian Astroparticle Physics Research Institute, Kingston, Ontario, K7L 3N6, Canada*

*Perimeter Institute for Theoretical Physics, Waterloo, Ontario, N2L 2Y5, Canada*

Nirmal Raj

*Centre for High Energy Physics, Indian Institute of Science, C.V. Raman Avenue, Bengaluru 560012, India*

---

## Abstract

White dwarfs and neutron stars are far-reaching and multi-faceted laboratories in the hunt for dark matter. We review detection prospects of wave-like, particulate, macroscopic and black hole dark matter that make use of several exceptional properties of compact stars, such as ultra-high densities, deep fermion degeneracies, low temperatures, nucleon superfluidity, strong magnetic fields, high rotational regularity, and significant gravitational wave emissivity. Foundational topics first made explicit in this document include the effect of the “propellor phase” on neutron star baryonic accretion, and the contribution of Auger and Cooper pair breaking effects to neutron star heating by dark matter capture.

---

## Contents

<b>1</b>	<b>Introduction</b>	<b>2</b>
<b>2</b>	<b>The physics of compact objects</b>	<b>3</b>
2.1	Fermi gas model and maximum masses . . . . .	4
2.2	Structure equations and equation of state . . . . .	6
2.3	Spin periods . . . . .	8
2.4	Neutron star substructure . . . . .	9
2.5	Thermonuclear explosions . . . . .	10
2.6	Cooling . . . . .	12
2.6.1	White dwarf cooling. . . . .	12
2.6.2	Neutron star cooling. . . . .	13
2.6.3	Comparison of white dwarf and neutron star late-stage cooling . . . . .	14
2.7	Nucleon superfluidity . . . . .	15
2.8	Neutron star magnetic field and spin-down . . . . .	16

---

*Email addresses:* joseph.bramante@queensu.ca (Joseph Bramante), nraj@iisc.ac.in (Nirmal Raj)

<b>3</b>	<b>The white dwarf as a dark matter laboratory</b>	<b>17</b>
3.1	Dark matter annihilation inside and heating white dwarfs	18
3.2	Non-annihilating dark matter converting white dwarfs into black holes	20
3.3	White dwarf explosions via dark matter	20
3.4	Dark matter's influence on white dwarf equations of state	23
<b>4</b>	<b>The neutron star as a dark matter laboratory</b>	<b>23</b>
4.1	Dark matter kinetic and annihilation heating of neutron stars	23
4.1.1	Capture and kinetic heating	23
4.1.2	Dark matter self-annihilations, nucleon co-annihilations, and induced nucleon decay	29
4.1.3	Improvements and uncertainties	31
4.1.4	Dark matter models that heat neutron stars through scattering and annihilation	31
4.1.5	Neutron star reheating mechanisms not involving dark matter	31
4.2	Neutron stars and halo substructure	33
4.3	Dark matter inducing superbursts in neutron stars	35
4.4	Dark matter that implodes neutron stars into black holes	35
4.4.1	Dark matter thermalization in neutron stars	36
4.4.2	Collapse of dark matter and formation of small black hole	37
4.4.3	Growth or evaporation of dark matter-formed black hole in the neutron star	39
4.4.4	Signatures of dark matter that implodes neutron stars	39
4.5	Primordial black hole dark matter and neutron stars	41
4.6	Neutron stars admixed with dark sectors	42
4.6.1	Impact on nuclear equation of state	42
4.6.2	More admixed neutron stars	44
4.7	Exotic compact stars	44
4.8	Dark sectors leading to internal heating of neutron stars	44
4.9	Dark matter signals in gravitational waves from neutron star mergers	47
4.10	Dark matter signals in pulsar timing	47
4.10.1	Pulsar timing arrays	48
4.10.2	Binary pulsar timing	49
4.10.3	Pulsar spin-down	49
4.11	Axion-like and very light dark matter, and neutron stars	50
<b>5</b>	<b>Conclusions and perspective</b>	<b>51</b>
	<b>References</b>	<b>52</b>

## 1. Introduction

Dark matter is one of the foremost scientific mysteries of our times. Given how little is known about its microphysical properties, its possible identities seem limitless. This is famously encapsulated in the 90+ orders of magnitude that dark matter (DM) masses could span, from  $10^{-24}$  eV, set by the maximum possible Compton wavelength containable within a dwarf galaxy, to  $10^8 M_\odot \simeq 10^{74}$  eV, the mass of DM in a small galaxy. Over this range of masses DM may be described as a wave/field, a particle, a macroscopic object, or galactic substructure – including black holes and topological defects. A promising strategy to

confront such remarkable diversity in possibility is to exploit physical systems with remarkable diversity in characteristics.

Compact stars – white dwarfs (WDs) and neutron stars (NSs) typically formed as relics of nuclear-powered stars – afford such an environment. Since their quantum properties were first described in the 1920s–30s by Fowler [1], Anderson [2], Stoner [3], Chandrasekhar [4], Zwicky and Baade [5] (and possibly Landau [6]), our understanding of compact stars has been enriched at the intersection of several branches of physics: astrophysics, general relativity, particle physics, nuclear physics, statistical physics, thermodynamics, and plasma physics. It is little wonder that they feature in numerous tests of fundamental physics [7, 8], and it should come as no surprise that they are also ideal laboratories to search for dark matter. Indeed, DM hunters would do well to take advantage of their striking properties: they have very high densities, with accompanying steep gravitational potentials, sometimes deeply degenerate constituent fermions, often very low temperatures, the presence of nucleon superfluidity, ultra-strong magnetic fields, extreme regularity in rotation rivalling the precision of atomic clocks, and powerful gravitational radiation emitted during binary mergers, to name a few.

The use of stars to look for evidence of DM dates to proposals that weakly interacting particle DM might alter nuclear reaction rates in the Sun [9, 10]. Shortly after, it was realized that NSs were useful for seeking out certain models of DM that could form black holes in their interior [11]. One immediate difference between a search for DM in compact stars and a terrestrial detector is that, since DM is accelerated in the deep gravitational well of a compact star, its interactions with stellar constituent particles occur at semi-relativistic velocities:  $O(10^{-2} - 10^{-1})c$  for a WD and  $O(0.5)c$  for a NS. This high DM speed provides enhanced sensitivity to theoretical models with velocity-suppressed rates for scattering on Standard Model (SM) states, since in the Milky Way’s Galactic halo (and by extension in terrestrial detectors) the velocity of DM particles is only  $O(10^{-3})c$ . In particular, the environs of a NS are greatly suited to testing the origin of DM, since the kinetic energy of DM at speeds  $\sim 0.7c$  are similar to that during cosmological production, particularly for “freeze-out” processes [12].

This review is organized as follows. In Section 2 we provide an overview of the properties of NSs and WDs, emphasizing aspects that will be important for dark matter searches. In Section 3, we describe WD searches for dark matter, treating dark matter annihilation and heating of WDs, conversion of WDs to black holes, ignition of Type Ia supernovae, and effects of dark matter on WD equations of state. In Section 4, we describe NS searches for dark matter, including dark matter heating NSs kinetically and via annihilations, models of dark matter that convert NSs to black holes, exotic compact stars that constitute dark matter, NSs admixed with dark matter, models of dark matter that lead to internal heating of NSs, signals of dark matter in NS-related gravitational waves and pulsar timing, and the utility of NSs in discovering axion-like and primordial black hole dark matter. In Section 5, we briefly discuss future research directions for dark matter in compact stars.

## 2. The physics of compact objects

A detailed account of the physical characteristics of WDs and NSs is beyond the scope of this review, and for these we refer the reader to Refs. [13] and [14]. Here we outline key properties of these stars that make them useful dark matter detectors.

**White dwarfs** are stellar remnants formed from main sequence stars that undergo a red giant phase not hot enough to fuse carbon. Depending on its mass, a WD will be composed of some proportion of helium, carbon, oxygen, neon and magnesium, which make up the bulk of the mass. A sea of electrons cohabiting with nuclei provide, as we will see, the Fermi degeneracy pressure that supports the WD against

gravitational collapse.

Super-giant progenitors of mass around 10–25  $M_\odot$  that undergo core-collapse leave behind short-lived “proto-NSs” through which neutrinos diffuse out carrying away 99% of the star’s binding energy, following which NSs are born. They are composed mainly of Fermi degenerate neutrons formed by electron-proton capture,  $e^- + p \rightarrow n + \nu_e$ , at extreme densities and temperatures. Due to beta chemical equilibrium, NSs are also thought to contain populations of protons, electrons, and muons; it is in fact the filled Fermi seas of these fermionic fields that keep neutrons from decaying to protons, electrons, and muons inside NSs. The supernova collapse is generically expected to be hydrodynamically asymmetric, resulting in a natal “kick” to the NS at 450-1000 km/s speeds in a random direction [15, 16, 17, 18, 19]; a 1% fractional anisotropy in the momenta of escaping neutrinos could be another source of the asymmetric kick [20, 21, 22].

### 2.1. Fermi gas model and maximum masses

Compact stars, especially WDs, are prevented from collapsing under their own gravity by Fermi degeneracy pressure. In a low-temperature Fermi gas of Fermi momentum  $p_F$ , the number of fermions (of spin degeneracy  $g_s = 2$ ) filling up a real volume  $V$  and Fermi sphere volume  $V_F = 4\pi p_F^3/3$ , is  $N_f = g_s V V_F / (2\pi)^3$ , from which we obtain:

$$p_F = (3\pi^2 n)^{1/3}, \quad (1)$$

where  $n$  is the fermion number density. The total energy of the Fermi gas given the energy of a state  $e(p)$  is

$$E = 4\pi g_s V \int_0^{p_F} dp p^2 e(p), \quad (2)$$

and for an energy density  $\varepsilon = E/V$  the pressure is obtained as

$$P = -\left(\frac{\partial E}{\partial V}\right)_{N_f} = n^2 \frac{d}{dn} \left(\frac{\varepsilon}{n}\right). \quad (3)$$

Setting  $e(p) = m_f + p^2/(2m_f)$  in the non-relativistic limit and  $e(p) = p$  in the relativistic limit, and using Eqs. (1),(2) and (3), we get the Fermi degeneracy pressure of a species as

$$P = \begin{cases} [(3\pi^2)^{2/3}/5m_f] n^{5/3}, & p_F \ll m_f, \\ [(3\pi^2)^{1/3}/4] n^{4/3}, & p_F \gg m_f. \end{cases} \quad (4)$$

The net pressure of the compact star is the sum of the contributions of constituent species. In WDs, the electrons are unbound – the electron-nucleus Coulomb energy  $\simeq Ze^2(n_e/Z)^{1/3}$  is  $O(10^{-2})$  times the typical kinetic energy,  $(3\pi^2 n_e)^{1/3}$  – and thus form their own Fermi gas system. It may be seen from Eq. (2) that due to their lightness and abundance, it is the *electrons* that contribute the greatest to the pressure of WDs. In contrast, in neutron stars the constituent neutrons contribute the most to both the stellar mass and pressure.

The total energy of the star in the non-relativistic limit is given by

$$\begin{aligned} E_{\text{tot}}^{\text{non-rel}} &\simeq (\text{total kinetic}) - (\text{gravitational binding}) \\ &= \frac{3}{5} N_f \frac{p_F^2}{2m_f} - \frac{3}{5} \frac{GM_\star^2}{R_\star} \\ &= \left(\frac{27\sqrt{3}\pi}{40\sqrt{10}}\right)^{2/3} \frac{1}{m_f R_\star^2} \left(\frac{ZM_\star}{Am_N}\right)^{5/3} - \frac{3}{5} \frac{GM_\star^2}{R_\star}, \end{aligned} \quad (5)$$



and in the relativistic limit,

$$\begin{aligned} E_{\text{tot}}^{\text{rel}} &= \frac{3}{4} N_f p_F - \frac{3}{5} \frac{GM_\star^2}{R_\star} \\ &= \left(\frac{243\pi}{256}\right)^{1/3} \frac{1}{R_\star} \left(\frac{ZM_\star}{Am_N}\right)^{4/3} - \frac{3}{5} \frac{GM_\star^2}{R_\star}. \end{aligned} \quad (6)$$

Eq. (5) shows that, in the ground state of the compact star where the virial theorem (potential energy =  $-2 \times$  kinetic energy) applies, we have  $R_\star \propto M_\star^{-1/3}$  as a mass-radius relation<sup>1</sup>. This implies that WDs, modeled accurately as a Fermi gas system, become smaller with increasing mass. Hence the heaviest WDs are the densest, and thus one expects electrons in them to be ultra-relativistic and Eq. (6) to apply. In Eq. (6) both the potential and kinetic terms fall as  $R_\star^{-1}$ , however the former grows faster with  $M_\star$  than the latter, implying a maximum WD mass above which the star will collapse. This ‘‘Chandrasekhar limit’’ [23] (see also Sec. 2.5) is given by

$$M_{\text{max-WD-rel}} = \sqrt{\frac{5\pi}{G^3}} \frac{15}{16} \left(\frac{Z}{Am_N}\right)^2 \simeq 1.7 \left(\frac{2Z}{A}\right)^2 M_\odot. \quad (7)$$

A similar limit may be obtained for NS masses by setting  $A \rightarrow 1, Z \rightarrow 1$ :

$$M_{\text{max-NS-rel}} = 6.8 M_\odot. \quad (8)$$

These estimates are not physically motivated: they assume relativistic fermions constituting the entire volume of the star (true for neither WDs nor NSs) and a non-interacting Fermi gas (not true for NSs). Nevertheless they ballpark the true limit to within  $\mathcal{O}(1)$  factors. A more precise treatment must account for the stellar structure, which we will discuss below, but first let us make two more estimates of the maximum mass of NSs.

(i) If we assume non-relativistic neutrons, the virial theorem using Eq. (6) gives a mass-radius relationship:

$$R_{\text{NS}} \simeq 12 \text{ km} \left(\frac{M_\odot}{M_{\text{NS}}}\right)^{1/3}. \quad (9)$$

In this picture the NS radius is a decreasing function of its mass; however it cannot become smaller than the Schwarzschild radius corresponding to a maximum mass,  $R_{\text{Schw}} = 3 \text{ km} (M/M_\odot)$ . This condition gives

$$M_{\text{max-NS-nonrel}} = 2.8 M_\odot. \quad (10)$$

(ii) Due to super-nuclear densities in the NS cores, strong interactions cannot be neglected in considerations of NS structure. A maximum mass can be obtained in the (unphysical) limit where such interactions solely support the star against gravitational collapse [24]. Strong interactions become repulsive at inter-nucleon distances roughly shorter than the reduced Compton wavelength of the mediating pion,  $m_\pi^{-1}$ . This gives a maximum neutron density  $m_N m_\pi^3$ , corresponding to a mass-radius relation of  $M_{\text{NS}} = 4\pi m_N m_\pi^3 R_{\text{NS}}^3 / 3$ . For a surface escape speed  $v_{\text{esc}}$ , we have  $R_{\text{NS}} = R_{\text{Schw}} v_{\text{esc}}^{-1} = 3 \text{ km} (M/M_\odot) v_{\text{esc}}^{-1}$ . Putting these together yields the maximum NS mass as

$$M_{\text{max-NS-strong}} = \sqrt{\frac{3}{32\pi}} v_{\text{esc}}^{3/2} \left(\frac{M_{\text{Pl}}^6}{m_N m_\pi^3}\right)^{1/2} \simeq 2 M_\odot \left(\frac{v_{\text{esc}}}{0.5c}\right)^{3/2}. \quad (11)$$

<sup>1</sup>This shows that more compact stars are generally denser, which we will see is relevant to determining the speed of DM passing through and the density of DM collected in compact stars.

As we will see below, this turns out to be an excellent estimate.

As argued in, e.g., Ref. [25], a more accurate reason for the existence of a maximum mass for NSs is that the sound speed  $c_s$  in NS material cannot be arbitrarily large. In particular,  $c_s^2/c^2 = (\partial P/\partial \varepsilon)_{\bar{s}} \leq 1$  must be satisfied everywhere in the NS, where  $\bar{s}$  is the specific entropy. Physically, increments in the self-gravitating energy density result in increments in equilibrium-restoring pressure, however this trend cannot extend forever due to the sound speed limitation, putting a cap on NS masses. This is also an important criterion in modelling the equation of state (EoS) of high-density NS matter.

Briefly, we review the argument for a *minimum* NS mass. For a given EoS of the NS core fluid, as the central density (hence mass) of the NS is decreased, the gravitational binding energy will decrease, and at some minimum density, the NS will be unstable to small radial perturbations. This EoS-dependent minimum NS mass is typically  $\sim 0.1M_\odot$  [26, 27]. Such an NS would be primarily composed of an  $O(100)$  km crust zone, with a percent-level fraction of mass in the central degenerate neutron fluid [27]. Be that as it may, a realistic minimum mass of NSs is about  $1M_\odot$ , after neutrino pressure and other thermal effects during the formation of a NS in a core collapse supernova are considered<sup>2</sup> [31].

## 2.2. Structure equations and equation of state

Detailed reviews of NS structure and the role of EoSs may be found in Refs. [32, 33, 34], while we present here the essentials. Accurate estimates of compact star macroscopic properties are best obtained by solving the spherically symmetric stellar structure equations:

$$\begin{aligned} \frac{dP}{dr} &= -\frac{Gm\varepsilon}{c^2r^2} \left(1 + \frac{P}{\varepsilon}\right) \left(1 + \frac{4\pi r^3 P}{mc^2}\right) \left(1 - \frac{2Gm}{c^2r}\right)^{-1}, \\ \frac{dm}{dr} &= 4\pi \frac{\varepsilon}{c^2} r^2, \end{aligned} \quad (12)$$

Here  $m$  is the mass enclosed within a radial distance  $r$ , and all other quantities are as defined above. The first equation, the **Tolman-Oppenheimer-Volkoff (TOV) equation**, describes hydrostatic equilibrium, and the second describes the conservation of mass in the star. Given an EoS  $P(\varepsilon)$  and the boundary conditions  $m(0) = 0$ ,  $\varepsilon(0) = \varepsilon_c$  (a ‘‘central density’’), the structure equations can be solved to obtain useful quantities: a mass-radius relation (which would capture the maximum allowed mass), radial profiles of pressure, energy or number density, chemical potential, and so on.

A reliable estimate of WD properties may be gained by assuming a polytropic EoS:  $P(\varepsilon) = K\varepsilon^\gamma$ . For WDs, one can set the second and third terms to unity on the right-hand side of the first equation in Eq. (12), as the  $c$ -dependent terms depict general relativistic corrections that are only important for NSs. It is then straightforward to solve Eq. (12) for polytropes [25, 46]. In particular, the cases of  $\gamma = 5/3$  and  $\gamma = 4/3$ , applicable respectively to the limit of non-relativistic and relativistic electrons, result in the  $M$ - $R$  scaling relations we derived from the virial theorem in Eqs. (5) and (6) with more refined numerical factors. Notably, for the relativistic case we obtain the Chandrasekhar mass as:

$$M_{\text{Ch-WD}} \simeq 1.4M_\odot. \quad (13)$$

Realistic EoSs are non-polytropes accounting for Coulomb corrections arising from electron-ion interactions, e.g., the Feynman-Metropolis-Teller EoS [35]. Figure 1 shows representative  $M$ - $R$  relations for WDs

<sup>2</sup>A compact object of mass  $0.77^{+0.20}_{-0.17}M_\odot$  has been observed in the supernova remnant HESS J1731–347 [28], exciting speculations as to its nature and the EoS of nuclear matter [29, 30].

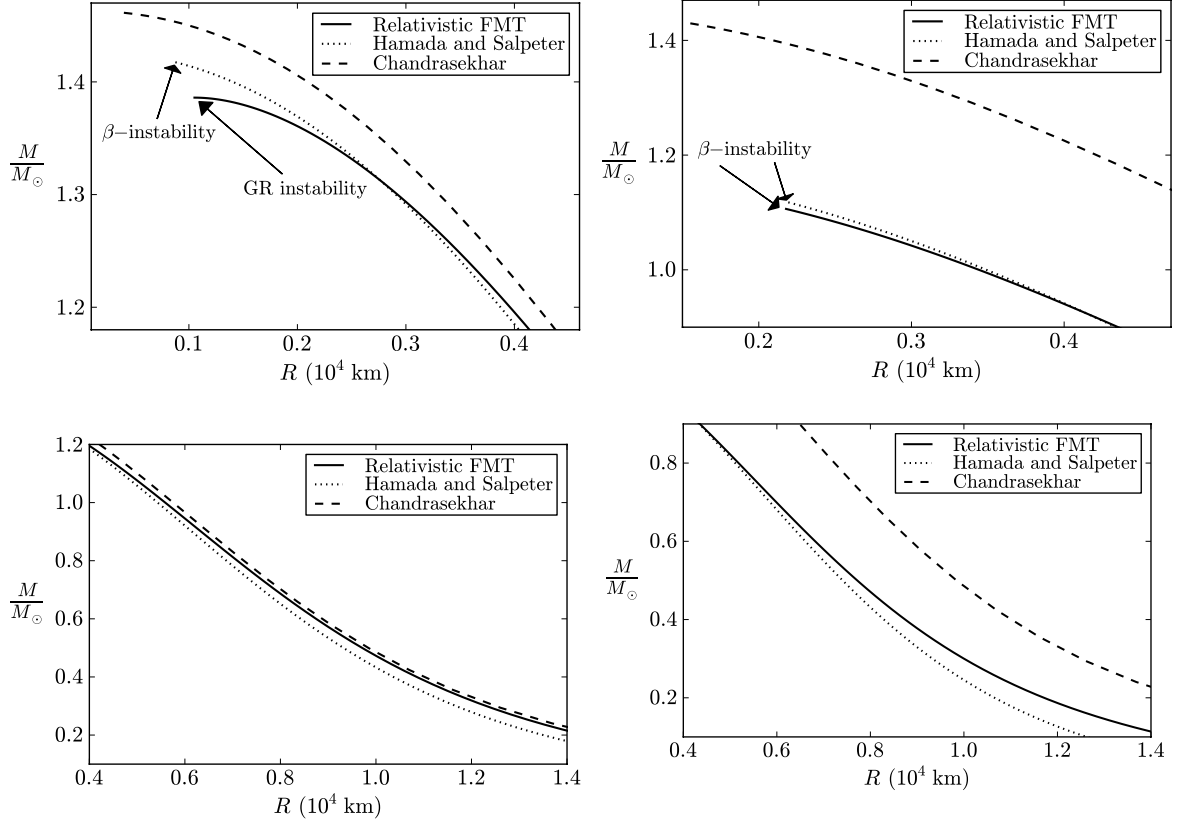


Figure 1: **Left.** WD mass-radius relations derived from three different equations of state for a  $^{12}\text{C}$  WD. The Chandrasekhar solution treats electrons as a free gas. The Hamada and Salpeter equation of state incorporates Coulomb corrections to the free gas approximation. The Relativistic FMT model additionally accounts for WD relativistic corrections to the Wigner-Seitz cell (Coulomb-corrected) treatment of the equation of state, [35]. Quantitatively similar curves are obtained for  $^4\text{He}$  and  $^{16}\text{O}$  WDs. The point marked “ $\beta$  instability” corresponds to where the central density is high enough that the WD is unstable against electron capture of nuclei resulting in  $(Z, A) \rightarrow (Z - 1, A)$  conversions. The point marked “GR instability” is where the general relativistic corrections shift an otherwise infinite central density to a finite value as the point at which the WD becomes gravitationally unstable. **Right.** Same as the left panels, but for  $^{56}\text{Fe}$  WDs. These plots are taken from Ref. [35].

of various nuclear compositions, taken from Ref. [35]. A simple analytical fit to translate between  $\rho$  and WD masses  $M_{\text{WD}} \in [0.1, 1.35]M_{\odot}$  is [47]

$$\left(\frac{\rho_{\text{WD}}}{1.95 \times 10^6 \text{ g/cm}^3}\right)^{2/3} + 1 \approx \left[\sum_{i=0}^6 c_i \left(\frac{M_{\text{WD}}}{M_{\odot}}\right)^i\right]^{-2}, \quad (14)$$

with  $\{c_i\} = \{1.003, -0.309, -1.165, 2.021, -2.060, 1.169, -0.281\}$ .

In NSs the EoS of nuclear matter is non-trivial due to the non-perturbative nature of QCD at the densities of the core. EoSs must account for nucleon-nucleon interactions, far more uncertain than Coulomb interactions, and must fit data on the per-nucleon binding energy in symmetric nuclear matter, the so-called symmetry energy that accounts for the energy above the  $N = Z$  ground state, the nuclear compressibility, and much else. For these reasons a wide range of EoSs has been proposed, resulting in multiple predictions for NS configurations. Figure 2 displays  $M$ - $R$  curves obtained from a few popular EoSs. The top left is a region where  $c_s > c$  and hence causality is violated; the NS mass for various EoSs is seen to reach a maximum close to this region.

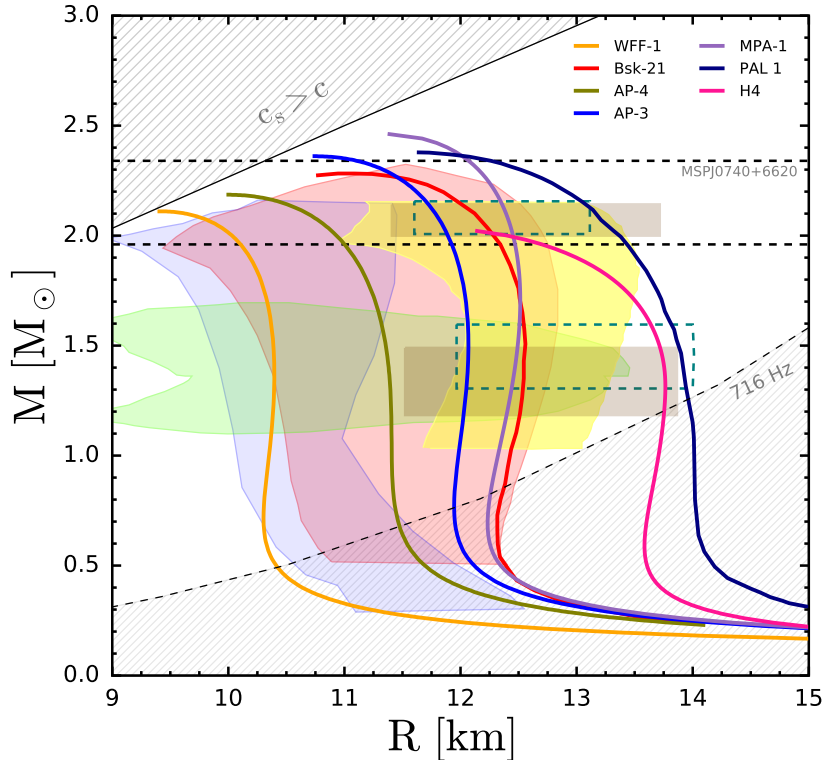


Figure 2: NS mass-radius relations for various equations of state for nuclear matter at high densities. The blue shaded region is preferred by pulsar observations [33], the yellow region is a fit to the observation of binary NS mergers using a hadronic EoS [36], the green region is the 90% C.L. preferred region from an EoS-insensitive fit to GW170817 [37], and the red regions are Bayesian fits at 90% C.L. from a combination of gravitational wave and low-energy nuclear and astrophysical data [38]. The horizontal thick-dashed lines depict the measured mass of the heaviest observed pulsar MSP J0740+6620 [39]. The line-shaded bottom right region is excluded by centrifugal mass loss, with the limit coming from observations of the fastest-spinning (716 Hz) pulsar [40]. The line-shaded top left region is excluded by the condition of causality: for any EoS the sound speed  $c_s \leq c$ . The rectangular regions are simultaneous fits at 68% C.L. of NS mass and radius by NICER (light brown by Refs. [41, 42] and dashed-green enclosed by Refs. [43, 44]). This plot is taken from Ref. [45].

### 2.3. Spin periods

Celestial bodies have a maximum angular speed: the gravitational force on a mass element on the equator must exceed the centrifugal force on it, giving a minimum spin period

$$P_{\min} \simeq \sqrt{\frac{3\pi}{G\rho}} = 10^4 \text{ s} \sqrt{\frac{\text{g/cm}^3}{\rho}}. \quad (15)$$

Thus for WDs with  $\rho = O(10^6) \text{ g/cm}^3$ ,  $P_{\min} \simeq 10 \text{ s}$ , and for NSs with  $\rho = O(10^{14}) \text{ g/cm}^3$ ,  $P_{\min} \simeq 10^{-3} \text{ s}$ . And indeed, the first pulsars historically espied were identified as such by their gradually lengthening sub-second spin periods. Moreover, no pulsars with spin periods smaller than  $O(\text{ms})$  have been observed; those observed near this limit are called millisecond pulsars. The bottom right region of Fig. 2 is excluded by the fastest spinning pulsar observed with rotation frequency 716 Hz [40], a limit given by  $(R/10 \text{ km})^{3/2} \geq 1280 \text{ Hz} (M/1.5 M_{\odot})^{1/2}$  [32].

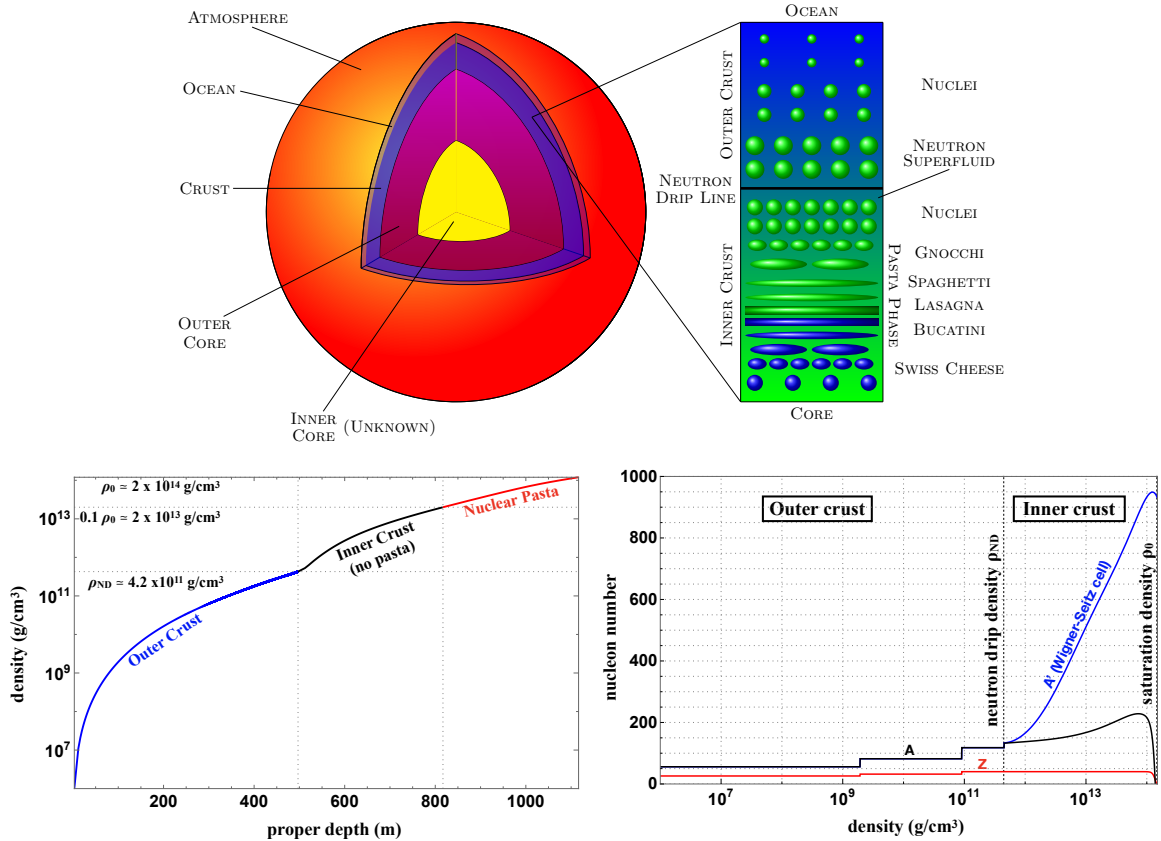


Figure 3: **Top.** Schematic of the internal structure of a NS, taken from Ref. [48]. The layers of the crust are shown in the zoom. **Bottom left.** Density profile of (various layers of) a NS crust. **Right.** Nucleon number as a function of NS crust density. See Sec. 2.4 for further details.

#### 2.4. Neutron star substructure

In the top panel of Figure 3 we show a schematic of the interior structure of a NS. The physics of substructure is obtained by solving Eq. (12) with the appropriate EoS for each stellar region. For illustration here we will make use of the Brussels-Montreal “unified” equation of state (“BSk”) accounting for all regions/densities in the NS, expressed in terms of analytic fits [49]. What follows is an overview of NS substructure; interested readers may gain further details from Ref. [50] and the references listed in Ref. [48].

The *crust*, about 1 km thick, spans over 10 decades in density and consists of several distinct layers corresponding to different phases of nuclear matter. The bottom left panel of Figure 3 shows the density of material as a function of the proper depth for the various crustal layers, and the bottom right panel shows nucleon numbers of nuclei as a function of densities spanning the entire crust; both plots were made using the EoS Bsk21 [48]. These plots do not show the *atmosphere* (density  $< 10^4$  g/cm³, thickness  $O(\mu\text{m})$ , composed of hydrogen and lighter elements) and *ocean* (density  $< 10^{10}$  g/cm³, thickness  $O(10)$  m, composed of carbon and heavy metals); these layers affect the star’s thermal spectrum, and are influenced by the star’s magnetic field.

The *outer crust* (density  $10^4 - 10^{11}$  g/cm³) is composed of nuclei forming a body-centered-cubic Coulomb crystal, interspersed with a degenerate and nearly-free relativistic gas of electrons. *À la* WDs,

electron degeneracy contributes dominantly to the pressure, while nuclei contribute dominantly to the mass. Deep in the crust, where the electron chemical potential is higher, nuclei become increasingly neutron-rich due to inverse beta decay. The outer crust terminates when the density and pressure become so high that free neutron states begin to appear.

The transition to the *inner crust* is marked by the neutron drip line, marked by density  $\rho_{\text{drip}} \simeq 4.2 \times 10^{11} \text{ g/cm}^3$  [51], beyond which a fraction of neutrons becomes unbound from nuclei. Up to densities about 0.1 times the nuclear saturation density  $\rho_0 \simeq 2 \times 10^{14} \text{ g/cm}^3$ , the inner crust comprises of heavy, neutron-rich nuclei (also known as proton clusters) forming a lattice, along with both an electron gas and a dripped-neutron gas. Such a system is inaccessible to terrestrial experiments, hence the composition of the inner crust is far more uncertain than the outer crust, and studies of this region are limited to theoretical calculations, *e.g.*, the Compressible Liquid Drop Model, the Thomas-Fermi approximation, and many-body quantum calculations. As the NS cools down, the dripped neutrons are expected to form a superfluid phase.

Further down, the inner crust density approaches the nuclear saturation point, and homogeneous nuclear matter appears [52, 53]. This has led to the prediction of the so-called nuclear “*pasta*” phase at the bottom of the inner crust [54, 55, 56, 57, 58, 59]. Intricate competition between nuclear attraction and Coulomb repulsion forms these extended non-spherical phases of nuclear matter; as the density increases, gnocchi, then spaghetti, and then lasagna pasta phases become more prevalent. In the deepest layer of the inner crust there are “inverted pasta phases” where nuclear density material predominates over sparser, sub-nuclear density voids. This includes bucatini (anti-spaghetti) and swiss cheese (anti-gnocchi) phases. Nuclear pasta is confined to a thin layer, yet they constitute a significant fraction of the crustal mass as they span densities of  $0.1 - 1 \rho_0$ . They may also impact several properties of the NS such as its thermal and electrical conductivity, and the elasticity and neutrino opacity of the crust.

The inner crust terminates when the density reaches  $\rho_0$ , beyond which nuclei “melt” into uniform nuclear matter, which form the core of the NS. The core is further sub-divided into the *outer core* (densities  $0.5-2 \rho_0$ ), where the nuclear matter is expected to be comprised of neutrons, protons, and electrons, and the *inner core* (densities  $2-10 \rho_0$ ), where exotic states of matter may possibly be present. These could be meson and hyperon condensates [60, 61, 62, 63]. These could also be deconfined quark matter, which is possible when the bag constant is large in the QCD bag model [63], either as *ud* matter [64] or *uds* matter [65, 66, 67, 68, 69, 70]. Deconfined quark matter is believed to be in a color superconducting (“CSC”) phase [71, 72, 73], which could be crystalline [74]. If strange-quark pairing is suppressed, a two-flavor superconducting (“2SC”) phase is formed involving *u* and *d* quarks. If not, the *uds* matter may exist in a color-flavor-locked (“CFL”) phase [75, 73] which may co-exist with confined states [76, 77, 78].

## 2.5. Thermonuclear explosions

Astrophysical situations may arise in which a WD exceeds its Chandrasekhar mass (Eq. (7)). For carbon-oxygen WDs, this would lead to ignition of runaway carbon fusion that unbinds the star. This is how Type Ia supernovae, conventionally used as “standard candles” in cosmological distance measurements, have been theorized to originate – via accreting material from a binary companion and going super-Chandrasekhar. This picture, however, is disputed by the lack of a specific “trigger” of the thermonuclear process along with a number of other observational inconsistencies [79]. As will be discussed later, other possible Type Ia progenitors include WD mergers and pyconuclear reactions in sub-Chandrasekhar mass WDs.

Yet another setting in which thermonuclear chain reactions create an explosion is in the ocean layer of NS crusts, and in particular the carbon component, which could be ignited by mass accretion from a binary companion. For accretion rates  $> 10\%$  of the Eddington limit, the result is “superbursts”, x-ray bursts

that spew  $O(10^{35})$  J of energy, lasting for hours, and in some cases recurring about every year [80, 81, 82, 83]. This must be distinguished from regular Type-I bursts in NSs, typically ignited by surface accretion, emitting  $10^3$  times less energy and lasting  $10^3$  times shorter.

Ref. [84] provides extended discussion on the physics of thermonuclear runaway fusion, while we provide here a brief summary. Two generic conditions must be satisfied: (1) a minimum energy  $Q_{\text{dep}}$  must be deposited to raise the temperature of a critical mass  $M_{\text{crit}}$  of density  $\rho$  to a critical temperature  $T_{\text{crit}}$  which can sustain fusion:

$$\begin{aligned} &\text{CONDITION 1} \\ &Q_{\text{dep}} \geq M_{\text{crit}}(\rho, T_{\text{crit}})\bar{c}_p(\rho, T_{\text{crit}})T_{\text{crit}}. \end{aligned} \quad (16)$$

The temperature prior to heating is here assumed  $\ll T_{\text{crit}}$ , and  $\bar{c}_p \simeq c_p^e/2 + c_p^\gamma/4 + c_p^{\text{ion}}$  is the average isobaric specific heat capacity, with

$$c_p^\ell(\rho, T_{\text{crit}}) = \frac{a_\ell b_\ell}{u} \left( \frac{T_{\text{crit}}}{E_F} \right)^{\alpha_\ell} \left[ 1 - \left( \frac{m_e}{E_F} \right)^2 \right]^{\beta_\ell}. \quad (17)$$

Here  $u$  is the atomic mass unit,  $m_e$  the electron mass, and for the {electronic, radiative, ionic} contributions,  $a_\ell = \{\pi^2, 4\pi^4/5, 5/2\}$ ,  $b_\ell = \{\sum X_i Z_i/A_i, \sum X_i Z_i/A_i, \sum X_i/A_i\}$  (with  $X_i, Z_i, A_i$  the mass fraction, charge and atomic number of the ion species  $i$  respectively),  $\alpha_\ell = \{1, 3, 0\}$ , and  $\beta_\ell = \{-1, -3/2, 0\}$ . The Fermi energy  $E_F = [m_e^2 + (3\pi^2 n_e)^{2/3}]^{1/2}$  with  $n_e = \rho b_e/u$  (Eq. (1)). The trigger energy in Eq. (16) ranges  $O(10^{17})$  GeV  $\rightarrow O(10^{24})$  GeV for WD central densities corresponding to WD masses ranging  $1.4 M_\odot \rightarrow 0.8 M_\odot$ .

Eq. (16) is necessary but not sufficient for runaway fusion. There is a second condition, through which the critical mass  $M_{\text{crit}} = 4\pi\rho\lambda_{\text{trig}}^3/3$  is also defined. To wit, the rate of energy gain via nuclear fusion must exceed the rate of energy loss via diffusion over the volume set by the ‘‘trigger length’’  $\lambda_{\text{trig}}$ :

$$\begin{aligned} &\text{CONDITION 2} \\ &\dot{Q}_{\text{nuc}} > \dot{Q}_{\text{diff}}. \end{aligned} \quad (18)$$

Here we have  $\dot{Q}_{\text{nuc}} = M_{\text{crit}}\dot{S}_{\text{nuc}}$  and  $\dot{Q}_{\text{diff}} \simeq 4\pi k\lambda_{\text{trig}}T_{\text{crit}}$  for a nuclear energy deposition rate per mass  $\dot{S}_{\text{nuc}}$  and thermal conductivity  $k$ . Conductive diffusion from relativistic electrons provides the dominant source of diffusion in WDs at the temperatures and densities relevant for igniting thermonuclear fusion; see Ref. [85, 86] for analytic expressions for  $\dot{Q}_{\text{diff}}$ .

The estimation of  $\dot{S}_{\text{nuc}}$  involves numerical simulations of flame propagation with a nuclear reaction network [84]. From this,

$$\begin{aligned} \lambda_{\text{trig}} &= \sqrt{\frac{3kT_{\text{crit}}}{\rho\dot{S}_{\text{nuc}}(\rho, T_{\text{crit}})}} \\ &= \begin{cases} \lambda_1 \left(\frac{\rho}{\rho_1}\right)^{-2} & , \rho \leq \rho_1 \\ \lambda_1 \left(\frac{\rho}{\rho_1}\right)^{\ln(\lambda_2/\lambda_1)/\ln(\rho_2/\rho_1)} & , \rho_1 < \rho \leq \rho_2 \end{cases} \end{aligned} \quad (19)$$

where for WDs  $\{\lambda_1^{\text{WD}}, \lambda_2^{\text{WD}}\} = \{1.3 \times 10^{-4} \text{ cm}, 2.5 \times 10^{-5} \text{ cm}\}$  and  $\{\rho_1, \rho_2\} = \{2 \times 10^8 \text{ g/cm}^3, 10^{10} \text{ g/cm}^3\}$ . This analytic form was obtained in Ref. [47] by fitting to Figure 6 of Ref. [84] – that is restricted to  $\rho_1 \leq \rho \leq \rho_2$  – and extrapolating to lower densities assuming plausible density-scalings of  $k$  and  $\dot{S}_{\text{nuc}}$ . The fit is for  $T_{\text{crit}} = 0.5$  MeV and assumes equal carbon and oxygen masses in WDs. In the NS ocean, the mass fraction of



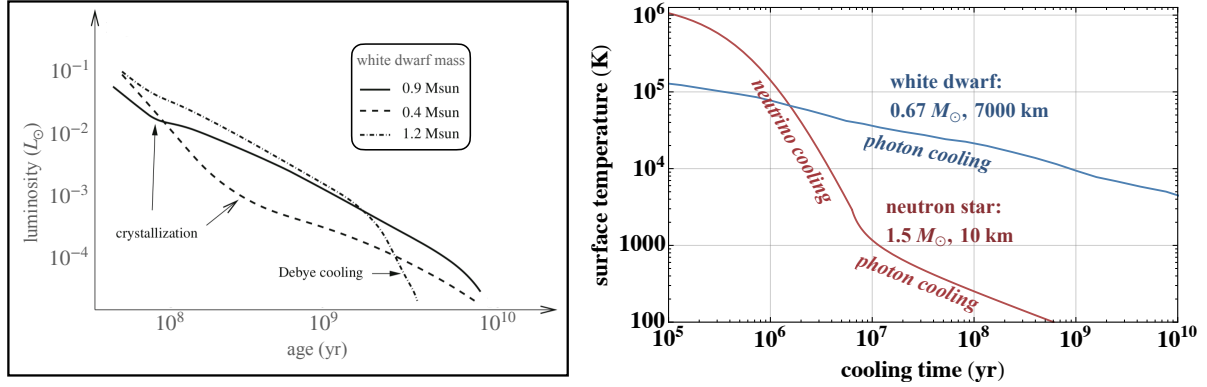


Figure 4: Cooling curves. *Left.* Luminosity versus time of WDs of various masses, taken from Ref. [87]. The onset of crystallization at about  $10^8$  yr takes cooling from the regime of thermal ions to the Debye regime. *Right.* Surface temperature versus time of a benchmark WD and NS. Early cooling dominated by emission of neutrinos is distinctly faster than that of photons. See Sec. 2.6 for further details.

carbon is 10% [80], implying  $\rho \rightarrow 0.1\rho$  in Eq. (19) if Eq. (19) holds for pure carbon burning<sup>3</sup>. One could also fit a relation among the WD central density, critical temperature and trigger mass [85]:

$$T_{\text{crit}} \gtrsim 10^{9.7} \text{ K} \left( \frac{\rho}{10^8 \text{ g/cm}^3} \right)^{3/140} \left( \frac{M_{\text{crit}}}{g} \right)^{3/70}. \quad (20)$$

## 2.6. Cooling

As no nuclear fuel is burnt in compact stars, they cool down continually from the moment of their birth unless energy is deposited into them by some means, as discussed in Sections 3 and 4. Observations of compact star cooling are an important handle on the physics governing their internal dynamics.

### 2.6.1. White dwarf cooling.

WDs initially cool by shedding the thermal energy of constituent ions. Given the specific heat per ion  $c_v = 3/2$ , the total WD energy in thermal ions is

$$U = \frac{3T}{2} \left( \frac{M_{\text{WD}}}{Am_N} \right). \quad (21)$$

The WD luminosity  $L = -dU/dt$ , and the cooling curve can be obtained from an independent expression for the luminosity in terms of the WD internal temperature  $T_{\text{int}}$ :

$$L = 0.2 \text{ J/s} \left( \frac{M_{\text{WD}}}{M_{\odot}} \right) \left( \frac{T_{\text{int}}}{\text{K}} \right)^{7/2}, \quad (22)$$

derived from photon diffusion in the WD surface layers assuming Kramer's opacity, and combining it with the EoS; see Ref. [26] for a detailed treatment. The cooling timescale is then obtained as

$$t_{\text{cool}} \approx \text{Gyr} \left( \frac{M/M_{\odot}}{L/(10^{-3}L_{\odot})} \right)^{5/7}. \quad (23)$$

<sup>3</sup>It probably does, for the scalings of Eq. (19) are seen to be similar to those in Table 3 of Ref. [84], for conductive burning.





layer for temperatures  $\gtrsim O(10^3)$  K, and becomes too thin for insulation at smaller temperatures [90, 94]. For an iron envelope at high temperatures [95, 96],

$$T_s = 10^6 \text{ K} \left[ \left( \frac{M_{\text{NS}}}{1.5 M_{\odot}} \right) \cdot \left( \frac{10 \text{ km}}{R_{\text{NS}}} \right)^2 \right]^{1/4} \left[ \frac{T}{9.43 \times 10^7 \text{ K}} \right]^{0.55}. \quad (29)$$

One can then identify the thin-envelope regime by solving for  $T_s = T$  in the above equation, which gives  $T_{\text{env}} = 3908 \text{ K}$ , below which one can simply set  $T_s = T$ .

The solution of Eq. (25) can now be written down as the time for the NS to cool to a temperature  $\tilde{T}_{\text{cool}}$  ( $\ll$  the initial temperature) [97]:

$$t_{\text{cool}}(\tilde{T}_9)/\text{yr} = \begin{cases} t_{\text{env}} = s_1^{-k} q^{-\gamma} [(1 + (s_1/q)^k \tilde{T}_9^{2-n})^{-\gamma/k} - 1], & \tilde{T}_{\text{cool}} > \tilde{T}_{\text{env}}, \\ t_{\text{env}} + (3s_2)^{-1} (\tilde{T}_9^{-2} - \tilde{T}_{\text{env}}^{-2}), & \tilde{T}_{\text{cool}} \leq \tilde{T}_{\text{env}}, \end{cases} \quad (30)$$

where  $\tilde{T}_9 = \tilde{T}_{\text{cool}}/(10^9 \text{ K})$ ,  $q = 2.75 \times 10^{-2}$ ,  $s_1 = 8.88 \times 10^{-6}$ ,  $s_2 = 8.35 \times 10^4$ ,  $k = (n-2)/(n-\alpha)$  and  $\gamma = (2-\alpha)/(n-\alpha)$  with  $\alpha = 2.2$  and  $n = 8$ ;  $\tilde{T}_{\text{env}} \simeq 4000 \text{ K}$  corresponds to the time after which the surface and internal temperatures equalize. The right-hand panel of Figure 4 shows the NS cooling curve plotted using the above expression, with the distinct regimes of neutrino and photon cooling labelled.

While in standard cooling scenarios NSs are expected to cool down to  $O(10^2)$  K over Gyr timescales (as in Fig. 4), temperatures as high as  $10^4 \text{ K}$  have been conjectured to persist if some additional astrophysical source of NS heating is present: we discuss such speculative reheating mechanisms in Sec. 4.1.5. We note that in the cases of magnetic field decay and rotochemical heating, the expectation is that late-stage NSs will still glow at below  $10^3 \text{ K}$ .

### 2.6.3. Comparison of white dwarf and neutron star late-stage cooling

From the discussion above, and from the right-hand panel of Fig. 4, we see that the temperature of an NS expected at late stages ( $t_{\text{cool}} \gtrsim \text{Gyr}$ ), about  $10^2 \text{ K}$ , is much smaller than the late-stage temperature of a WD, about  $10^{3.3-4} \text{ K}$ . It is natural to wonder why, as one may expect both to have a similar late-stage temperature since both are low-temperature degenerate stars. The crucial difference is that the late-stage WD heat capacity is determined by vibrational modes of the nuclear ionic Coulomb lattice forming its interior, while the NS heat capacity is that of a degenerate Fermi gas.

In the WD case, the heat capacity per ion is [26]

$$c_v^{\text{WD}} \simeq \int_0^{\kappa_{\text{max}}} \frac{\kappa^2 d\kappa}{2\pi^2 n} \sum_{\lambda=1}^3 \frac{e^{\omega_{\lambda}(\kappa)/T} (\omega_{\lambda}(\kappa)/T)^2}{(e^{\omega_{\lambda}(\kappa)/T} - 1)^2}, \quad (31)$$

where  $\omega_{\lambda}$  is the vibrational energy,  $\kappa$  is the wavenumber of the normal modes of the Coulomb lattice, and  $\lambda$  labels transverse and longitudinal modes. Using the linear approximation  $\omega_{\lambda} = \kappa c_s$ , where  $c_s$  is the sound speed in the lattice, and changing variables in the integral to  $\kappa \rightarrow yT/c_s$ , it can be immediately seen that  $c_v^{\text{WD}} \propto T^3$ .

In the case of the NS, in the limit where the temperature  $T$  drops below the Fermi energy  $E_F$ , only a fraction  $T/E_F$  of the fermions close to the Fermi surface will be excited and raise the bulk temperature. Hence the energy per fermion  $\propto T(T/E_F)$ , and it follows that the heat capacity  $c_v^{\text{NS}} \propto T$ .

From Eq. (25), setting the photon luminosity  $\propto T^4$ , we obtain  $t_{\text{cool}} \propto \log T$  for WDs and  $t_{\text{cool}} \propto 1/\sqrt{T}$  for NSs. Thus, WDs indeed cool much slower than NSs at later stages.

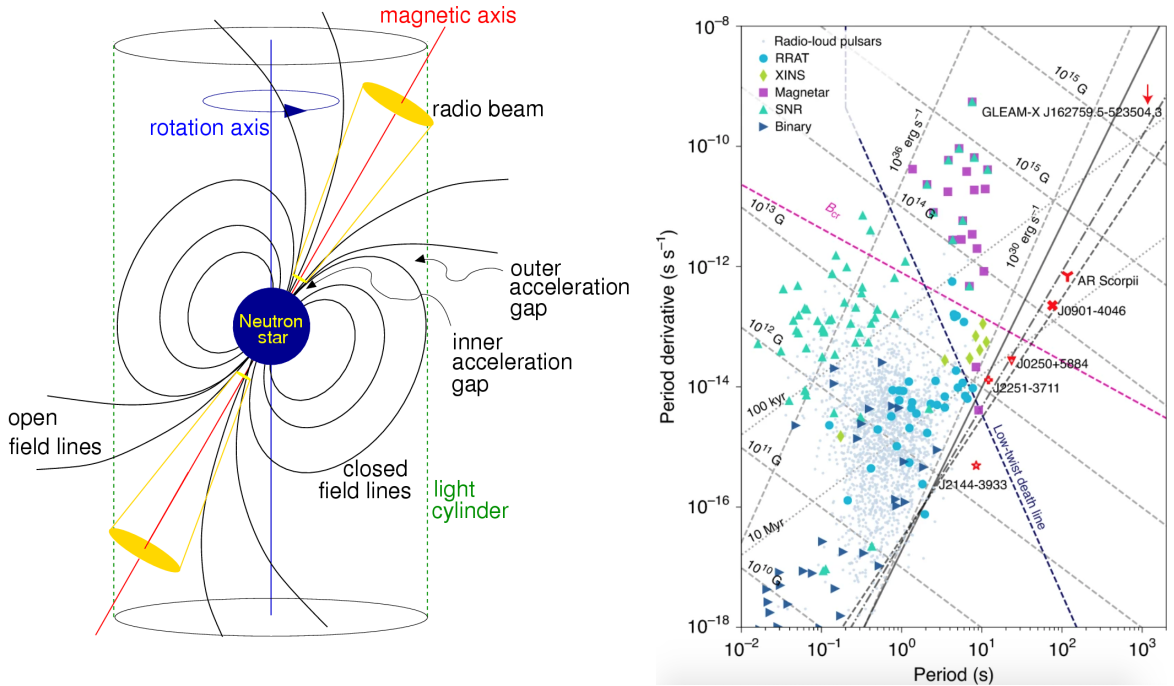


Figure 5: **Left.** The “light cylinder” around a NS within which the co-rotating magnetosphere is confined [102]. Acceleration of charges in this region are thought to produce electromagnetic beams that are detected terrestrially as regular pulses, making young NSs “pulsars”. **Right.**  $P-\dot{P}$  diagram taken from Ref. [103], illustrating the evolution of pulsars. For a description of the types of pulsars displayed here, see Ref. [102]. See Sec. 2.8 for further details.

## 2.7. Nucleon superfluidity

It has been recognized since 1959 that nucleons in a NS could be in a superfluid state [98], a hypothesis supported by observational fits to cooling curves [94]. Neutron superfluidity and proton superconductivity arise due to their Cooper pairing with a 0.1 MeV energy gap, corresponding to a critical temperature  $T_c \approx 10^{10}$  K [99, 63, 100]. Pairing occurs mainly close to the Fermi surface, hence superfluidity does not influence the EoS of NS matter (therefore bearing no consequence on NS mass-radius relations), but does play a major role in setting the NS’ heat capacity and neutrino emissivity. This is because these quantities are sensitive to particle-hole excitations close to the Fermi surface: the energy gap exponentially suppresses the nucleon contribution to the heat capacity for NS temperatures  $\ll T_c$ .

Neutrons in the NS inner crust are expected to form Cooper pairs in the singlet  $^1S_0$  state and in the core in a triplet  $^3P_2$  state: at higher densities, singlet pairing becomes repulsive [100]. The less dense protons are expected to pair in the singlet state in the NS core. A quark core in the NS could give rise to “color superconductivity” with  $ud$ ,  $ds$ ,  $su$  Cooper pairs carrying color charges [101]. Nucleon pairing models play a central role in the possibility of rotochemical heating, as discussed in Sec. 4.1.5. The presence of superfluidity in NSs also gives rise to macroscopic vortices and flux tubes, the former of which may play a role in late-stage reheating of NSs (Sec.4.1.5).

## 2.8. Neutron star magnetic field and spin-down

When a progenitor star turns into an NS, its surface area shrinks by a factor of about  $10^{10}$ . As a result, thanks to conservation of magnetic flux (Gauss' law for magnetism,  $B \times R_{\text{NS}}^2 = \text{constant}$ ) the stellar magnetic fields increase by this factor, and thanks to conservation of angular momentum the rotational speed also rises by this factor. Flux conservation also implies that the total energy in the NS due to the magnetic field decreases with the NS size:

$$E_B^{\text{NS}} = \frac{B^2}{8\pi} \cdot \frac{4\pi R_{\text{NS}}^3}{3} = \frac{\text{const.}}{R_{\text{NS}}}, \quad (32)$$

hence the presence of  $B$  fields tends to enlarge the NS. However  $E_B^{\text{NS}}$  is bounded by the gravitational binding energy of the NS, giving the condition

$$B \leq \sqrt{\frac{18 GM_{\text{NS}}^2}{5 R_{\text{NS}}^4}} \simeq 10^{18} \text{ Gauss} \left( \frac{M_{\text{NS}}}{M_{\odot}} \right) \left( \frac{10 \text{ km}}{R_{\text{NS}}} \right)^2. \quad (33)$$

A stricter upper limit can be obtained from considerations of hydromagnetic stability [104]. Measurements from pulsar spin-down (discussed here) find that millisecond pulsars typically have  $B$  field strengths of about  $10^8$  Gauss, classical pulsars about  $10^{12}$  Gauss, and magnetars about  $10^{15}$  Gauss. NSs have a ‘‘magnetosphere’’, a region of plasma surrounding the NS and co-rotating with it due to their coupling through the  $B$  field. One can see that this region is finite by simply locating the equatorial radius at which its tangential speed =  $c$  for a spin period  $P$ :

$$R_{\perp}^{\text{LC}} = \frac{cP}{2\pi} = 48 \text{ km} \left( \frac{P}{\text{ms}} \right). \quad (34)$$

This region defines the ‘‘light cylinder’’ shown in Figure 5, left panel. The presence of strong moving magnetic fields in the light cylinder generates electric fields that accelerate charged particles at the stellar surface, leading to emission of electromagnetic beams from near the magnetic poles of the NS. This beam, as we will soon see, is powered by the rotational energy of the NS. The lighthouse-like sweep of the beam, detected as regular pulses on Earth, serves to reveal NSs as pulsars<sup>4</sup>. This is how NSs were historically discovered by Bell and Hewish, and continues to be the primary method for finding NSs in the sky [107].

The NS spin varies over the lifetime of the NS due to a number of factors, chief among which is magnetic dipole radiation extracting rotational kinetic energy, an effect known as pulsar spin-down. The radiation power of a rotating magnetic dipole of moment  $m$ , with a component  $m_{\perp}$  perpendicular to the NS spin axis, and angular speed  $\omega = 2\pi/P$ , is given by [102]

$$\dot{E}_{\text{rad,B}} = \frac{2}{3c^3} m_{\perp}^2 \omega^4 = \frac{2}{3c^3} (B_{\perp} R_{\text{NS}})^3 \left( \frac{2\pi}{P} \right)^4, \quad (35)$$

where in the second equation we have used the expression for a sphere uniformly magnetized with field strength  $B$ . The rotational power of an NS of moment of inertia  $I = 2M_{\text{NS}}R_{\text{NS}}^2/5$  is given by

$$\dot{E}_{\text{rot}} = I\omega\dot{\omega} = -4\pi^2 \frac{I\dot{P}}{P^3}. \quad (36)$$

For sub-kHz frequencies this radiation cannot penetrate the ISM nebula surrounding the NS, and is hence deposited in it; the observed  $P$ ,  $\dot{P}$  and luminosities of supernova remnants such as the Crab Nebula ( $P =$

<sup>4</sup>At the time of writing, two ‘‘white dwarf pulsars’’ have been discovered [105, 106], but these refer to regular pulsation corresponding to the beat frequency of orbital rotation with a binary companion and the spin of the WD.

0.033 sec,  $\dot{P} = 1 \text{ sec}/80,000 \text{ yr}$ , luminosity =  $10^5 L_\odot$ , much higher than that of the Crab Pulsar within) bears out the supposition that  $-\dot{E}_{\text{rot}} \simeq \dot{E}_{\text{rad,B}}$  [102].

NS spin-down provides a remarkably valuable handle on the age of an NS through measurement of just its  $P$  and  $\dot{P}$ , i.e. without requiring knowledge of its radius, mass and  $B$  field. Assuming the  $B$  field remains constant, by equating Eqs. (35) and (36) we see that  $P\dot{P}$  is constant over time. For an initial spin period  $P_0$ ,

$$\begin{aligned} \int_0^\tau dt(P'\dot{P}') &= \int_{P_0}^P dP' P' \\ \Rightarrow P\dot{P}\tau &= \frac{P^2 - P_0^2}{2} \\ \Rightarrow \tau &= \frac{P}{2\dot{P}}, \end{aligned} \quad (37)$$

where the last equality assumed that the initial period  $P_0 \ll P$ . This *characteristic age*  $\tau$  due to spin-down is often an excellent order-of-magnitude estimate of an observed NS's true age. It slightly overestimates the latter for young NSs as an NS' spin may initially decelerate via gravitational radiation due to an oblate shape. For instance, for the Crab Pulsar, whose supernova was observed in 1054 A.D., one finds  $\tau = 1300$  years. In the case of older pulsars, Eq. (37) must again be used with special care, specifically when being applied to NSs that are thought to have spun up at some point in their life. These could be, *e.g.*, millisecond pulsars that are modelled as accreting mass and angular momentum from a binary companion; these have been observed with a characteristic age older their actual age [108]. In particular, there are millisecond pulsars with  $\tau > 13.8 \text{ Gyr}$  [107], the measured age of the universe [109].

We note in passing that for NSs for which precise data on distances and proper motions are available, their *kinematic age* may also be estimated by tracing back their trajectories and locating a plausible birth site [110]. This technique is possible thanks to the kick velocity imparted to the NS by the asymmetric explosion of the progenitor, as mentioned in the beginning of Sec. 2.

The pulsar braking index  $n$  is defined via  $\dot{\omega} \propto \omega^n$ . With a little elementary calculus, it may be seen that

$$n \equiv \frac{\omega\dot{\omega}}{\dot{\omega}^2} = 2 - \frac{P\ddot{P}}{\dot{P}^2}. \quad (38)$$

For spin-down induced by magnetic dipole radiation, one finds by equating Eqs. (35) and (36) that  $n = 3$ , although pulsars with braking indices of 1.4–3 have been observed, suggesting other spin-down mechanisms [102].

It is useful to place observed pulsars on a  $P$ - $\dot{P}$  diagram such as the one shown in Fig. 5 right panel. Pulsars typically begin life at the north-west region of the diagram, and move south-east along contours of constant  $B$  strengths while crossing contours of constant spin-down age. Eventually as they age to about 10 Myr the rotational energy is insufficient to generate the pulsar beam, and they cross the “pulsar death line”, sometimes referred to as the “death valley”. However, the death line is not well-understood, for the exact mechanism by which pulsar beams are created is still unknown and is an active area of research. This is evident in the  $P$ - $\dot{P}$  diagram: quite a few pulsars lie beyond various models of the death line [111, 112, 113, 114], with PSR J2144-3933 lying well beyond all the canonical death lines. We will re-encounter this oddball pulsar, which also happens to be the coldest NS observed, in Sec. 4.1.

### 3. The white dwarf as a dark matter laboratory

WDs have been used as DM detectors via a number of mechanisms. There are four main effects, which we will detail in the rest of the section: (1) DM can collect and annihilate inside WDs, heating them to

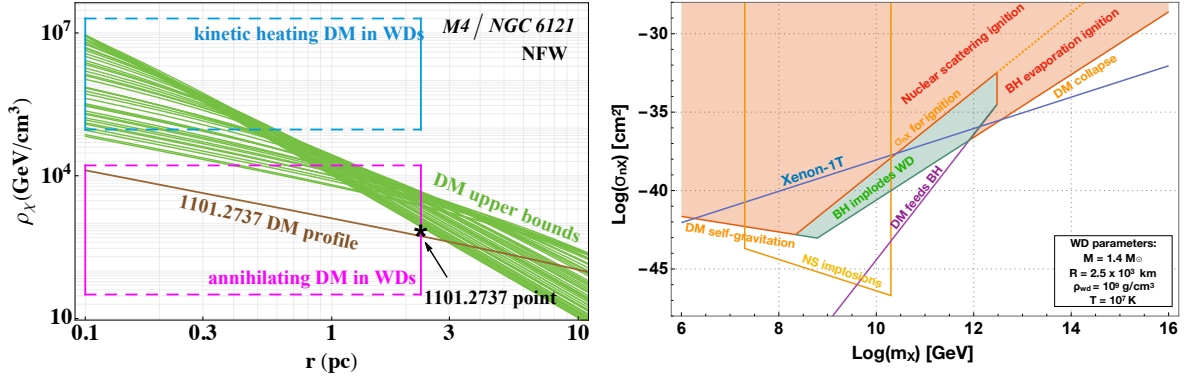


Figure 6: *Left*. Upper bounds from Ref. [116] on DM density distributions in the globular cluster M4, compared with an estimate of the DM densities (labelled “1101.2737”) from Ref. [117] using a spherical collapse model. Also shown are the range of DM densities required to match the observed luminosities of WDs in M4 via DM annihilations within the WD as well as kinetic heating by infalling DM; the horizontal range of the rectangles spans the uncertainty in the positions of the WDs. *Right*. Bounds on dark matter using an old WD in the Milky Way taken from [86]. See Secs. 3.1 and 3.2 for further details.

above the temperature that would be expected from a standard WD cooling curve such as in Sec. 2.6. (2) So much non-annihilating DM accumulates in a WD that the DM collapses and forms a black hole deep in the WD interior. This small black hole can grow to accrete the entire WD, thereby converting its host into a solar mass black hole. (3) DM encounters with and collection in the WD can cause it to explode. (4) WDs’ internal structure could be altered if a substantial fraction of its mass were comprised of DM.

In addition, resonant conversion of axion-like particle DM to photons in the corona of a magnetic WD may be observed [115]; we relegate discussion of this phenomenon in the context of NSs to Sec. 4.11.

### 3.1. Dark matter annihilation inside and heating white dwarfs

The possibility that dark matter can accumulate inside and change the internal thermal properties of stars has long been appreciated [9, 10]. A number of works has proposed that old WDs could have their late-time temperature altered through accumulation and annihilation of DM in the interior [118, 117, 119, 120]. To a good approximation the amount of collisionless DM (for local DM density  $\rho_\chi$  and average DM-WD relative speed  $v_{\text{rel}}$ ) flowing through a WD with mass  $M_{\text{WD}} = 1.2 M_\odot$ , radius  $R_{\text{WD}} = 4000$  km, and surface escape velocity  $v_{\text{esc}} = \sqrt{2GM_{\text{WD}}/R_{\text{WD}}}$  is

$$\dot{M} = \rho_\chi v_{\text{rel}} \times \pi \left( \frac{R_{\text{WD}} v_{\text{esc}}}{v_{\text{rel}}} \right)^2 = 10^{-7} \frac{M_\odot}{\text{Gyr}} \left( \frac{R_{\text{WD}}}{4000 \text{ km}} \right)^2 \left( \frac{M_{\text{WD}}}{1.2 M_\odot} \right) \left( \frac{\rho_\chi}{0.4 \text{ GeV/cm}^3} \right), \quad (39)$$

where we have normalized to the mass accumulated over a gigayear to emphasize that the DM mass accumulated inside the WD over the lifetime of the universe is only a tiny fraction of the stellar mass. This expression assumes that all DM incident on the WD is captured; for the DM-nucleon or DM-electron cross section dependence of the capture rate, see Refs. [121, 86].

The late-time temperature of a benchmark WD described above, assuming it is determined by the capture and annihilation of all DM transiting the WD, is given by [116]

$$T_{\text{WD}} \approx 4000 \text{ K} \left( \frac{350 \text{ km/s}}{v_{\text{rel}}} \right)^{1/4} \left( \frac{\rho_\chi}{10^3 \text{ GeV/cm}^3} \right)^{1/4}, \quad (40)$$



where here we have normalized this expression to a typical  $v_{\text{rel}}$ , but have chosen  $\rho_\chi$  more than three orders of magnitude greater than the inferred DM density near most WDs whose temperatures have been determined. This is the DM density required for heating WDs above their expected late-time temperature shown in Figure 4. In practice, this means that in order to find or exclude DM this way, one would need to find an ancient WD in a region that conclusively has a high DM density.

Reference [117] studied the heating effect that certain inelastic DM models would have on the late-stage temperature of WDs, and found that for a background DM density of  $\rho_\chi \simeq 3 \times 10^4 \text{ GeV/cm}^3$ , they would be sensitive to inelastic inter-state mass splittings of about  $10 - 10^3 \text{ keV}$  and per-nucleon scattering cross sections  $\sigma_{n\chi} \gtrsim 10^{-41} \text{ cm}^2$ . These authors proceeded to investigate whether WDs observed in a very dense self-bound stellar system, the globular cluster NGC 6121, a.k.a. Messier 4 (M4), might reside in a background density of DM large enough to observe heating from DM. Assuming that M4 was formed from a subhalo that was then tidally stripped by the Milky Way parent halo, using a spherical collapse model first derived in Ref. [118], adopting an NFW density profile, and accounting for the slight adiabatic contraction of densities from the baryon potential, they estimated that the DM density was approximately  $800 \text{ GeV/cm}^3$  at a cluster-centric distance  $r = 2.3 \text{ pc}$ , where the farthest WDs were observed in the Hubble Space Telescope. Following this, a number of authors investigated the implications of DM in globular clusters capturing in celestial bodies, under the assumption of a large ( $10^3$ - $10^4 \text{ GeV/cm}^3$ ) DM density [122, 123, 124, 125, 126, 127, 128, 129].

A recent study [116] set empirical limits on the DM densities in M4 using measurements of stellar line-of-sight velocities and performing a spherical Jeans analysis; Figure 6 shows these limits on various DM density profiles corresponding to upper bounds on NFW scale parameters. The density estimate of Ref. [117], denoted by an asterisk, is safe from these limits. Nevertheless, it was argued that the use of globular clusters as copious sources of DM resulting in far-reaching conclusions about its microscopic properties is problematic for several reasons.

1. The origin story of globular clusters is unclear. While Ref. [117] echoed a popular theory – corroborated in  $N$ -body simulations – that globular clusters originate in DM subhalos that then strip tidally [130, 131, 132], alternative simulations suggest they may form with no aid from dark matter via the collapse of giant molecular clouds [133, 134, 135, 136].
2. The V-band mass-to-light ratios of globular clusters in solar units is 1–5, which is equivocal about the presence of DM in them, unlike, say, dwarf galaxies (10–100), the Coma Cluster of galaxies (660) or the Milky Way (25) which are known to harbor significant amounts of DM. In fact, a structure defined as a stellar “cluster” is *defined* as a system whose dynamics need not be explained by DM, unlike a “galaxy” [137]. Accordingly, studies of more than 20 globular clusters looking for DM in them have either failed to detect DM or come to ambiguous conclusions [116].
3. There is no guarantee that any invisible mass favored in globular cluster data is in fact DM, as it may also be from faint stellar remnants [138].
4. The interpretation of the presence or absence of DM in ambiguous datasets is sensitive to priors and parametrizations. Ref. [139] found no evidence for DM when analyzing NGC 2419 by fitting a Michie model for the stellar and a generalized NFW profile for the DM distributions, but found strong evidence for DM when fitting these quantities with *no* analytic form, floating instead 389 free parameters.

One could conclude that, due to these significant uncertainties and the related infeasibility of determining DM density distributions in globulars with current and imminent measurement sensitivities, globular clus-

ters are systems that are far from robust for making statements about DM interactions. On that note, there are proposals for finding WDs in dwarf galaxies like Segue I and II [140].

### 3.2. Non-annihilating dark matter converting white dwarfs into black holes

If enough non-annihilating DM accumulates in WDs, the DM can collapse, and subsequently form a small black hole that accretes surrounding WD material, eventually consuming the entire WD [122, 86, 141]. Typically the DM is assumed to be “asymmetric” since in such models DM typically does not self-annihilate [142]. If in the process of accumulation and collapse DM self-annihilates efficiently, too much of it may be lost to form a black hole in the WD core.

The routine by which DM could form a small black hole in the interior of a WD is very similar to the more studied case of DM forming black holes in NSs<sup>5</sup>, which is detailed in length in Section 4.4. To avoid repetition, here we will emphasize aspects that are distinct from the case of the NS. The WD-to-BH conversion process is as follows. First, DM accumulates in the WD over time, through scattering on nuclei or electrons in its interior. Then, the captured DM thermalizes with the WD interior, i.e., after repeated scattering it is expected to localize within a small volume determined by the WD’s internal temperature and gravitational potential.

One chief difference here between WDs and NSs is that during thermalization, DM will scatter with a Coulomb lattice of ions in the core of the WD, which is stabilized by relativistic electron degeneracy pressure. This effect considerably suppresses DM-nucleus scattering rates at low momentum transfers, the regime that determines the thermalization timescale  $t_{\text{th}}^{\text{WD}}$ . For a carbon WD, this is given by [86]

$$t_{\text{th}}^{\text{WD}} \simeq 20 \text{ yr} \left( \frac{10^{-40} \text{ cm}^2}{\sigma_{n\chi}} \right) \left( \frac{m_\chi}{10^6 \text{ GeV}} \right)^2 \left( \frac{10^7 \text{ K}}{T_{\text{WD}}} \right)^{5/2}. \quad (41)$$

Thus for  $m_\chi > 10^{10}$  GeV, it can take  $> \text{Gyr}$  for DM to thermalize with the WD interior. Another difference between DM collapsing to form black holes in WDs and NSs is that, during the collapse inside a WD, DM may trigger a star-destroying thermonuclear explosion. We now turn to this topic.

### 3.3. White dwarf explosions via dark matter

Dark matter accumulated inside WDs might trigger a Type Ia-like supernova explosion through the deposition of enough energy to prompt runaway fusion reactions in the carbon/oxygen/neon interior of the WD [85, 146]; see also Ref. [147] for an early discussion of DM cores affecting Type Ia supernovae.

More generally, DM triggering WDs into supernovae can proceed in a number of ways:

- Attendant to DM converting WDs to black holes, DM can collect into a core region of the WD, collapse, and as a result of the collapse, deposit enough energy to ignite the WD. Ignition can occur either directly through nuclear scattering during the collapse of the DM core [85, 146, 47] or through the evaporation of a small black hole that forms out of the collapsed DM core [148, 141, 47].
- DM can have internal properties that result in energy being liberated as WD particles enter the DM state. A simple example of this is captured (and possibly thermalized) DM annihilating and depositing

---

<sup>5</sup>See also Ref. [143, 144, 145], which study black hole formation in other astrophysical bodies like the Earth, Sun, and Population III stars.



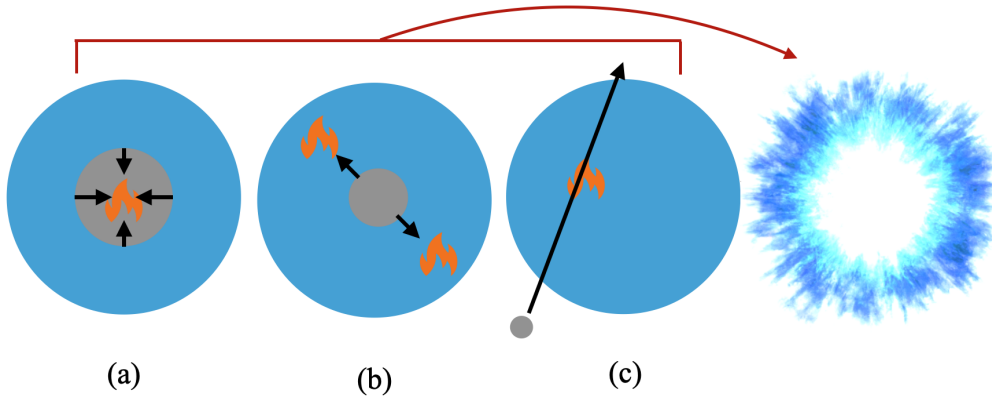


Figure 7: Illustration of mechanisms by which WDs may be prompted to explode by dark matter. (a) DM accumulates to the point of collapse in the center of the WD, then while collapsing (or after collapsing and forming a black hole) heats the WD to a temperature inducing a thermonuclear chain reaction. (b) The internal potential or mass energy of spatially extended DM is deposited as WD nuclei enter its state, prompting local heating that initiates the thermonuclear runaway. (c) Macroscopic DM transiting the WD transfers explosive kinetic energy via scattering on WD constituents.

energy in the WD medium with which it is admixed [149]. Other interesting possibilities are composite DM with an internal potential for baryons [150], solitonic Q-ball DM that absorbs baryonic charge and dissociates nuclei in the process [149], monopoles that possibly induce nucleon decay in similar fashion (Sec. 4.1.2), and accretion of WD carbon ions onto a black hole formed from collapse of electrically charged DM states [47].

- During an initial transit through the WD, DM can deposit kinetic energy gained by falling into the WD’s gravitational potential. The DM could be in the form of primordial black holes (PBHs), in which case energy is transferred via dynamical friction [146, 151], or particles inducing nuclear scatter recoils [149, 152, 153]. Tightly bound asteroid-like DM triggering WD explosions via stellar shocks has also been suggested [154].

However the WD is heated, a number of requirements must be met for thermonuclear reactions sparked to sustain themselves and cause the WD to explode. These requirements are described in Sec. 3.3. We now discuss some subtle aspects of this phenomenon as explored in the literature.

A detailed simulation of PBH energy deposition in a WD, including the effect of turbulent flows in the wake of the passing PBH, found that heavier PBHs were required to ignite WDs [151] compared to initial estimates [146]. This study employed a 1D+1D hydrodynamic simulation of the shock front created by a transiting PBH, and found that the development of hydrodynamic instabilities dissipating heat deposited through dynamical friction appeared to occur more rapidly than ignition processes, which were modeled using the same carbon fusion reaction rates used in Ref. [84]. Instead of a burning reaction, the prompt detonation of WD material by transiting PBHs was further studied in Ref. [155]. Another study investigated ignition during DM core collapse using a system of differential equations that track the evolution of per-particle energies [156] - this tracked carbon fusion inside the collapse region, and found carbon depleted before the WD ignition temperature in Ref. [84] was reached. Future work could build on this result in a number of directions, *e.g.* by studying C-O burning and employing the full nuclear reaction network used in Ref. [84] to obtain WD ignition temperatures. In addition, future WD ignition estimates should also consider convective flows of heated WD material moving carbon through the collapse region replenishing carbon and oxygen, and whether WD ignition occurs via thermal energy transported out of the collapse

region. This is especially important, since studies on carbon fusion occurring inside DM bound states found that fusion can be induced in the region surrounding the collapsing region that is the source of heat, either through the evaporation of black holes of size much smaller than the ignition region, or through effluence of thermal energy outside of the transiting DM composite [86, 141, 150, 47]. Finally, the ignition of WD supernovae via oxygen burning typically requires a temperature somewhat higher than that of carbon<sup>6</sup> [84], and future detailed treatments of WD ignition by collapsing DM should account for this possibility.

Ref. [149] set limits on a wide range of DM-nucleus scattering cross sections and DM masses assuming point-like elastic scattering of DM particles on carbon in WDs. These constraints were placed using the condition for the minimum stopping power,

$$n_T \sigma_{T\chi} m_T v_{\text{esc}}^2 \gtrsim \rho \bar{c}_p T_{\text{crit}} \lambda_{\text{trig}}^2 \quad (42)$$

for a heating region of size  $\leq \lambda_{\text{trig}}$ . However, this condition does not account for the finite number of nuclei that the DM particle would encounter during its transit through the heating region. Suitably modified, the above condition should be

$$\begin{aligned} N_{\text{hit}} \frac{m_T v_{\text{esc}}^2}{\lambda_{\text{trig}}} &\gtrsim \rho \bar{c}_p T_{\text{crit}} \lambda_{\text{trig}}^2, \\ N_{\text{hit}} &= \max[n_T \sigma_{T\chi} \lambda_{\text{trig}}, n_T^{1/3} \lambda_{\text{trig}}] \end{aligned} \quad (43)$$

where  $N_{\text{hit}}$  is the number of point-like scatters on nuclei as the DM particle traverses the length  $\lambda_{\text{trig}}$ . One can see that Eq. (43) reduces to Eq. (42) for  $\sigma_{T\chi} < n_T^{-2/3}$ . Ref. [149] considers a  $1.25 M_{\odot}$  WD to set limits, for which  $n_T \simeq 10^{-31} \text{ cm}^{-3}$ , implying that  $\sigma_{T\chi} \lesssim 2 \times 10^{-21}$  for Eq. (42) to be valid. However,  $\sigma_{T\chi} > 10^{-12} \text{ cm}^2$  is shown to be excluded in Ref. [149]. One could also see the error in this result by estimating the maximum energy transferred by DM elastic recoils by a linear transit across a length  $\lambda_{\text{trig}}$ . This is  $(n_T^{1/3} \lambda_{\text{trig}})(m_T v_{\text{esc}}^2) \simeq 10^{4.5} \text{ GeV}$ , which may be compared with the trigger energies ranging across WD masses,  $10^{17-24} \text{ GeV}$  (Sec. 2.5). One could contrast this analysis against Refs. [152, 153], which considered WD explosions triggered by the transit of macroscopic composite DM. In these studies, the requisite number of WD nuclei within a trigger volume may indeed be excited to ignite the region into runaway fusion. In Fig. 11 bottom left panel we show the masses and radii of DM mini-clusters constrained by the observed existence of WDs in our Galaxy, taken from Ref. [153]. Overlaid here are contours of the minimum DM-nucleus elastic scattering cross sections required to transfer sufficient kinetic energy to the WD trigger volume to induce stellar explosion.

A number of phenomena have been linked to the DM-induced ignition of thermonuclear explosions in WDs. It has been posited that DM core collapse in WDs might account for a large fraction of observed Type Ia supernovae [85], as a solution to the Type Ia progenitor problem [79] and consistent with the apparent observation of sub-Chandrasekhar WDs as the origin of most Type Ia supernovae [157]. Reference [85] also found that a trend in existing Type Ia data [158], showing that more massive progenitors explode sooner, is consistent with certain DM models that induce WD explosions through DM core collapse, where this would occur sooner for heavier WDs. The accumulation in certain sub-Chandrasekhar WDs of charged massive particles (CHAMPs) making up DM, which might occur preferentially outside galaxies with magnetic fields that serve to deflect CHAMPs, could be an explanation of the distribution of calcium-rich gap transient WD supernovae [47] that do explode preferentially on the outskirts of galaxies [159]. The distribution of Type Ia supernovae in galaxies could be tied to local properties like velocity dispersion, especially in the

---

<sup>6</sup>We thank Melissa Diamond for correspondence on this point.

effect	change in capture rate	applicability	reference
EoS of star effects	$O(1)$ : BSk20 $\rightarrow$ 21	all $m_\chi$	[167]
	none: QMC-2 $\rightarrow$ BSk24	all $m_\chi$	[168]
mass-radius configuration	$O(100)$ as $1 \rightarrow 2.2M_\odot$	all $m_\chi$	[169]
nuclear self-energies nucleon structure	30–100	$m_\chi > 100$ MeV, any EoS	[170]
		$O(10^3)$ for $2 M_\odot$ NSs	[168]
non-elastic scattering	subdominant	–	[168]
“collective” effects	$O(1 - 10^3)$	$2 M_\odot$ NS, $m_\chi < 100$ MeV, $A'$ mediator	[171]
superfluidity: energy gap	maybe $O(1)$	$m_\chi \lesssim 35$ MeV, single phonon excitation	[48] [164]
NS opacity/ extinction factor	$O(1)$	$m_\chi > \text{GeV}$	[169]
relativistic kinematics	$\sim 4$	$m_\chi > \text{GeV}$	[169]
	$\sim 10$	$m_\chi < \text{GeV}$	[169]
gravitational focusing	$< 2$	all $m_\chi$	[169]
light mediator kinematics	$O(1)$ voided	$m_\phi/\mu_{\text{red}} < 10^{-1}$ $m_\phi/m_\chi < 10^{-4}$	[172]
DM halo velocity distribution	$< 2$	all $m_\chi$	[173]

Table 1: Known effects that modify the rates of dark matter capture in NSs. See Sec. 4.1.3 for further description.

case of PBH-ignition [160]. Finally, a separate study has investigated whether WD explosions from DM could explain the aforementioned Ca-rich gap transient distribution, through the ignition of WDs in dwarf spheroidal galaxies expected to be located at some distance from larger galactic DM halos [161].

### 3.4. Dark matter’s influence on white dwarf equations of state

WD mass-radius relationships can also be observably impacted by DM. If a substantially massive core of DM accumulated in the interior of a WD, its stable configurations would be altered through revised TOV equations [147, 162, 163]. For a typical circumambient DM density, the amount of collisionless DM required to induce these effects,  $10^{-4}M_\odot - 10^{-1} M_\odot$ , well exceeds what could be collected in the WD over the lifetime of the universe; see Eq. (39). However, future studies could investigate whether such a large quantity of DM might be collected through collisional accretion, analogous to the NS treatment in Ref. [164] (discussed in Sec. 4.2). Another effect comes through the axion: its existence implies that its non-derivative coupling to nucleons would displace it from its usual minimum in a finite-density medium. This results in a reduction of the nucleon mass and alters the TOV equations [165].

## 4. The neutron star as a dark matter laboratory

### 4.1. Dark matter kinetic and annihilation heating of neutron stars

#### 4.1.1. Capture and kinetic heating

NSs are excellent captors of particle dark matter by virtue of their extreme densities and steep gravitational potentials, and also quite serviceable as thermal detectors thanks to their typically small temperatures. While the capture of DM in NSs and its subsequent thermal relaxation was first treated in Ref. [11], it was

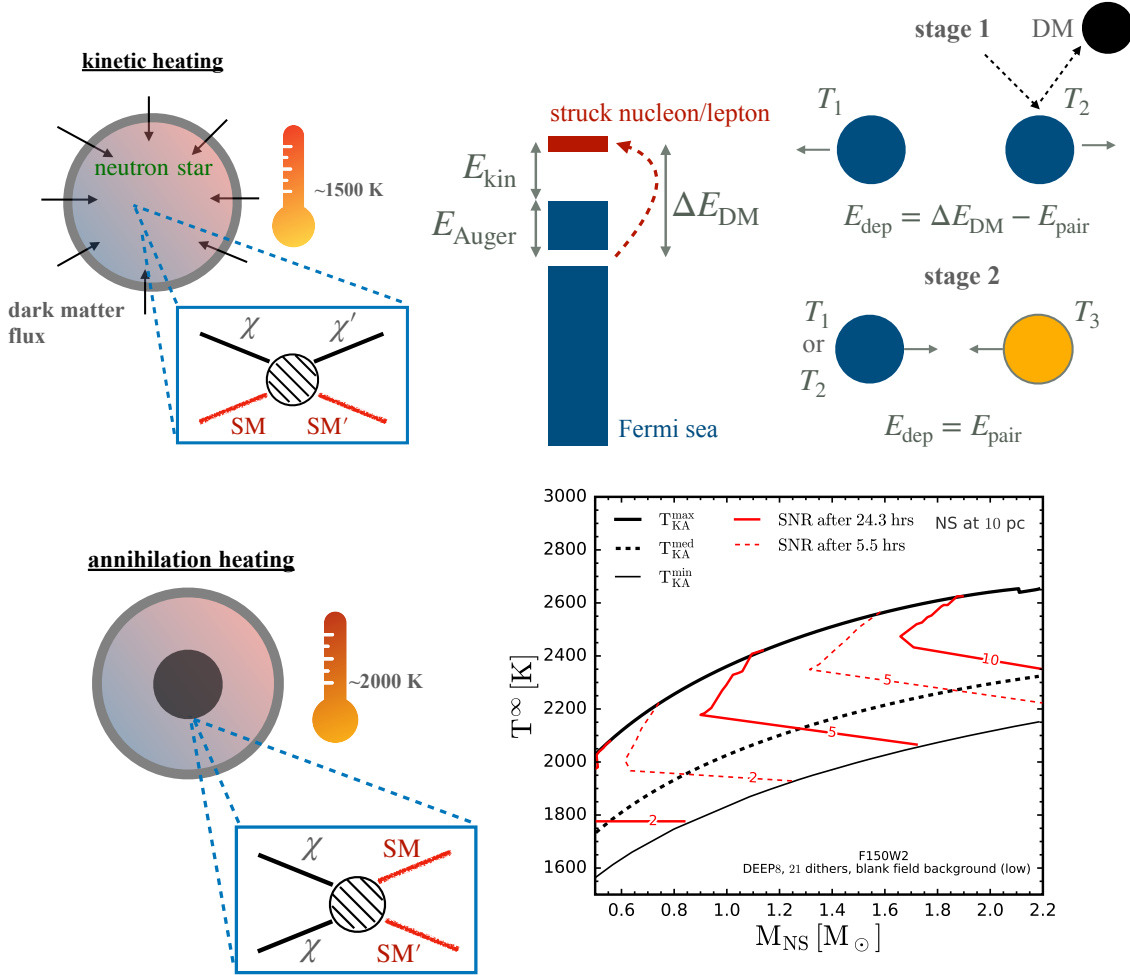


Figure 8: **Top left.** Cartoon showing the dark kinetic heating effect in NSs. Scattering interactions of the infalling dark matter flux contribute to the luminosity of a typical NS at the level of a 1500 K blackbody temperature. **Top middle.** The nucleon Auger effect that contributes to kinetic (and possibly annihilation) heating by dark matter in NSs. The total energy deposited after scattering turns out to be the dark matter energy transfer, although physically it comes as the sum of two contributions: the energy spilled during the rapid filling of the hole left behind by the struck target, and the energy carried by the target in excess of the Fermi energy. **Top right.** The breaking and re-pairing of Cooper pairs that contributes to kinetic (and possibly annihilation) heating by dark matter in NSs. This phenomenon takes place for dark matter with mass above about 35 MeV; for smaller masses, dark matter capture proceeds through collective excitations in the nucleon superfluid medium. **Bottom left.** Cartoon showing possible additional heating of NSs via self-annihilations of dark matter possibly collected in a thermalized volume. This highly model-dependent process could heat the NS to blackbody temperatures around 2000 K. **Bottom right.** As a function of NS mass, NS effective temperatures imparted by dark kinetic+annihilation heating that can be measured at the James Webb Space Telescope at various signal-to-noise ratios, taken from Ref. [45]. The band denotes variations over NS radii predicted by numerous equations of state as well as NS-DM relative velocities from estimates by various NS population models. See Sec. 4.1.1 for further details.

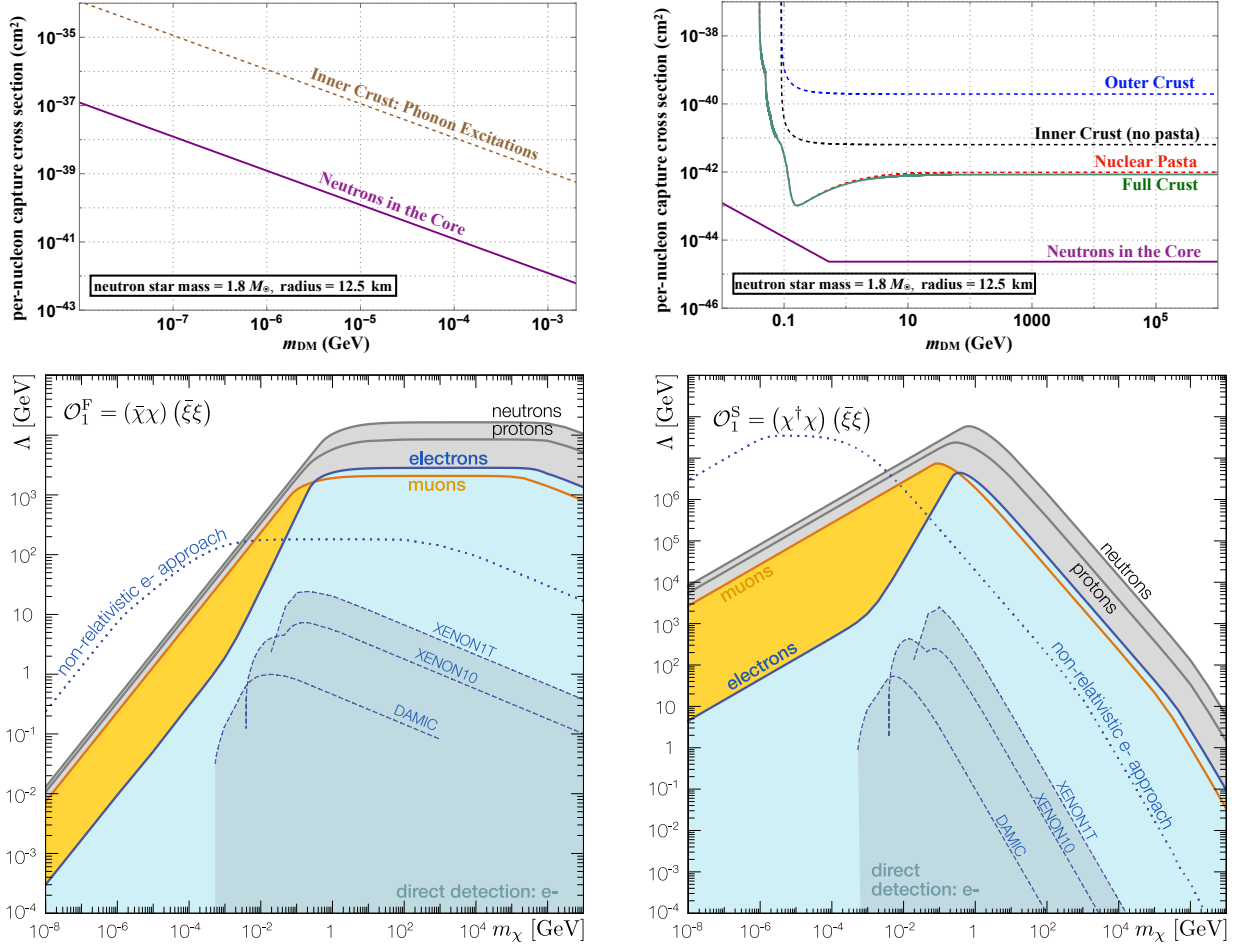


Figure 9: **Top.** Capture cross section sensitivities for light dark matter scattering in a NS crust (*left*) (via excitation of superfluid phonons in the inner core) and in the NS core (via Pauli-blocked contact scattering on neutrons, although see Sec. 4.1.1 for a discussion on scattering in the superfluid core), and for heavier dark matter scattering in various layers of the crust and the core (*right*). These two plots are taken from Ref. [48]. See Sec. 4.1.1 for further details. **Bottom.** Sensitivities to the cutoff of effective CP-even scalar interactions of dark matter with relativistic, degenerate electrons in a NS, for DM that is spin-1/2 (*left*) and spin-0 (*right*). Also shown are the sensitivities for interactions with muons, protons and neutrons. The electron scattering limits are seen to widely complement terrestrial searches. These two plots are taken from Ref. [166]. See Sec. 4.1.1 for further details.

only recently realized that this could be a minimal probe of dark matter scattering on Standard Model (SM) states: the transfer of DM kinetic energy to the NS's constituent particles during the infall of DM at semi-relativistic speeds overheats the NS [174]. It was also proposed that upcoming infrared telescopes, *e.g.*, the Thirty Meter Telescope (TMT) [175] and the Extremely Large Telescope (ELT) [176] are sensitive to this “dark kinetic heating” mechanism [174] for NSs out to about 100 pc from Earth; a study has also been dedicated to the sensitivity at the recently launched James Webb Space Telescope (JWST) [177, 45], which has shown that finding an NS much closer than 100 pc would likely be required. Thermal observations of nearer pulsars could be made following the discovery of old, isolated NSs in radio telescopes such as FAST [178], CHIME [179] and SKA [180]. Though their  $B$  fields and rotational velocities are expected to be low, implying they populate regions near the “pulsar death line” in  $P$ - $\dot{P}$  space beyond which NSs are supposed to stop pulsing, NSs have been observed beyond the death line [113, 111, 114, 112] calling into question models of NS pulsation (as also discussed in Sec. 2.8). It is estimated that about  $10^5$  NSs in the Galaxy lie beyond the death line [113].

To illustrate the idea of dark kinetic heating let us consider the following representative NS configuration:

$$\begin{aligned} M_{\text{NS}} &= 1.5 M_{\odot}, \quad R_{\text{NS}} = 12.85 \text{ km} \\ \Rightarrow v_{\text{esc}} &= \sqrt{\frac{2GM_{\text{NS}}}{R_{\text{NS}}}} \simeq 0.59. \end{aligned} \quad (44)$$

where  $v_{\text{esc}}$  is the escape speed at the surface. This configuration is obtained for a Quark Meson Coupling (QMC) EoS of matter [168].

For local DM density  $\rho_{\chi}$  and average DM-NS relative speed  $v_{\text{rel}}$  (which in the solar vicinity are  $0.4 \text{ GeV/cm}^3$  and  $350 \text{ km/s}$  [181]), the DM mass capture rate is given by [11]

$$\begin{aligned} \dot{M} = m_{\chi} C_{n_{\chi}} &= \rho_{\chi} v_{\text{rel}} \times \pi b_{\text{max}}^2 \times p_v \times p_{\sigma}, \\ &= p_v p_{\sigma} \times 1.76 \times 10^{25} \text{ GeV/s}, \end{aligned} \quad (45)$$

where  $b_{\text{max}} = R_{\text{NS}}(1+z)(v_{\text{esc}}/v_{\text{rel}})$  is the maximum impact parameter of DM intersecting the NS, with  $1+z = (1-v_{\text{esc}}^2)^{-1/2}$  a blueshift factor magnifying the NS radius to a distant observer, and  $p_v$  is the probability that a scattered DM particle loses sufficient energy to be captured. For instance, this probability  $\simeq 1$  for scalar- or vector-mediated scatters, but may be suppressed for pseudoscalar-mediated interactions that favor soft forward scatters [172]. Eq. (45) is, of course, the DM capture rate for an isolated NS; an NS in a binary system could capture DM at a rate greater by up to a factor of a few thanks to gravitational assist [182].

The probability that incident DM is scattered is given by  $p_{\sigma} = 1 - e^{-\tau} \simeq \tau = \sigma_{n_{\chi}}/\sigma_{\text{cap}}$  where, for optical depth  $\tau$ , the approximate equality in the first line holds in the optically thin limit. The “capture cross section” above which  $\tau > 1$  in the NS core is:

$$\sigma_{\text{cap}} = \begin{cases} \sigma_0(\bar{m}_n/m_{\chi}) & , \quad m_{\text{evap}} < m_{\chi} < \bar{m}_n, \\ \sigma_0 & , \quad \bar{m}_n \leq m_{\chi} \leq \text{PeV}, \\ \sigma_0(m_{\chi}/\text{PeV}) & , \quad m_{\chi} > \text{PeV}, \end{cases} \quad (46)$$

where the NS geometric cross section  $\sigma_0 = \pi(\bar{m}_n/M_{\text{NS}})R_{\text{NS}}^2 \simeq 2.2 \times 10^{-45} \text{ cm}^2$ . One understands the dependence on  $m_{\chi}$  in Eq. (46) by considering the typical neutron recoil energy in the neutron rest frame:

$$\Delta E_{\text{DM}} \simeq \frac{\bar{m}_n m_{\chi}^2 (1+z)^2 v_{\text{esc}}^2}{(\bar{m}_n^2 + m_{\chi}^2 + 2(1+z)\bar{m}_n m_{\chi})}, \quad (47)$$



The above expression is a good approximation to describe DM-neutron scattering in the stellar rest frame as well, since the neutrons are typically non-relativistic: their Fermi momenta, varying over a few 100 MeV across the NS, are smaller than their  $\sim$ GeV mass. For  $m_\chi < \bar{m}_n$ , only a fraction  $\approx 3\Delta p/p_F$  of degenerate neutrons close enough to their Fermi surface receive the typical momentum transfer  $\Delta p = \sqrt{2\bar{m}_n\Delta E_{\text{DM}}}$  to scatter to a state above the Fermi momentum  $p_F \approx 0.4$  GeV. This ‘‘Pauli-blocking’’ effect gives  $\sigma_{\text{cap}} \propto \Delta E_{\text{DM}}^{-1/2} \propto m_\chi^{-1}$ . The so-called evaporation mass,

$$m_{\text{evap}} \approx 20 \text{ eV} \left( \frac{T_{\text{NS}}}{10^3 \text{ K}} \right), \quad (48)$$

is the DM mass below which the thermal energy of the NS would kinetically eject the captured DM from the stellar potential well [167, 183]. For  $\bar{m}_n \leq m_\chi \leq 10^6$  GeV, a single scatter suffices for capture:  $\Delta E_{\text{DM}} \approx \bar{m}_n v_{\text{esc}}^2 \gamma^2 > \text{KE}_{\text{halo}}$ , the DM halo kinetic energy. For  $m_\chi > \text{PeV}$ , multiple scatters are required for capture, so that approximately  $\sigma_{\text{cap}} \propto \text{KE}_{\text{halo}}/\Delta E_{\text{DM}} \propto m_\chi$ . The expression in Eq. (45) can be refined to account for the velocity distribution of DM far from the NS [184].

The heating of the NS comes not only from the recoil of incident DM but from two other secondary effects. As depicted in Fig. 8, a target neutron (or a lepton) that is upscattered by DM leaves behind a hole in the Fermi sea. The hole is filled up immediately by a nearby neutron from a higher energy level, which in turn leaves a hole, and so on. This process spills over energy in the form of radiation and kinetic energy, and is reminiscent of the Auger effect observed in electron levels in superconductors; we will re-encounter this effect as a means of NS internal heating in Sec. 4.8. The net energy deposited in the NS by this effect,  $E_{\text{Auger}}$ , is simply the difference in energy between the Fermi surface and the position of the original hole. The energy carried by the struck nucleon/lepton in excess of the Fermi energy,  $E_{\text{kin}}$ , is dissipated as kinetic energy above the Fermi surface. Thus the total energy deposit  $E_{\text{Auger}} + E_{\text{kin}}$  comes out to be simply the DM recoil energy  $\Delta E_{\text{DM}}$ . Yet another effect comes from the superfluidity of nucleons (see Sec. 2.7). For  $m_\chi \gtrsim 35$  MeV, DM participates in elastic scattering by first breaking a nucleon Cooper pair, which is bound with an energy given by the superfluidity energy gap  $\sim$  MeV. The absorbed  $\sim$  MeV energy is redeposited into the NS when the free nucleon finds another and pairs up, liberating the gap energy. For  $m_\chi \lesssim 35$  MeV nucleons in the NS might not scatter elastically as there isn’t enough energy transfer to break nucleon Cooper pairs, leaving DM to capture via collective excitations instead [48, 164]. Light DM capture in certain models through collective effects in NSs has been studied [171]. The presence of DM self-interactions can enhance the capture rate by orders of magnitude as initially captured DM particles can serve as captors of ambient DM [185].

Once captured in the potential well, a DM particle repeatedly scatters on and thermalizes with the NS until its orbit shrinks to within the radius of the star, by which times most of its kinetic energy is transferred. Under equilibrium, the kinetic power of the infalling dark matter, constituting the NS heating rate, equals the rate at which photons are emitted from the NS surface, constituting the NS cooling rate. The latter is dominated by such photon emission for NSs older than  $\sim$ Myr, as we saw in Sec. 2.6. The NS luminosity corresponding to a temperature  $T$  (in the NS frame) is then  $L = z\dot{M} = 4\pi R_{\text{NS}}^2 T^4$ , which attains a maximum value  $L_{\text{max}}$  for unit capture probabilities  $p_\sigma$  and  $p_\nu$ . For our representative NS configuration (Eq. (44)),  $L_{\text{max}} = 7.6 \times 10^{24}$  GeV/s, corresponding to a NS temperature seen by a distant observer  $\tilde{T} = T/(1+z)$  of  $\tilde{T} = 1400$  K. Temperatures in this range are measurable within reasonable integration times at current and imminent infrared telescope missions [174, 186], in particular at the recently launched JWST [45], and the forthcoming ELT and TMT. For instance, the NIRCам instrument at JWST could constrain the surface NS temperature at 1750 K with a signal-to-noise ratio (SNR) of 2 in  $27.8 \text{ hr}(d/10 \text{ pc})^4$ , where  $d$  is the distance to the NS [174]; the IRIS instrument at TMT could do the same in  $19.4 \text{ hr}(d/10 \text{ pc})^4$ . In the bottom right panel of Fig. 8 are displayed the NS effective temperatures constrainable at JWST at various SNRs for integration

times of 5.5 hr and 24.3 hr, using the F150W2 filter on NIRCcam. In this plot taken from Ref. [45], the band spans the range of the NS radii (which determines the range of DM capture rates) predicted by various EoSs, and integrates over the NS-DM relative velocities predicted by various NS population models in Ref. [187, 188]. These sensitivities are for the case of NSs being heated not only by the kinetic energy of infalling DM but also by DM annihilations, which we will discuss in Sec. 4.1.2. Searches for DM using NS thermal emissions are best carried out with NSs whose “standard” temperatures are expected to be below approx. 1000 K. Thus one would need NSs older than 10 Myr (Fig. 4), making the determination of their age via spin-down or kinematic considerations (Sec. 2.8) crucial. One would also need them sufficiently isolated to ensure no accretion of material from a binary companion.

The DM-nucleon scattering cross section may be so large that DM scatters dominantly with the  $\sim$ km-thick low-density crust of the NS before reaching the  $\sim$ 20 km-diameter denser core. Moreover, the core may consist of exotic phases of high-density matter such as meson condensates and deconfined  $ud$  or  $uds$  quark matter, the latter of which may exist in any of the multiple phases discussed in Sec. 2.4; in such cases, the dynamics governing DM scattering cannot be unambiguously computed, whereas the better understood crust can be treated robustly as a DM captor. DM scattering with the NS crust leads to surface emission of photons under thermal equilibrium analogous to capture in the NS core discussed above, hence the observational signatures of NS heating are unchanged. In Figure 9 we show the DM capture cross section  $\sigma_{\text{cap}}$  for every layer of the NS described in Sec. 2.4, derived in Ref. [48] for a  $1.8 M_{\odot}$  mass, 12.5 km radius NS. For DM masses below about 10 MeV (left panel), DM capture can occur by scattering on superfluid neutrons in the inner crust, and exciting phonons. The single-phonon emission mode is expected to dominate, which proceeds via a static structure function  $= \Delta p / (2m_n c_s)$  that relates the per-nucleon cross section to the phonon-excitation cross section. Here  $c_s$  is the phonon speed. Due to the proportionality to the transfer momentum,  $\sigma_{\text{cap}} \propto m_{\chi}^{-1}$  similar to the Pauli-blocking regime of the NS core discussed above. The latter sensitivity (applicable to when the core is populated mainly by neutrons) is also shown for comparison in the plot. For DM masses above about 100 MeV (right panel), DM capture can occur by scattering on individual nucleons locked up in nuclei in the outer crust by transferring energies greater than their  $\sim$ MeV binding energy. Scattering on nuclei is generally suppressed: large  $\Delta p$  leads to loss of nuclear coherence over multiple nucleons, and small  $\Delta p$  leads to loss of coherence over multiple nuclei, described by a lattice structure function. Deeper down in the inner crust, heavier-than-100-MeV DM capture proceeds by scattering on loosely bound nucleons, and even further down, by scattering on the pasta phase. Pasta scattering may either be on individual nucleons at high DM masses or on multiple nucleons at low DM masses as described by response functions accounting for inter-nucleon correlations. A resonant peak in the response function is seen to enhance the capture sensitivity near  $m_{\chi} \simeq 100$  MeV. For comparison is also shown the DM capture cross section for scattering in an NS core dominated by neutrons.

Even in the absence of exotic phases, NS cores are expected to contain  $\sim$ 10% level populations of protons, electrons, and muons thanks to beta chemical equilibrium. DM may be possibly be leptophilic, such that scattering at tree level is solely on  $e^{-}$  and/or  $\mu^{-}$ , or iso-spin violating, such that scattering is dominantly on protons. NS capture and heating applies to these scenarios, too [174]. While the Fermi momenta of protons and muons are smaller than their mass, making them non-relativistic and amenable to the above treatment, that of electrons are 1–2 orders of magnitude greater than  $m_e$ , warranting relativistic kinematics to treat their DM capture in the stellar rest frame [189, 167, 190, 191, 192, 193, 194, 166]. This also makes the treatment of Pauli-blocking non-trivial [192, 166]. In particular, the capture probability accounting for Pauli-blocking, relativistic scattering and summing over multiple scatters is [166]

$$df = \sum_{N_{\text{hit}}} d\sigma_{\text{CM}} v_{\text{Mol}} dn_{\text{T}} \frac{\Delta t}{N_{\text{hit}}} \Theta\left(\Delta E - \frac{E_{\text{halo}}}{N_{\text{hit}}}\right) \Theta\left(\frac{E_{\text{halo}}}{N_{\text{hit}} - 1} - \Delta E\right) \Theta(\Delta E + E_p - E_{\text{F}}), \quad (49)$$



where  $v_{\text{Mol}}$  is the Möller velocity that relates the cross section in any frame to that in the center of momentum frame ( $d\sigma_{\text{CM}}$ ),  $dn_{\text{T}}$  is the differential volume of the target momentum space normalized to the Fermi volume,  $E_{\text{halo}}$  is the DM halo kinetic energy, and  $\Delta E$  is the energy transfer. We refer the reader to Ref. [166] for a detailed formalism. In Figure 9's bottom panels we show the NS capture sensitivity to contact interaction cutoffs versus  $m_\chi$  for scalar-type operators involving spin-1/2 and spin-0 DM. For electron scattering the NS capture reach is seen to be orders of magnitude greater than that of terrestrial direct searches for  $m_\chi > \text{MeV}$ , and indeed completely complements the latter for sub-MeV DM masses.

NS capture-and-heating can also provide orders-of-magnitude improvement over Earth-bound searches for DM with scattering that is

1. spin-dependent, since scattering directly on fermions instead of nuclei does not lead to the loss of nuclear coherence that limits spin-dependent searches at direct detection [186, 169, 195],
2. and/or velocity-dependent [186, 169, 195], since semi-relativistic DM speeds at the point of capture overcome velocity-suppressed scattering rates,
3. inelastic [174, 196, 197], since again the high DM speeds ensure that  $\mathcal{O}(100)$  MeV mass splittings between the DM and its excited state can be probed, as opposed to  $\mathcal{O}(100)$  keV at direct detection, and
4. below the so-called neutrino floor at direct searches, coming from irreducible neutrino backgrounds that are irrelevant for NS capture; see Fig. 9 top right panel,
5. with heavier-than-PeV DM, where DM capture proceeds mainly through multiple scattering in transit [198, 199, 174].

#### 4.1.2. Dark matter self-annihilations, nucleon co-annihilations, and induced nucleon decay

While the discussion above focused NS heating from the transfer of captured DM kinetic energy, applicable to any particulate dark matter model – in particular to non-annihilating DM such as asymmetric DM – certain scenarios may lead to DM annihilation inside the NS that further brightens it [184, 200] and thereby facilitate observations [174, 186, 48, 45], in some cases reducing telescope integration times by a factor of 10. For instance, JWST/NIRCam could constrain a 2480 K NS, heated by local DM kinetic energy + annihilations, with SNR 2 in 2.5 hr  $(d/10\text{pc})^4$ , and TMR/IRIS could do so in 0.56 hr  $(d/10\text{pc})^4$  [174]; compare these with kinetic heating-only exposure times in Sec. 4.1.1. Fig. 8 shows JWST sensitivities in more detail, as discussed in Sec. 4.1.1.

Self-annihilations of DM into most SM states would result in NS heating, the exception being neutrinos with sub-100 MeV energies as their optical depth in the NS material is too small to be trapped [201]. In any case, this phenomenon relies intricately on whether or not the DM thermalizes with the NS within its lifetime, since DM may possibly annihilate much more efficiently if it is collected within a small volume in the NS core; this is a highly model-dependent question [189, 194, 48] as discussed in Sec. 4.4.1. To understand this, consider the evolution of the number of DM particles  $N_\chi$  within a volume  $V$  of the NS self-annihilating with a thermally averaged cross section  $\langle\sigma_{\text{ann}}v\rangle$ , and its solution:

$$\begin{aligned}\frac{dN_\chi}{dt} &= C_\chi - \frac{\langle\sigma_{\text{ann}}v\rangle N_\chi^2}{V}, \\ N_\chi(t) &= \sqrt{\frac{C_\chi V}{\langle\sigma_{\text{ann}}v\rangle}} \tanh\left(\frac{t}{\tau_{\text{eq}}}\right),\end{aligned}\tag{50}$$

$$\tau_{\text{eq}} = \sqrt{\frac{V}{C_{\chi} \langle \sigma_{\text{ann}} v \rangle}},$$

where  $C_{\chi} = C_{n\chi} + C_{\chi\chi}$  is the total DM capture rate via scattering on nucleons (Eq. (45)) and, through self-interactions, on DM already accumulated in the NS, and  $\tau_{\text{eq}}$  is the characteristic timescale for equilibrium between capture and annihilation to establish, after which  $N_{\chi}(t)$  achieves a steady state ( $dN_{\chi}/dt \rightarrow 0$ ). Thus for  $t > \tau_{\text{eq}}$ , the total annihilation rate equals the capture rate. When  $V$  is the thermal volume (Eq. (52)), one can then compute the minimum annihilation cross section required for capture-annihilation equilibrium to occur well within the age of an observed NS,  $\tau_{\text{NS}}$ . Using a partial-wave expansion  $\langle \sigma_{\text{ann}} v \rangle = a + bv^2$ , the condition may be written for  $s$ -wave and  $p$ -wave domination as [194]

$$\begin{aligned} a &> 7.4 \times 10^{-54} \text{ cm}^3/\text{s} \left( \frac{\text{Gyr}}{\tau_{\text{NS}}} \right)^2 \left( \frac{C_{\text{max}}}{C_{\chi}} \right) \left( \frac{\text{GeV}}{m_{\chi}} \frac{T_{\text{NS}}}{10^3 \text{ K}} \right)^{3/2}, \\ b &> 2.9 \times 10^{-44} \text{ cm}^3/\text{s} \left( \frac{\text{Gyr}}{\tau_{\text{NS}}} \right)^2 \left( \frac{C_{\text{max}}}{C_{\chi}} \right) \left( \frac{\text{GeV}}{m_{\chi}} \frac{T_{\text{NS}}}{10^3 \text{ K}} \right)^{1/2}, \end{aligned} \quad (51)$$

where  $C_{\text{max}}$  is the maximum capture rate achieved at the saturation cross section.

Interestingly, a thermal Higgsino of 1.1 TeV mass, a largely unconstrained true electroweak WIMP [140]), would thermalize with just the NS crust rapidly enough to heat a reasonably old NS through annihilations in equilibrium with the rate of capture [48]. We also remark that due to different scalings of the NS luminosity from kinetic or annihilation heating on the NS mass and radius, in principle it must be possible to distinguish between the two heating mechanisms using an ensemble of NSs [174, 45].

An interesting way to probe DM self-annihilations in NSs is possible if the primary annihilation products are feebly interacting DM-SM mediators that live long enough to exit the star before decaying to SM states. One could search for a flux of these states sourced by DM “focused” in celestial bodies via capture. For gamma-ray final states, limits have been imposed with Fermi and H.E.S.S. data on DM-nucleon scattering and DM self-annihilation cross sections using brown dwarfs for sub-GeV DM and NSs for TeV mass DM [126]. For neutrino final states, limits in the TeV-PeV range come from IceCube, KM3NeT and ANTARES [202, 203].

Dark matter species that carry negative baryon number, arising for instance from “hylogenesis” models, could annihilate with baryons in a NS post-capture leading to possibly observable heating signals [204, 205, 206]. Such co-annihilations with nucleons are also possible in models of “dark baryons” that undergo quantum mixing with the neutron [207]. Yet another co-annihilation-like scenario resulting in NS heating is when a component of the DM comes in the form of magnetically charged black holes (MBHs) [208]. Subspecies that come with electroweak-symmetric coronas are expected to be near-extremal in mass, however upon encountering NSs they may become non-extremal: first they may capture in the NS by stopping due to the Fermi-degenerate gas, then they could absorb nucleons that are emitted back as (baryon number-violating) Hawking radiation, overheating NSs. A smaller deposit of heat could come from mergers of captured MBHs that enhance Hawking radiation, mimicking a self-annihilation process. Energy depositions from DM annihilations may also possibly nucleate quark matter bubbles in the NS interior, resulting in emission of radiation, cosmic rays and gravitational waves [209].

The production of x-rays and other high-energy effluents emitted from NSs, resulting from monopoles passing through and catalyzing nucleon decay, have been studied [210, 211]. This provides a strong bound on the abundance of monopole species that induce nucleon decay, which is a well-motivated class of monopoles arising from symmetry-breaking in Grand Unified Theories.

#### 4.1.3. Improvements and uncertainties

The above treatment has been improved by accounting for a number of physical effects in the NS, which in some cases leads to observational uncertainties; these effects are collected in Table 1. The largest uncertainty in the capture rate, spanning two orders of magnitude, comes from the unknown mass of the NS candidate that will be observed [169], unless some precise mass-radius measurement is performed. Other effects that may modify the DM capture rate, applicable to different DM and NS mass ranges, are variations in the EoS of NS matter, self-energies from the nuclear potential, nucleon structure that suppresses coherent scattering, nucleon superfluidity, extinction in the NS in the optically thick regime, scattering on relativistic nucleons, gravitational focusing in the NS interior layers, suppression of scattering via the propagator of a mediator of mass smaller than the transfer momentum, and the Galactic velocity distribution of DM. Table 1 lists the appropriate references that treat these effects.

#### 4.1.4. Dark matter models that heat neutron stars through scattering and annihilation

Making use of the general effects discussed above, specific UV-complete and self-consistent DM models have been explored in the context of NS capture and heating. These include the supersymmetric partner of the Higgs field, the Higgsino, that captures through inelastic scattering to electrically neutral and charged excited states [174, 48], a generalization of this to electroweak multiplets [213], a model of DM with a vector force-carrier of a gauged  $L_\mu - L_\tau$  interaction [191], DM in the form of a GeV-scale “dark baryon” that mixes with the neutron [207], simplified models of DM (specifying a single state each for DM and the mediator) with various mediator species [214, 215, 216], DM that arises as a pseudo-Goldstone boson [217], models of dark sectors that can explain the muon  $g - 2$  anomaly [218], and consistent models of DM interacting with nucleons through a pseudoscalar mediator: axion-like particles and a CP-odd state that arises in a Two-Higgs doublet model [195]. The sensitivities to parameters of some of these scenarios are shown in Fig. 10.

#### 4.1.5. Neutron star reheating mechanisms not involving dark matter

A search for DM reheating NSs in the late stages of their cooling must encompass understanding other astrophysical mechanisms that could possibly do the same. We discuss below those that feature prominently in the literature.

1. DM capture in NSs would not encounter a “neutrino floor” due to very dilute ambient neutrino densities that produce suppressed recoils/absorption on NS constituents, owing to low cross sections and Pauli-blocking. However, it is natural to ask if there is an “ISM floor” from accretion of interstellar material. It turns out that old, isolated NSs that have spin periods  $< 1000$  seconds do not accrete ISM as they are in an *ejector phase* [219]: a “pulsar wind” of ISM outflow powered by the NS’ magnetic field, being much denser than the inflowing material attempting accretion, would pre-empt accretion via kinetic pressure. Even if the pulsar wind happens to be weak enough for the ISM to overcome it, there is a second barrier to accretion: the magnetosphere co-rotating with the NS will impart centrifugal acceleration to the ISM, spraying away the gas – the *propellor phase*. For NSs with unusually large spin periods of  $> 1000$  seconds, these arguments do not apply, instead infalling ISM would be deflected along the magnetic field lines of the NS and accretion will be confined to a small polar region, which can be distinguished from all-surface thermal emission. In any case, the ISM density in the local 100 pc is  $10^{-3}$  GeV/cm<sup>3</sup> [220] so that any ISM accretion will be outdone by present-day DM capture near geometric cross sections.

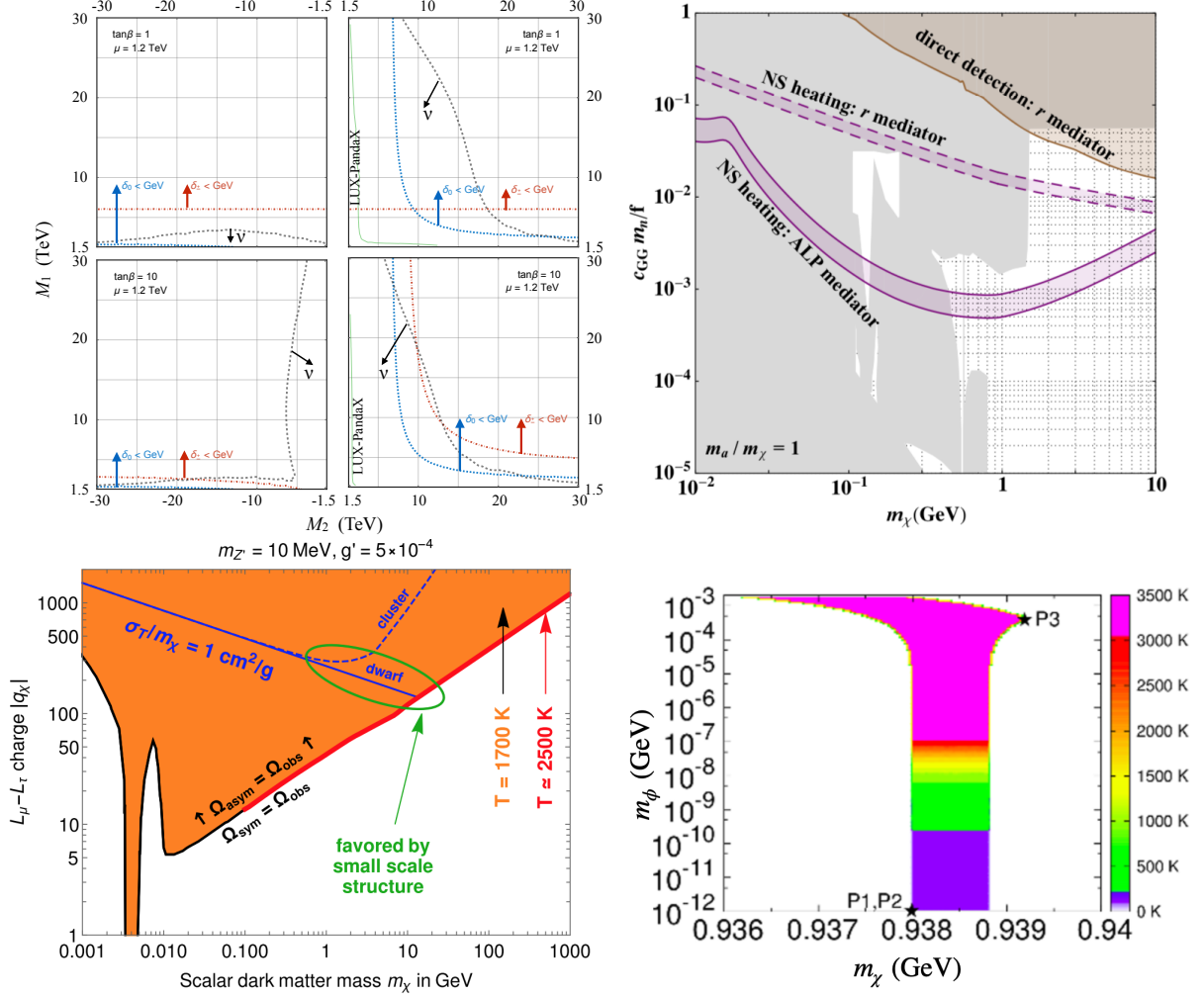


Figure 10: Sensitivities of self-consistent dark matter models to NS kinetic heating; see Sec. 4.1.4. **Top left.** [174] Electroweakino singlet and doublet mass parameters for various  $\tan\beta \equiv$  ratio of Higgs VEVs, that may be cornered through inelastic scattering of thermal Higgsino DM in the NS via excitation to charged and neutral states (regions marked by “ $\delta < \text{GeV}$ ”). **Top right.** [195] As a function of DM mass, gluonic coupling to an axion-like particle that mediates velocity-dependent scattering interactions. The gray region depicts limits from beam dumps, rare meson decays, and astrophysics. NS capture can also proceed through mediation by a CP-even scalar in the theory, which gives rise to limits from direct detection. **Bottom left.** [212] The orange region can be probed for spin-0 DM scattering on muons in the NS by exchanging a  $U(1)_{L_\mu-L_\tau}$  gauge boson. Also shown are constraints from DM self-interactions. **Bottom right.** [207] NS temperatures achieved by capture and heating of the anti-particle of DM carrying baryon number = 1, in a scenario where DM self-interacts repulsively and annihilates to the mediator  $\phi$  that then decays to SM states that deposit heat.

2. *Rotochemical heating* could result from an imbalance in chemical potentials as the NS material is driven out of beta chemical equilibrium by deceleration in the rotation of NSs. Reactions that seek to restore chemical equilibrium deposit heat in the NS. This mechanism could occur for NSs with small (sub-7 ms) pulsar spin periods at birth for certain nucleon pairing models [221] – a requirement in tension with studies that find that natal spin periods are likely  $\mathcal{O}(10 - 100)$  ms (see the references listed in Ref. [222]).
3. Other astrophysical late-time NS reheating mechanisms include [223, 224] *magnetic field decay* that dissipates energy into the NS material, *crust cracking* which arises when the NS crust breaks as the NS relaxes from an oblate to spherical shape, releasing accumulated strain energy, and *vortex creep* which develops as superfluid vortex lines travel outward as the NS spins down, and get pinned to the nuclear lattice in the inner crust thereby introducing a velocity difference between the crust and the superfluid core, which dissipates energy in the star.

We note that these mechanisms are speculative, and none have been unequivocally observed. An exclusion set by non-observation of DM-induced heating at imminent telescopes would also rule out these mechanisms. Another notable point is that while the rotational power of NSs goes into dipole radiation, which in turn illuminates the nebula surrounding the pulsar as we saw in Sec. 2.8, it very likely does not contribute to the NS thermal luminosity. This is already apparent in the Crab Nebula example discussed in Sec. 2.8, but can also be inferred from x-ray emission bounds on observed pulsars which have thermal luminosities 5-6 orders smaller than the rotational power: see Table 5 of Ref. [225]. Further, the diffusion of the  $B$  field in the NS is also unlikely to heat the NS; as argued in Ref. [226], NSs older than about Myr are cool enough for magnetic diffusion timescales to exceed the NS age, effectively shutting off  $B$  field dissipation regardless of the initial strength of the field.

#### 4.2. Neutron stars and halo substructure

Numerous cosmologies predict enhanced small-scale power, for instance via an early matter-dominated era or DM self-interactions assisting primordial density perturbations, resulting in a substantial fraction of DM surviving in substructure termed variously as clumps, subhalos, minihalos and miniclusters [228, 229, 230, 231, 232, 233, 234, 235]. If DM has scattering interactions with the SM, and if the interacting component resides in clumps, direct searches may have observed no conclusive signal simply because the Earth has yet to encounter a subhalo since their inception. In this scenario, subhalo DM may be observed by its heating of old, nearby NSs: the latter may travel through DM clumps and capture constituent DM particles, giving rise to kinetic and/or annihilation heating.

In the top left panel of Fig. 11, taken from Ref. [164], is shown the cooling time of NSs as a function of the NS surface temperature in green, and in the same plot is shown the energy deposited by clumps in NSs during encounters,  $E_{\text{meet}}^T$ , as a function of the time between NS-clump encounters for various clump sizes. The  $E_{\text{meet}}^T$  in the top x-axis correspond to the NS temperatures imparted in the bottom x-axis immediately following the encounter. For encounter times shorter than cooling times, the NS will glow at a steady-state luminosity, whereas for those longer than cooling times, NSs would be expected to glow brightly for short durations following encounters before dimming. In the latter case, sky surveys of large populations of NSs may be able to pick out the fraction that is still above some temperature to which the telescope is sensitive. In the top right panel, also taken from Ref. [164], are shown clump mass vs radius regions that may be discovered by observing more than 100 NSs above  $10^4$  K in the local kiloparsec, e.g., by Roman/WFIRST and Rubin/LSST, and excluded by observing a single NS with temperature  $< 1000$  K, e.g. by JWST, ELT and TMT. Also shown is a region that is already excluded by the observation of the coldest ( $< 30,000$  K)

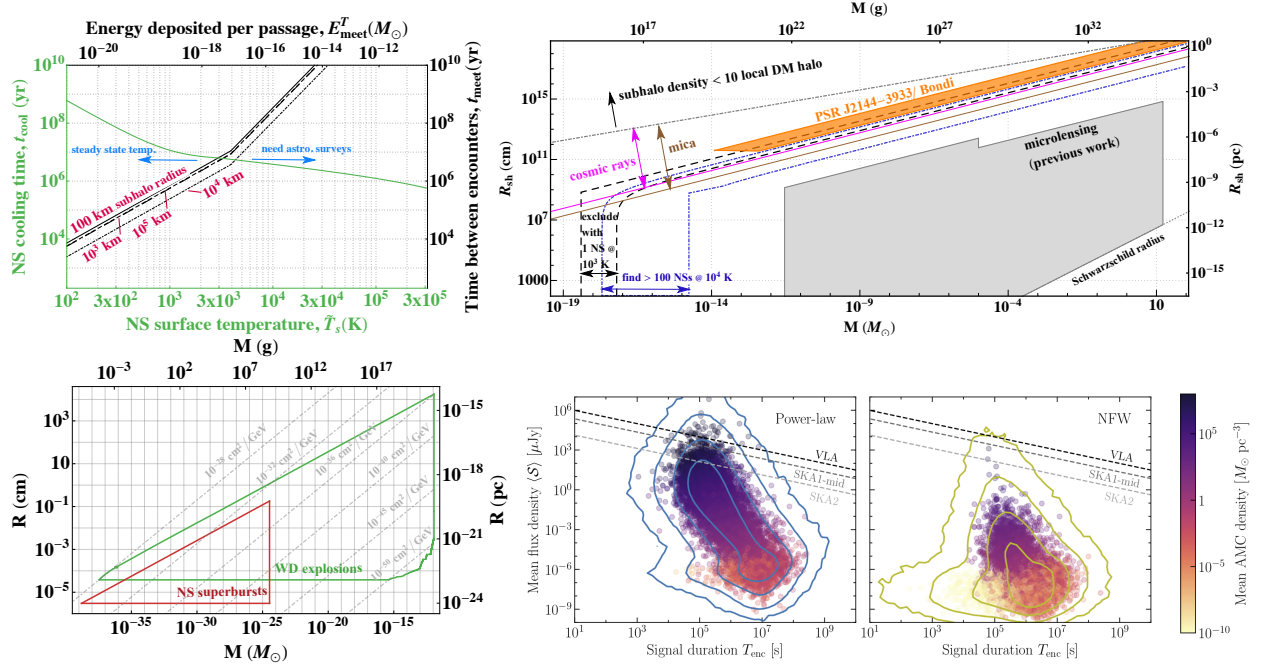


Figure 11: **Top**. NS cooling timescale versus surface temperature (obtained from Eq. (30)), superimposed on a plot of time between DM clump-NS encounters versus the energy deposited by kinetic heating during the passage of a clump for various NS radii (*left*). The ticks on either x-axis and either y-axis correspond one-to-one to each other. This plot shows the region in which NSs are expected to glow at a steady temperature, so that observing a single NS is enough to set constraints, and the region where overheated NSs cool down rapidly between clump encounters, so that astronomical surveys are required to observe the fraction of overheated NSs in an ensemble. On the *right* are future sensitivities of astronomical observations of NSs on DM clump radii and masses, exploiting dark kinetic heating, seen to be complementary to limits from other experiments. These limits are valid for DM-nucleon cross sections greater than the values for which the effects in these searches are relevant. These two plots are taken from Ref. [164]; see Sec.4.2 for further details. **Bottom left** Dark clump masses and radii constrained by compact stellar thermonuclear explosions, occurring for the minimum DM-nucleus cross sections per DM mass overlaid; see Sec.4.2. **Bottom right**. For two different internal density profiles, the mean flux density of transient radio signals at various telescopes from encounters of axion miniclusters as a function of the transit time (= signal burst duration), taken from Ref. [227]. See Ref. 4.11 for further details.



known NS PSR J2144–3933 by the Hubble Space Telescope (HST) [236] for clumps made of dissipative or strongly self-interacting DM, which would accrete onto NSs through the Bondi–Hoyle–Lyttleton mechanism [237, 238, 239].

In addition, in the presence of a long-range fifth force, NS heating by clumps may be enhanced by greater focusing effects, greater DM kinetic energies upon arrival at the NS surface, and seismic oscillations induced by an effective tidal force. In the bottom right panel of Fig. 16, taken from Ref. [240], is shown the limit from overheating PSR J2144–3933 on the effective NS-clump coupling versus clump mass, for four values of the range of the fifth force arising from a Yukawa potential [241]. (We do note that the DM need not be in the form of a clump for these limits to apply, but could also be a tightly bound composite.) The curve labelled “NS kinetic heating” corresponds to having an additional short-range interaction enhance DM capture. These limits are complementary to those coming from the Bullet Cluster on DM self-interactions mediated by the light mediator, from weak equivalence principle tests using Galacto-centric motions of celestial bodies on the inter-baryonic force mediated by the same, and from the 15 year dataset of the NANOGrav pulsar timing array (see also Sec. 4.10.1).

Yet another signature of clumps with nucleon scattering interactions is thermonuclear explosions induced in compact stars, as discussed in Sec. 3.3. These could be Type Ia-like supernovae in carbon-oxygen WDs or x-ray superbursts in the carbon ocean layer in NS crusts (Sec. 2.5). Constraints from the observed frequency of NS superbursts (Sec. 4.3) and from the existence of WDs (Sec. 3.3) are shown in the left bottom panel of Fig. 11 in the plane of clump size and mass; the contours overlaid are the minimum reduced nuclear cross sections required to ignite a trigger mass of the stellar material. This method of constraining clumps could be extended to those with baryonic long-range forces discussed above. In that case, limits on the effective coupling apply to far smaller values (all the way to unity) than shown in Fig. 16 bottom right panel, and to much higher clump masses. See Ref. [153].

Clumps encountering NSs can also be made of axions, leading to interesting signatures depicted in the right bottom right panel of Fig. 11, which we discuss in Sec. 4.11. We also note that the phenomenology of black hole formation inside NSs (Sec. 4.4) would be applicable here if NS-clump encounters are frequent enough.

#### 4.3. Dark matter inducing superbursts in neutron stars

Superbursts in NS carbon oceans, described in Sec. 2.5, can be induced by transiting DM if it is sufficiently heavy to deposit the requisite trigger energy. Ref. [152] set limits on the cross sections and (super-Planckian) masses of macroscopic DM opaque to nuclei by satisfying the runaway criteria (Eqs. (16) and (18)) and requiring that the time between DM-NS encounters is smaller than the inferred maximum recurrence time of the superburst 4U 1820+30. Ref. [153] set limits on the masses, radii and interaction strengths of dark clumps (shown in Fig. 11 bottom left panel) and nuggets with long-range baryonic forces, using inferred recurrence times of the six superbursts (out of 16 detected in total) that have been observed to repeat [82, 83].

#### 4.4. Dark matter that implodes neutron stars into black holes

Dark matter that is captured by an NS, after repeated re-scattering with the NS medium, will settle into a small thermalized region at the center of the NS. As more DM is collected, this spherical agglomeration can grow to a large enough mass that it collapses and forms a small black hole, which may (depending on its mass) subsequently accrete the entirety of the NS, transforming it into a solar mass black hole [11]. The processes of DM capture in NSs, thermalization, accumulation to the point of collapse, collapse, formation

of a black hole, and its possible evaporation via Hawking radiation or growth consuming the NS, have been investigated in Refs. [242, 184, 118, 200, 243, 244, 245, 246, 247, 248, 249, 85, 250, 251, 252, 253, 254, 148, 141, 255, 256, 257, 258, 143, 150, 259, 260, 261]. In addition, possible astrophysical signatures of DM converting NSs to black holes have been identified in, *e.g.*, Refs. [249, 262, 251, 252].

The kind of DM that is by and large studied in this context is “asymmetric dark matter”, DM primarily made of its *particles* as opposed to a symmetric population of *particles and anti-particles*. This emulates the visible universe, which is primarily matter (electrons, nucleons) and not anti-matter; indeed, the asymmetry in DM may be linked to that of the visible sector [142, 263], but this is not necessary for the discussion that follows. The primary feature that permits asymmetric DM to convert NSs into black holes is that it is typically<sup>7</sup> non-annihilating, and so as it collects inside the NS, it is not expected to annihilate to Standard Model states. This may be compared with symmetric, annihilating DM discussed in Sec. 4.1.2. Investigation into what fraction of the DM may self-annihilate or co-annihilate with nucleons, while still forming a black hole inside the NS, was undertaken in Refs. [247, 248, 265].

Another kind of DM which could convert NSs into black holes is primordial black holes [266, 267]. A PBH captured in an NS can settle inside, accrete NS material, and convert the NS into another black hole [268, 269, 270, 271, 272, 251, 273, 274, 275, 145, 276, 277, 278]; this is detailed in Section 4.5. For the remainder of this sub-section we will focus on particle DM.

We now turn to details of the processes leading asymmetric dark matter to convert NSs into black holes. They proceed as follows: (1) DM is captured in the NS and thermalizes with the NS interior, forming a small ball of DM at the center, (2) the DM ball reaches a critical mass at which it collapses, and through some cooling process continues to collapse until (3) a small black hole forms which, provided accretion of NS material outstrips Hawking radiation, will result in the conversion of the NS to a black hole. Figure 12 left panel shows a simple schematic of this process.

#### 4.4.1. Dark matter thermalization in neutron stars

In step (1) above, the size of the thermalized region is determined by the temperature of the NS, which sets the final temperature of the DM particles, and by the central density of the NS, which sets the gravitational potential binding energy. A simple application of the virial theorem yields an estimated DM thermal radius of [247]

$$r_{\text{th}} \approx 20 \text{ cm} \left( \frac{\text{GeV}}{m_\chi} \right)^{1/2} \left( \frac{T_{\text{NS}}}{10^3 \text{ K}} \right)^{1/2} \left( \frac{10^{15} \text{ g/cm}^3}{\rho_{\text{NSc}}} \right)^{1/2}, \quad (52)$$

where  $\rho_{\text{NSc}}$  is the NS central density. The time it takes for DM to sink to this region depends on a few timescales (see *e.g.*, Ref. [143], Section 3 for a review), but usually the longest is the time it takes for DM to scatter with its lowest velocities/temperatures on nucleons, after having mostly settled inside the NS. A detailed calculation of this timescale requires modeling the NS core, and so the result will depend on the density, degeneracy, and possibly even new QCD phases in the NS interior. For neutrons treated as a degenerate fluid, we have [189]

$$t_{\text{th}} \approx 3000 \text{ yr} \frac{\frac{m_\chi}{m_n}}{\left(1 + \frac{m_\chi}{m_n}\right)^2} \left( \frac{2 \times 10^{-45} \text{ cm}^2}{\sigma_{n\chi}} \right) \left( \frac{T_{\text{NS}}}{10^5 \text{ K}} \right)^2, \quad (53)$$

where this expression assumes a momentum-independent cross section for spin-1/2 DM scattering on nucleons via a heavy mediator. Extensions to spin-0 DM, Lorentz structures of DM-nucleon interactions leading

---

<sup>7</sup>For the exception, see Ref. [264].



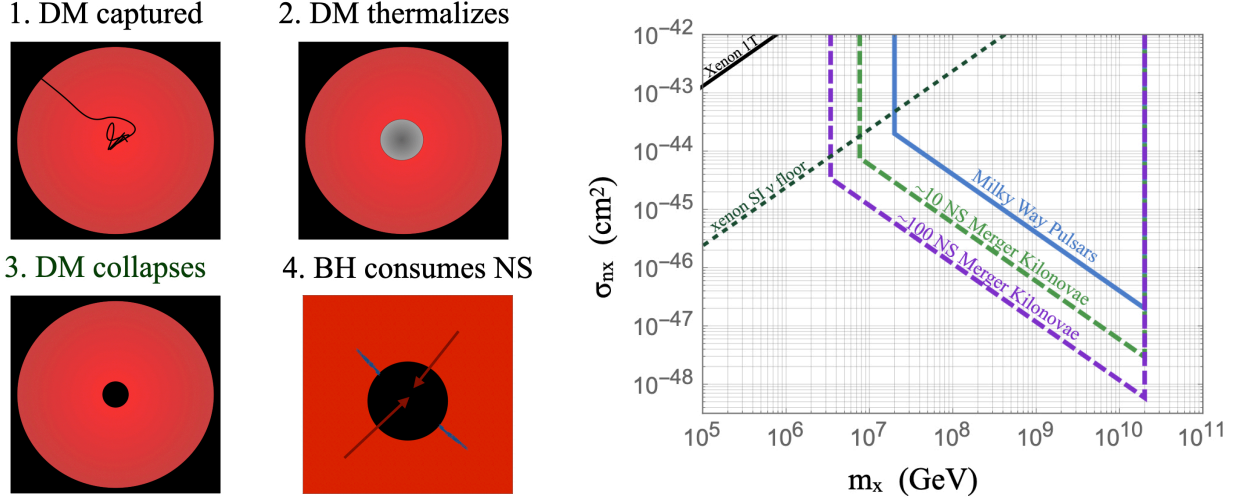


Figure 12: **Left.** Schematic of asymmetric dark matter converting a NS into a black hole. **Right.** Dark matter per-nucleon scattering cross section versus mass bounds on heavy fermionic asymmetric dark matter from the observation of old Milky Way pulsars that have not been converted to black holes [251], compared with terrestrial direct search limits and their neutrino floor. Also shown are prospects for observing NS mergers with accompanying kilonovae, localized to 1 kpc precision inside Milky Way-like spiral galaxies. A detailed discussion of Milky Way pulsar ages, and in particular PSR J1738+0333, which has a characteristic age confirmed by the age of its WD companion, can be found in Ref. [279].

to momentum-dependent cross sections, and light mediators were investigated in Ref. [194]. In the above expression, the thermalization timescale counter-intuitively *decreases* with increasing DM mass above  $m_n$ : one would naively expect that heavier DM takes *longer* to thermalize. But the effect comes about because  $t_{\text{th}}$  is set by the inverse of the energy loss rate (in turn depending on the DM-nucleon scattering rate) in the NS degenerate medium with phase space restrictions, and this rate goes as positive powers of the (continually degrading) DM momentum  $k_{\text{cold}}$ . For DM energies close to the NS temperature,  $k_{\text{cold}} \simeq \sqrt{3m_\chi T_{\text{NS}}}$ , implying energy is lost faster in the last few scatters for heavier DM, i.e., implying quicker thermalization. In Figure 13 we show the per-nucleon cross section or effective field theory coupling necessary for DM to thermalize inside an NS on 10 Gyr year timescales for certain models.

As discussed in Sec. 4.1.2, depending on the DM annihilation cross section, thermalized DM collected within  $r_{\text{th}}$  can annihilate efficiently enough to yield interesting signals.

#### 4.4.2. Collapse of dark matter and formation of small black hole

In step (2), after enough DM has collected in the thermalized region in the NS, it will reach a critical mass at which it collapses. The exact density of DM required to initiate collapse will depend on its self-interactions, and by extension its EoS and sound speed while contained in the NS. Assuming negligible self-interactions, the critical mass required for collapse is

$$M_{\text{crit}} \approx 7 \times 10^{46} \text{ GeV} \left( \frac{10^7 \text{ GeV}}{m_\chi} \right)^{3/2} \left( \frac{T_{\text{NS}}}{10^3 \text{ K}} \right)^{3/2} \left( \frac{10^{15} \text{ g/cm}^3}{\rho_{\text{NSc}}} \right)^{1/2}. \quad (54)$$

For a detailed review of the conditions for collapse see *e.g.*, Section 4 of [143]. It is generally the case that if DM thermalizes rapidly through scattering with neutrons in the NS interior, then when it reaches the point of collapse it will also rapidly shed the gravitational energy required to form a black hole. This is because the temperature is higher during collapse and hence the time to shed gravitational energy is

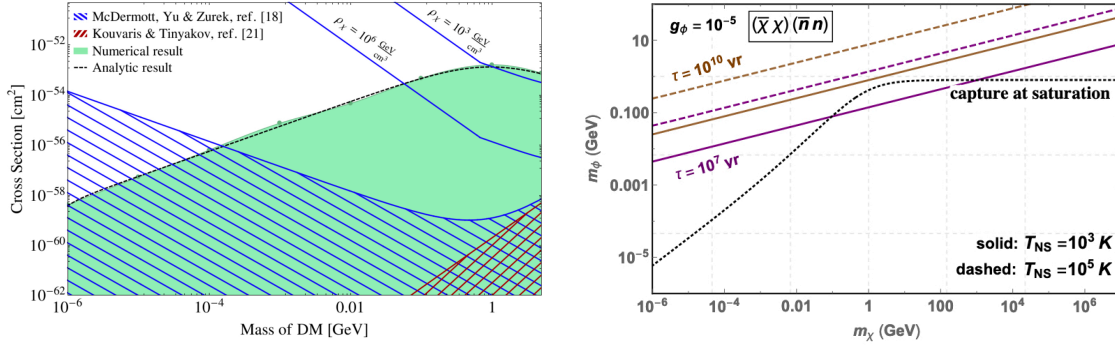


Figure 13: **Left.** [189] Cross section for dark matter to thermalize in a neutron star in 10 billion years, assuming a momentum-independent cross section with neutrons. **Right.** [194] The case of scattering on neutrons through the scalar current operator indicated in the figure with mediator mass  $m_\phi$ . Thermalization in 10 Myr and 10 Gyr for different NS temperatures, and a curve indicating parameters that lead to DM capture in the NS through geometric cross sections, are shown.

typically shorter. As the shortness of this timeframe is common, this part of the collapse dynamics is not always treated explicitly, but Refs. [85, 143, 148, 11] provide more detailed treatment, both in compact stars and other astrophysical bodies. The time for the DM sphere to collapse below its Schwarzschild radius will depend on whether it cools via scattering with neutrons or through other radiative process, *e.g.*, emission of a light particle in the dark sector [85].

An additional consideration is whether enough DM will have collected to exceed the dark sector Chandrasekhar mass (analogous to Eq. (7)), parametrically of order

$$M_{\text{Chand,f}} \approx \frac{M_{\text{Pl}}^3}{m_\chi^2} \approx M_\odot \left( \frac{\text{GeV}^2}{m_\chi^2} \right), \quad (55)$$

while for bosons this is

$$M_{\text{Chand,b}} \approx \frac{2M_{\text{Pl}}^2}{m_\chi} \left( 1 + \frac{\lambda}{32\pi} \frac{m_{\text{pl}}^2}{m_\chi^2} \right)^{1/2} \rightarrow \begin{cases} 2 \frac{M_{\text{Pl}}^2}{m_\chi}, & \lambda \ll 1, \\ \frac{\lambda}{2\sqrt{2}} \frac{M_{\text{Pl}}^3}{m_\chi^2}, & \lambda > 100 m_\chi / M_{\text{Pl}}, \end{cases} \quad (56)$$

where  $\lambda$  is the boson  $\phi$ 's repulsive self-interaction coupling arising in the Lagrangian  $\mathcal{L} \supset -(\lambda/4!) \phi^4$ .

Attractive DM self-interactions could alter the amount of asymmetric fermionic DM necessary for collapse to a black hole [246, 265, 279]. The collapse of light fermionic DM is in principle permitted by the attractive self-interaction mediated by a light scalar, however, a detailed study of the final stage collapse to a black hole has pointed out an important caveat [280]: for a simple scalar field potential consisting only of a mass term and a coupling to the fermions, the effective mass of the scalar could grow during DM fermion collapse, preventing collapse to a black hole. Whether bosonic self-interactions let DM form black holes in NSs is a non-trivial question. In particular, a large value of  $\lambda$  can shift bosonic asymmetric DM bounds from old NSs to higher DM masses [245, 247, 248]. Bosonic asymmetric DM forming black holes inside a NS do so by forming a Bose-Einstein condensate (BEC) [245, 244, 281, 247, 248, 252], from which collapse will proceed for GeV-mass DM. The dynamics of the BEC prior to and following collapse would affect whether a black hole is produced and is an area of investigation [281, 247, 248, 252, 282].

#### 4.4.3. Growth or evaporation of dark matter-formed black hole in the neutron star

After a black hole is formed inside the NS, step (3) is to determine whether it is so small that it will rapidly evaporate away via Hawking radiation, or whether it is so large that through accumulating surrounding baryonic material it will grow to consume the NS in a relatively short timeframe. Initial studies of this process estimated whether Bondi accretion by the black hole would proceed faster than Hawking radiation, which is entirely determined by the initial mass of the black hole [245, 244]. Later studies incorporated the accumulation of DM particles additionally collected into the NS and onto the black hole, finding that this can substantially influence whether the black hole would grow to consume the NS [247, 248, 265].

Altogether, the requirement that the black hole grows in the NS is given by

$$\dot{M}^{(\text{NS accretion})} + \dot{M}^{(\text{DM accretion})} - \dot{M}^{(\text{Hawking})} > 0, \quad (57)$$

where the first term is the NS accretion rate onto the black hole, the second is the DM accretion rate onto the black hole, and the third is the Hawking radiation rate. Each of these terms has been individually studied in the context of asymmetric DM which causes NSs to implode:

1. *NS accretion*: The simplest treatment of NS accretion onto the black hole assumes Bondi accretion. In practice, angular momentum of the NS fluid around the black hole, for a rapidly spinning NS, can diminish accretion relative to naïve Bondi accretion, but the high viscosity of the NS fluid results in infall rates consistent with spherical Bondi accretion despite angular momentum effects [283]. Sufficiently small black holes will have a quantum penalty to accumulation of neutrons due to the neutron de Broglie wavelength; this effect can be pronounced for black hole masses near the edge of growth vs. evaporation [260]. The accretion of the NS fluid onto the black hole inside a NS has been studied in a detailed simulation that accounts for hydrodynamic and general relativistic effects [255], finding that in the final stages of accretion, the mass of NS fluid ejected from the accretion zone is likely less than about  $10^{-4} M_{\odot}$ .
2. *DM accretion*: The accretion of DM onto the small black hole inside the NS can substantially affect whether it grows or shrinks, especially when the DM accretion rate onto the NS is maximized [247, 248, 265, 252].
3. *Hawking radiation*: There is a correction to the evaporation rate of black holes inside NSs, coming from the Pauli blocking of Hawking radiation, since the region around the black hole will be inhabited by a degenerate sea of SM fermions [284].

#### 4.4.4. Signatures of dark matter that implodes neutron stars

A number of striking astrophysical signatures arise from DM that converts NSs to black holes. Firstly, the oldest known pulsars can be used to set limits on asymmetric DM, since for a given background DM density, the existence of these pulsars limits the accumulation of DM [242, 243, 244, 245, 246, 247, 248, 249, 184, 200]. However, the “characteristic age” of pulsars comes with caveats: it is not always a good indicator of the actual age of the pulsar as discussed in Sec. 2.8. One particular pulsar, PSR J1738+0333, is in a binary system with an old WD, and thus to go with its characteristic age, has an additional age-marker in its WD companion, both of which point to a  $\gtrsim 5$  Gyr-old NS. Hence this pulsar has been used to set bounds on asymmetric DM [279, 251]. A recent work [285] integrates over the density of DM that NSs traverse during their orbits around the Milky Way, refining bounds that use characteristic ages of old, nearby pulsars.

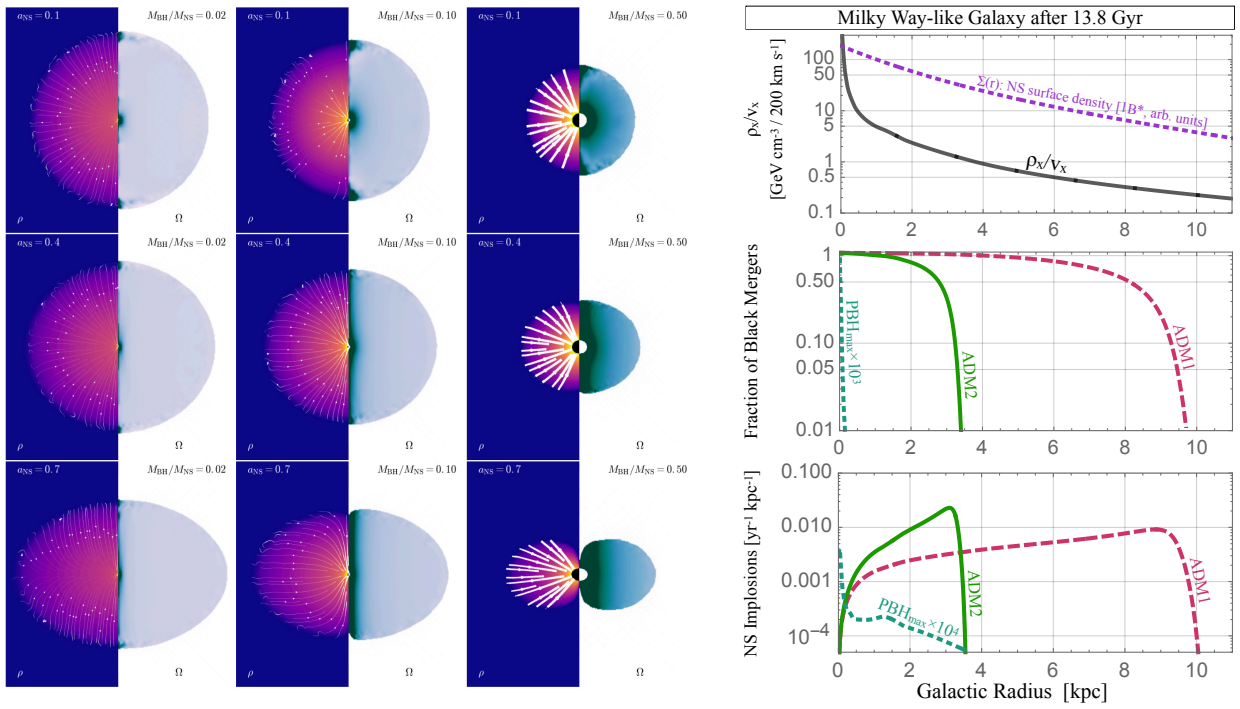


Figure 14: **Left.** From a simulation of a NS accreting onto a black hole at its center [255]. NS fluid density and velocity vectors are shown in the left half of these figures, with angular momentum density shown on the right half, for a different NS spin parameters  $\Omega$ . **Right.** Number of NSs converted to black holes in a Milky Way-like galaxy, along with the current NS implosion rate for dark matter models that would cause NSs near Earth to implode in 10 Gyr (“ADM1”) and 50 Gyr (“ADM2”) [251].

A number of prompt and delayed signatures may be sought if DM is converting Gyr-old NSs to black holes in regions where DM is denser than in the outer regions of the Milky Way. In particular, the absence of millisecond pulsars in the Galactic Center [286, 287] has been linked to models of DM that would convert old NSs to black holes [249, 200]. These studies predict a maximum pulsar age that increases with Galactocentric distance, corresponding to a decrease in the amount of DM accumulating in pulsars. It has been shown that collapsing NSs can shed their magnetospheres and emit a radio pulse about a millisecond in duration, and thus the implosion of pulsars via DM is a possible origin of non-repeating fast radio bursts (FRBs) [262]. The Galactic localization of FRBs sourced from DM-induced NS implosions could be used to confirm or limit this hypothesis [251]. Based on these estimates, approximately ten FRBs localized in Milky Way-equivalent galaxies would be required to differentiate between an FRB population sourced by DM-induced NS implosions and one that simply matches the NS distribution in these galaxies.

The implosion of NSs into black holes has also been explored as a source of  $r$ -process elements. NS fluid ejected during the implosion could undergo  $r$ -process enrichment, sourcing early  $r$ -process elements observed in ultra-faint dwarf spheroidal galaxies [250, 251].  $r$ -process enrichment has also been studied for rapidly spinning NSs and NSs that capture primordial black holes [288], along with associated high-energy events [273, 274]. However, the dynamics of ejecta from NS implosions later investigated in simulations [255, 276, 289] disfavor large amounts of NS material being ejected in any single NS implosion event. In particular, Ref. [255] found in their simulations that even maximally spinning NSs would eject less than  $10^{-4} M_{\odot}$  of their material during implosion. Recently, neutrinos produced during DM-induced NS implosions, and the prospects for detecting them as a diffuse background were studied [290].

Figure 14, from Ref. [255], shows a detailed simulation of the final stages of NS accretion onto a black hole in its interior, and the expected rate of these NS implosions in Milky Way-like galaxies for a generalized NS-implosion-DM framework laid out in Ref. [251]. Since the accumulated mass of DM onto NSs will be proportional to DM density and inversely proportional to the DM-NS relative velocity, one can parameterize how quickly particle DM will convert NSs into black holes:

$$\left(\frac{t_{\text{convert}}}{\text{Gyr}}\right)\left(\frac{\rho_{\chi}}{\text{GeV}/\text{cm}^3}\right)\left(\frac{200 \text{ km/s}}{v_{\chi}}\right) \lesssim 2, \quad (58)$$

where we have quoted the bound from Ref. [251] using the  $\gtrsim 5$  Gyr-old PSR J1738-0333.

Many additional pathways for discovering DM that implodes NSs arise from the population of solar mass black holes that would be created, which would reside preferentially in the centers of galaxies [251, 253]. The number of NS merger events with accompanying kilonovae required to increase sensitivity to these DM models was estimated for 10–100 kilonovae in Ref. [251]. As stated in that study, kilonovae would not occur following an apparent “neutron star merger” if both solar mass compact objects were black holes converted from NSs. The prospects of gravitational wave observatories like LIGO/VIRGO and their successors for finding a population of NSs converted to black holes have been detailed in Refs. [251, 253, 257, 256, 258, 156, 291]. The capability of future gravitational wave observatories to differentiate solar mass black hole mergers from solar mass NS mergers, depending on minute variations in the waveform just prior to the merger, was examined in Ref. [292], which noted that a large population of mergers may be needed to find evidence for a solar mass black hole population.

#### 4.5. Primordial black hole dark matter and neutron stars

Black holes could form in the infant universe through some mechanism producing sub-horizon overdensities, and for masses above  $5 \times 10^{14}$  g these “primordial black holes” do not evaporate away within the age of the universe [267, 266] – thus constituting non-baryonic dark matter. PBHs are constrained by



a number of phenomena they give rise to: evaporation, gravitational (micro)lensing, disruption of dwarf galaxies and wide binaries, gravitational waves, and accretion [266]. Wide-ranging as they are, these limits nevertheless leave open a mass window in which PBHs could make up all the DM: roughly  $10^{17} - 10^{22}$  g (or  $10^{-16} - 10^{-11} M_{\odot}$ ).

PBHs encountering NSs may capture through the energy loss mechanism of dynamical friction: the NS constituent particles absorb the momentum of the transiting PBH [293]. In this picture there are no collective excitations of the NS medium, as the PBH travels at supersonic speeds after being accelerated by the NS’ gravity. An alternative treatment of the energy loss is by considering oscillations of the NS medium excited by the passing PBH<sup>8</sup>, which seemingly extracts more energy from the PBH [294]. However, these approaches were shown to be equivalent by modelling the NS as a semi-infinite incompressible fluid [295]. All said and done, the captured PBH proceeds to grow via Bondi accretion of the NS material [293, 296, 297] (see Section 4.4 for additional considerations regarding black hole growth in NSs), eventually destroying the NS in a catastrophic event that emits telltale electromagnetic signals and gravitational waves [251, 275]. Collisions between PBHs and NSs may also explain fast radio bursts [262, 251, 298]. In the case that black holes are charged, their capture and consumption of the NS is treated differently [145], where specifically this work employed the capture rate for monopoles and a different accretion rate appropriate for extremal black holes. Finally, as mentioned in Sec. 4.1, magnetically charged black holes that may constitute DM could capture in NSs and heat them via Hawking radiation of absorbed nucleons.

#### 4.6. Neutron stars admixed with dark sectors

NSs that contain an appreciable fraction of exotic particle species could give rise to interesting observational signatures such as modified NS mass-radius relations and distinct gravitational wave signals. But to obtain such “admixed” NSs one cannot rely on their capture of ambient DM. One can see this immediately from Eq. (45): for an NS of age  $10 \text{ Gyr} \approx 3 \times 10^{17} \text{ s}$  in the solar vicinity, the total DM mass accumulated over its lifetime is only about  $5 \times 10^{-15} M_{\odot}$ . Thus other mechanisms must be in play, like a conversion of a large fraction of the NS’s interior to dark sector particles. We detail some such exotic DM accumulation mechanisms below.

##### 4.6.1. Impact on nuclear equation of state

Hidden GeV-mass states charged with baryon number  $B$  could explain the long-standing neutron lifetime puzzle [304] and take a crucial part in baryogenesis (see, *e.g.*, Refs. [305, 306]). One consequential species is the “**dark neutron**” with  $B = 1$  that can mix with the standard neutron, and could arise either as an elementary particle [304] or as a composite in, *e.g.*, mirror matter models [307]. The dark neutron could be cosmologically long-lived if its interactions with the visible sector are small enough, in which case it could constitute the dark matter of the universe. Dark neutrons  $\chi$  may be produced in NSs in neutron-nucleon scattering processes  $nN \rightarrow \chi N$  and neutron decay  $n \rightarrow \chi + \text{anything}$ . If the production of  $\chi$  occurs on timescales shorter than NS lifetimes, the  $\chi$  fluid that is in chemical equilibrium with the nucleonic fluid would generally soften the EoS of NS matter. Consequently, the maximum mass of these admixed NSs is reduced compared to standard NSs, giving rise to constraints on dark neutrons (or other dark sectors) from observations of high-mass NSs [299, 308, 309, 310, 311, 312, 313, 314]; see Figure 15 for representative limits. For related studies of millisecond pulsars and NSs as dark matter admixed quark stars, see Refs. [315, 316, 317]. In the case of neutron decay to dark neutrons, the above arguments regarding neutron decay also apply to a variation of the dark neutron  $\chi$  with  $B = 1/3$  such that it is produced in the NS via the

---

<sup>8</sup>This analysis was reused in Ref. [241] to treat the tidal heating of NSs by composite particulate DM.



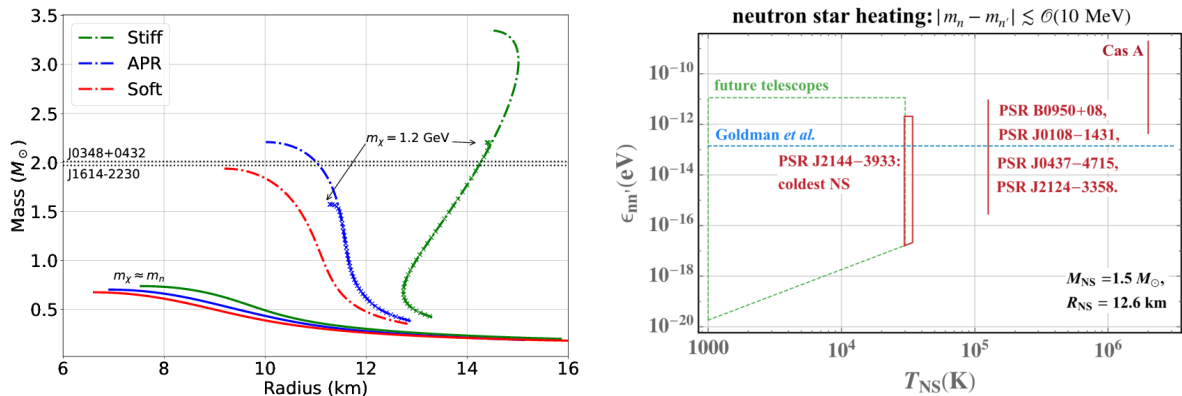


Figure 15: **Left.** Mass-radius relations of NSs admixed with a large population of dark baryons, taken from Ref. [299]. The presence of dark baryons without self-interactions softens the EoS, resulting in a maximum NS mass smaller than those observed above  $2 M_{\odot}$  (dashed horizontal lines). [Since the appearance of Ref. [299], an even heavier  $2.35 \pm 0.17 M_{\odot}$  NS has been observed [300].] Analogous constraints could apply to dibaryons/hexaquarks, a QCD bound state that could make up dark matter [301]. **Right.** Limits on the neutron mixing amplitude of dark/hidden/mirror neutrons from the heating of NSs via the “nucleon Auger effect”, taken from Ref. [302]. These are shown for NSs of various surface temperatures, with the ceiling for each set by the timescale of neutron-to-dark-neutron conversions being smaller than the NS age. While these limits are valid for neutron-dark neutron mass splittings of up to the NS nuclear self-energy  $\approx 10\text{--}100 \text{ MeV}$ , terrestrial limits from ultracold neutron facilities are only valid for mass splittings up to the Zeeman splitting from the Earth’s magnetic field, which is 19 decades smaller. Also shown is a weaker bound from Ref. [303] from NS mass loss due to neutron-to-dark-neutron conversions, measured with binary pulsar timing (Sec. 4.10.2). See Secs. 4.6.1 and 4.8 for further details.

decay  $n \rightarrow \chi\chi\chi$  [318]. These constraints can be evaded in models that introduce repulsive self-interactions between the dark neutrons, which would pre-empt the softening of the EoS [319, 320]. Admixed NSs also exhibit mass-radius relations that could span a 2-dimensional area rather than follow a 1-dimensional sequence [321]. Another interesting diagnostic of admixed NSs is the tidal Love number impacted by the formation of extended atmospheres [322, 323], and the second Love number [324]. This is measurable as a phase shift in a binary merger gravitational wave signal at the forthcoming Advanced LIGO and the third-generation observatories Einstein Telescope and Cosmic Explorer. Yet another diagnostic, stemming from the modification of NS mass-radius relations, is the NS pulse profile as measured by precision probes such as NICER [325]. In the case where the production of  $\chi$  takes longer than NS lifetimes, other effects come into play, chief among which is the overheating of NSs due to formation of holes in the nucleon Fermi sea; we review this in Section 4.8.

A **sexaquark/hexaquark** electrically neutral state  $uuddss$  that is elusive to accelerator searches has been proposed as a dark matter candidate [326]; to ensure nuclear stability and cosmological lifetimes for the hexaquark, its mass must lie between 1860–1890 MeV [327]. It was shown that due to rapid thermalization in the early universe, the hexaquark freezes out at an abundance of  $10^{-11}$  of the total baryon number, and can thus only be a minuscule relic [328]. Moreover, hexaquarks in this mass range would be produced within seconds of the birth of a proto-NS during a core-collapse supernova, and the energy released in this process would unbind the proto-NS, strongly disfavoring the existence of this state [301]. As the latter authors argue, even if the proto-NS somehow survives, since all baryons are converted rapidly to hexaquarks, the EoS of the resulting star would be softer than that of a standard NS, which would run afoul of observations of high NS masses as in the case of dark neutrons. Nevertheless, the latter limit may be satisfied if the NS undergoes early quark deconfinement such that hexaquarks are not present, or a later deconfinement that leaves a quark core inside a neutron-hexaquark shell [329].

#### 4.6.2. More admixed neutron stars

Further mechanisms to obtain NSs admixed with dark sectors have been proposed. In analogy with dark neutrons, spin-0 states  $\phi_\chi$  carrying baryon number may interact with the neutron via the vertex  $\mathcal{L} \supset y_{n\nu} n \phi_\chi \bar{\nu}$ , giving rise to  $n \rightarrow \nu \phi_\chi$  decays producing  $\phi_\chi$  that could constitute 1-10% of the NS mass [311]. In a different model with  $\mathcal{L} \supset y_{nn} n \phi_\chi \bar{n}$ , nucleon bremsstrahlung  $nn \rightarrow nn \phi_\chi$  could populate NSs with  $\phi_\chi$  for NS internal temperatures  $T_{\text{NS}}$  satisfying  $m_{\phi_\chi}/3 < T_{\text{NS}} \lesssim m_{\phi_\chi}/2$  [299, 311]. This condition is to ensure that neutron kinetic energies are sufficient to produce  $\phi_\chi$  while keeping the products from escaping the NS' gravity. For  $m_{\phi_\chi} = 100$  MeV one obtains percent-level NS mass fractions of  $\phi_\chi$ . Dark compact stars formed from a possibly dissipative dark sector [330, 331] could accrete surrounding baryonic matter to form admixed stars [311], though the exact mechanism required to obtain comparable amounts of exotica and nucleons in these structures is far from clear. One probe of admixed NSs orthogonal to EoS effects is the NS cooling curve [332]; in particular, sub-GeV DM that annihilates to neutrino final states and participating in the NS' thermal conduction could have an observable effect on NS cooling.

#### 4.7. Exotic compact stars

Dark baryons such as mirror neutrons may give rise not only to NSs admixed with them, but also to compact stars composed entirely of them. Such exotic “**mirror neutron stars**” may constitute an appreciable fraction of DM, providing smoking gun signatures in tidal deformability measurements from gravitational waves and binary pulsar observations [333, 321]. A mirror-like hidden sector may also give rise to **exotic white dwarfs** that can be detected using their mergers via gravitational waves [334]. In the presence of kinetic mixing between the photon and its hidden counterpart, mirror NSs may capture interstellar material and emit radiation observable at Gaia [335]. Mirror stars made of mirror anti-neutrons may grow a population of SM anti-matter in their cores which can accrete ISM and produce radiation observable at Fermi-LAT [336].

Analogously, asymmetric DM with large self-interactions could form **dark compact stars** [337] that could capture ISM protons and electrons which consequently sink to the core and form a hot radiative gas, observable in telescopes as X-ray or gamma-ray point sources [338]. Other exotic compact objects with near-Schwarzschild compactness may exist and constitute DM, *e.g.*, some classes of **boson stars**, **Q-balls**, **non-topological solitons**, and **ultra-compact minihalos**. For reviews see Ref. [339, 340, 341, 342].

In the vein of a first-order QCD phase transition giving rise to expanding bubbles of the low-temperature phase compressing regions of the high-temperature phase into dense quark nuggets [343], an excess of “dark quarks” charged under a confining gauge group and residing in a false vacuum may be compressed by the true vacuum of a first-order transition [344]. In the case of fermionic dark quarks heavier than the confinement scale, this process can lead to compact “**dark dwarf**” stars supported by Fermi degeneracy pressure *à la* WDs [345]. The compression may even go on to form primordial black holes, which is the only end state for bosonic dark quarks.

#### 4.8. Dark sectors leading to internal heating of neutron stars

In Sec. 4.6 we mentioned that neutron scattering and decay processes producing dark baryons  $n'$  occurring within the lifetime of the NS would give rise to dark neutron-admixed NSs. The two-state Hamiltonian for the  $|n\rangle$ - $|n'\rangle$  system with  $m_n \simeq m_{n'}$  and mixing amplitude  $\epsilon_{nn'}$  is

$$H = \begin{pmatrix} m_n + \Delta E & \epsilon_{nn'} \\ \epsilon_{nn'} & m_{n'} \end{pmatrix}, \quad (59)$$

where  $\Delta E$  is the medium-dependent energy splitting. The dominant channel of  $n'$  production is neutron-nucleon scattering,  $nN \rightarrow n'N$ , with cross section [302]

$$\sigma_{n'N} \simeq g_N \left( \frac{\epsilon_{nn'}}{\Delta E} \right)^2 \sigma_{nN \rightarrow nN}, \quad (60)$$

where  $\sigma_{nN \rightarrow nN}$  is the neutron-nucleon cross section determined experimentally,  $g_n(g_p) = 2(1)$  is a multiplicity factor, and  $\epsilon_{nn'}/\Delta E$  an effective in-medium  $n$ - $n'$  mixing angle. The typical rate of  $n'$  production in an NS may then be computed from the above as

$$\Gamma_{n'} = \frac{1}{10^7 \text{ yr}} \left( \frac{\epsilon_{nn'}}{10^{-15} \text{ eV}} \right)^2 \left( \frac{n_{\text{nuc}}}{0.3 \text{ fm}^{-3}} \right), \quad (61)$$

for a total nucleon density  $n_{\text{nuc}}$ .

If the timescale of  $n'$  production  $\Gamma_{n'}^{-1}$  exceeds NS lifetimes, which typically occurs in parametric regions where  $n'$  also constitutes (the cosmologically long-lived) DM, it would give rise to NS overheating via the ‘‘nucleon Auger effect’’ discussed in the context of DM capture in Sec. 4.1.1. When nucleons leave behind holes in their Fermi seas, through either conversion to  $\chi$  or upscattering, higher-energy ambient nucleons rapidly fill them in, in the process liberating heat in the form of electromagnetic and kinetic energy. The total power liberated by  $n \rightarrow n'$  conversions in the NS is [302]

$$L_{n \rightarrow n'} = \int d^3r n_n(\mathbf{r}) \dot{E}_{n'}(\mathbf{r}), \quad \text{with } \dot{E}_{n'} = \sum_{N=n,p} f_{NN} n_N \left\langle \left( \tilde{\mu}_n - \frac{p_{n'}^2}{2m_{n'}} \right) \sigma_{n'NV} \right\rangle_{p_N > p_{F_N}}, \quad (62)$$

where the subscript in the second equation denotes the inclusion only of scattering events that result in spectator nucleons kicked above their Fermi sea.

This effect arrests the passive cooling of NSs, and very stringent constraints on dark neutrons [346, 302] may be placed using HST observations of the coldest ( $< 30,000$  K) observed pulsar PSR J2144–3933 [236]. The reach on the mixing between neutrons and dark neutrons could be further extended with present and forthcoming ultraviolet, optical and infrared campaigns suited to observe colder NSs: LUVUOIR [347], Rubin [348, 349], DES [350], Roman [351], JWST [177], TMT [175], and ELT [176]. This is depicted in the right panel of Fig. 15 in the plane of the off-diagonal mass or transition amplitude versus the surface temperature of various NSs. The ceiling for these limits arises from the fact that the nucleon Auger effect is effectively non-existent if the timescale of dark neutron production is smaller than the NS age, in which case the Fermi sea of the dark neutron is filled up and thus neutron conversion is Pauli-blocked. It must also be noted that these limits apply to dark neutron masses in excess of the neutron mass (939.6 MeV) by 10–100 MeV, the values of neutron self-energies from the nuclear potential of the NS medium that effectively raise  $m_n$ . Above this mass conversions of neutrons to dark neutrons are kinematically suppressed.

One scenario in which the above limits may be weakened is when the dark neutron arises as a mirror equivalent of the neutron in mirror world theories, with exact mass degeneracies [352]. In this case, mirror electrons produced via mirror beta decay could take away heat by scattering with electrons via a millicharge, and emit mirror bremsstrahlung via mirror photons. Internal heating of NSs can also occur by baryon number-violating neutron decays, depositing nearly the mass energy of the neutrons, and for some models with long-range potentials this provides the strongest limits from observations of PSR J2144–3933 [353].

The heating of NSs from neutron losses via baryon number-conserving and violating processes, and from NS capture of DM in the various ways described in Sec. 4.1, provide compelling fundamental physics motivations for upcoming astronomical missions to perform systematic measurements of NS luminosities, masses and radii.

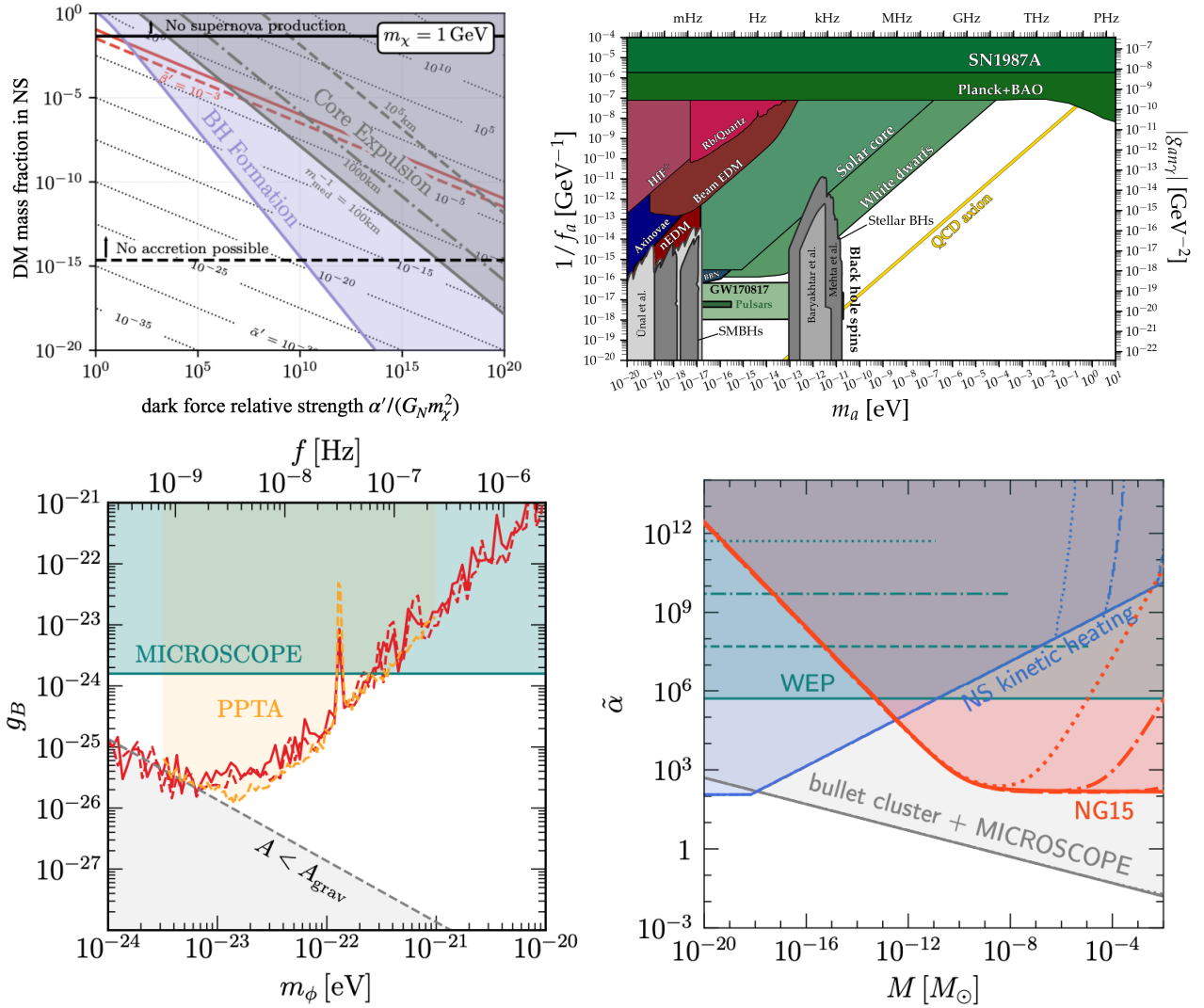


Figure 16: **Top left.** Limits on the mass fraction of dark matter in NSs in a binary as a function of the coupling of an attractive long-range dark force relative to gravity, for DM mass = 1 GeV. The solid red contour indicates the minimum value of the effective dark force coupling  $\alpha'$  that will have a detectable impact at LIGO; the dashed red contour depicts the value of the coupling when the dark charge resides in only one NS. In the purple region, the NSs turn into black holes. In the gray region, DM is expelled from the NSs when screening due to the dark force lifts. See Ref. [254] for further details. **Top right.** Future limits from gravitational waves on an axion-like species sourced by inspiraling binary NSs: the region bounded by  $m_a \lesssim 10^{-12}$  eV and  $f_a \gtrsim 10^{15}$  GeV can be probed by Advanced LIGO. For particulars on the other limits shown here, see Ref. [354]. **Bottom left.** Limits on the coupling of ultralight dark matter to baryons as a function of its mass from the 15-year dataset of the NANOGrav pulsar timing array [240] for correlated (red solid) and uncorrelated (red dashed) signals. Also shown are erstwhile limits from the Parkes Pulsar Timing Array (PPTA) and MICROSCOPE's equivalence principle test, and the region where the signal amplitude is smaller than a gravitational one. **Bottom right.** Limits on the effective baryonic long-range Yukawa coupling of dark matter subhalos/nuggets versus DM mass using NANOGrav [240] (red region). The {solid, dashed, dot-dashed, dotted} curves correspond to the range of the force  $10^{[0,-1,-2,-3]}$  pc. Stronger limits from WD explosions and NS superbursts, not shown here, could come into play for certain additional DM properties [153]. Also shown are limits from kinetic heating of the coldest observed pulsar PSR J2144–3933 (see Sec. 4.2), weak equivalence principle tests, and the Bullet Cluster.

#### 4.9. Dark matter signals in gravitational waves from neutron star mergers

Admixed NSs containing large quantities of DM could interact with each other via a long-range force (either attractive or repulsive) acting on the dark component. This could leave a distinct signature in the waveforms of the gravitational waves (GWs) picked up during their mergers at detectors such as LIGO and VIRGO [355, 254, 356]. However, for the effects of DM admixed in NSs to be seen, something beyond standard DM accumulation (which results in DM cores with masses  $\ll 10^{-10} M_{\odot}$ ) is required. As previously noted, one might consider a sizable fraction of the NSs mass converting to dark sector particles, or *e.g.* some process of DM accumulation through fluid-like accretion in an exceptionally dense region of dark matter [164]. New GW signatures from highly admixed NSs would be visible via two effects: one, a modification to the measured chirp mass  $\mathcal{M} \equiv \mu^{3/5} (M_1 + M_2)^{2/5}$  where  $M_{1,2}$  are the NS masses and  $\mu$  their reduced mass, since the effect of the new force on the evolution of the binary period is degenerate with a shift in NS masses; two, energy loss through dipole radiation of the force-carrier, which would again show up in the binary period evolution.

Other interesting effects are observable in mergers of DM-admixed NSs. The post-merger GW spectrum could exhibit additional peaks, as was shown by a simple mechanical model in Ref. [357].

In general, the equation of state and structure of an admixed NSs will depend on DM model properties, including whether the DM is bosonic [314, 312, 358], and whether such a bosonic core of DM is fully contained within the admixed NS or extends outside the baryonic component of the admixed NS [359]. In the latter case, it has been shown that the bosonic DM extending beyond the surface of the admixed NSs can lead to a “mass-shedding” phenomenon in binary systems of DM-admixed NSs [358, 359], resulting from inter-NS tidal forces.

It has also been investigated whether the DM components in a binary admixed NS system might remain gravitationally bound and orbit inside the merger remnant, after the NS component have merged. Assuming the DM components remain intact, [360] found that orbital separations of typically a few km, resulted in a kHz-band GW signal that could be sought in GW searches.

In Fig. 16 top left panel we show limits from Ref. [254] on the NS mass fraction of DM as a function of the dark force strength relative to gravity. For sizeable abelian forces, the charge carried by the DM must not be too large lest it unbind the star, limiting the hidden force to be weaker than gravity if gravitational tests are to be made [361]. A long-range dark sector force such as felt by muons in the NS could also induce the effects above [362].

Axions may be sourced by NSs due to in-medium corrections to the axion potential, giving rise to inter-NS forces that can be detected during the inspiral [363]. In Fig. 16 top right panel we show ensuing limits from Ref. [363, 354] on the decay constant as a function of the mass of an axion-like species. Ultra-light scalar DM with baryonic interactions can induce time-varying mass shifts in the NS from their coherent background, which could show up in broadband measurements [364]. Ultra-light DM could also modify the dispersion relation of neutrinos escaping a proto-NS, giving rise to asymmetric emission and hence the natal kick of the NS (Sec. 2) as well as a non-oscillating permanent strain in the local metric, a “gravitational memory” signal, that can be picked up at GW detectors [365]. Dark photons [366] and axions [367] produced in NS mergers could convert to detectably luminous  $\gamma$ -rays.

#### 4.10. Dark matter signals in pulsar timing

Pulsating NSs are incredibly precise celestial metronomes. As discussed in Sec. 2.8, their spin periods slow down at rates smaller than 1 sec per  $10^{12}$  sec, affording a pulse regularity second only to atomic clocks. This precision is exploited to probe fundamental physics in a number of ways, and in this section we collect the implications for dark matter searches.



#### 4.10.1. Pulsar timing arrays

Pulsar timing arrays (PTAs), by constraining correlations in the arrival times of pulses emitted by  $O(10)$  millisecond pulsars<sup>9</sup>, are primarily detectors of nanoHertz to milliHertz gravitational waves [368, 369]. These measurements can also be used to constrain DM substructure (including primordial black holes): their transits could induce a shift in the signal phase,

$$\varphi(t) = \varphi_0 + vt + \frac{1}{2}\dot{v}t^2 + \frac{1}{6}\ddot{v}t^3 + O(t^4), \quad (63)$$

from a shift in the frequency via two effects:

$$\begin{aligned} \left(\frac{\delta\nu}{\nu}\right)_{\text{Dopp}} &= \hat{\mathbf{d}} \cdot \int \nabla\Phi dt, \\ \left(\frac{\delta\nu}{\nu}\right)_{\text{Shap}} &= 2 \int \mathbf{v}_\chi \cdot \nabla\Phi dz, \end{aligned} \quad (64)$$

where  $\hat{\mathbf{d}}$  is the Earth-to-pulsar direction,  $\mathbf{v}_\chi$  the velocity of the DM structure,  $\Phi$  the gravitational potential due to it, and  $z$  traces the pulsar-to-Earth path of photons. The first line of Eq. (64) describes a *Doppler time delay* in the observed period of the pulsar brought about by the acceleration of the NS or Earth due to transiting DM [370]. The second line describes a *Shapiro time delay* coming from a change in the arriving photon's geodesic due to DM structure's gravitational potential [371]. Signals of DM substructure could either be *dynamic* [371, 370, 372, 373, 374], as when the transit times are much smaller than the total observation time, giving rise to blips in the data, or could be *static* [375, 376, 377], as when they are much larger, showing up as a sizeable contribution to the  $\ddot{v}$  term in Eq. (63). Detailed analyses of dynamic and static signals, treating Doppler and Shapiro time delays, can be found in Refs. [378, 379, 380], with implications for DM substructure origins explored in Ref. [381]. Limits from North American Nanohertz Observatory for Gravitational Waves (NANOGrav) data [382, 383] are derived in Ref. [241, 240] on dark nuggets (that could range from point-like to  $> 10^9$  km in size) interacting with baryons through a long-range Yukawa force; see Fig. 16 bottom right panel.

Another scenario amenable to searches at PTAs is that of ultralight ( $10^{-24}$ - $10^{-22}$  eV) DM, which could induce oscillations of the gravitational potential of the Galactic halo at nanohertz frequencies [384, 385]. Various PTAs have constrained these models [386, 387, 388, 240]; see Fig. 16 bottom left panel. In addition, a network of topological defects that alter fundamental constants could be uncovered through a variation of pulsar periods across a network of well-timed pulsars [389].

PTAs currently operational are the European Pulsar Timing Array (EPTA) [390] that uses the Westerbork Synthesis, Effelsberg, Lovell, Nancay and Sardinia radio telescopes, Parkes Pulsar Timing Array (PPTA) [391], NANOGrav [392] that uses the Green Bank Telescope, Arecibo Observatory and Very Large Array, Indian Pulsar Timing Array (InPTA) [393] that uses the Upgraded Giant Meterwave Radio Telescope (uGMRT) (these four make up the International Pulsar Timing Array (IPTA) [394]), MeerTime at MeerKAT [395], and the Chinese Pulsar Timing Array (CPTA) [396] that uses the Five-hundred-meter Aperture Spherical Telescope (FAST). The future has the Square Kilometer Array (SKA) [397, 398]. It would be of significant interest to look for various DM substructure as well as ultra-light DM in the datasets of all these PTAs, an exercise we urge of expert authors.

<sup>9</sup>Although about 3000 pulsars have been discovered [107], only these many provide the level of stability and noise-free emission required to achieve interesting precision at PTAs.



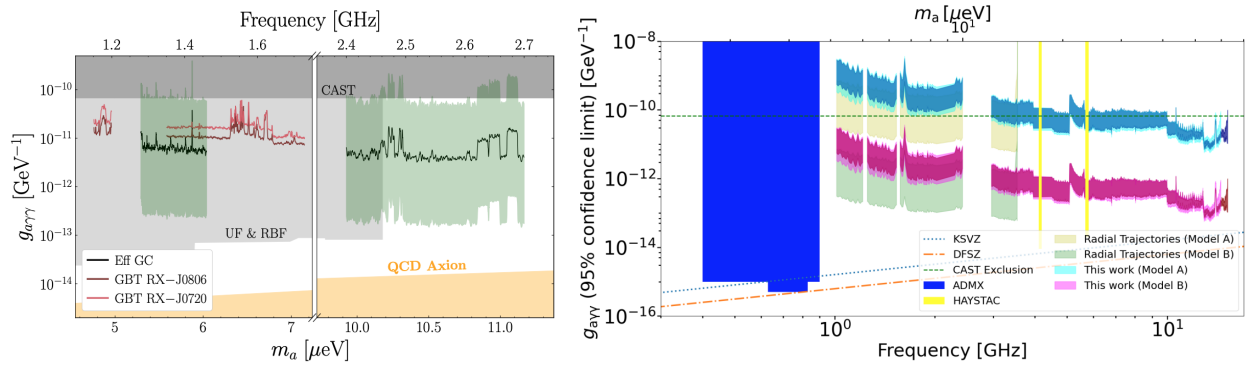


Figure 17: *Left.* 95% C.L. bounds on the ALP-photon coupling versus ALP mass from Ref. [418] using the Green Bank and Effelsberg Radio Telescopes’ observations of NSs nearby and in the Galactic Center. The green bands span theoretical uncertainties in the Effelsberg analysis. Also shown are limits from CAST (helioscope), and UF and RBF (haloscopes), and the region where the ALP could be the QCD axion. *Right.* Same as the left panel, from Ref. [419], using VLA data on the pulsar J1745–2900 and ray-tracing models. The bands depict uncertainties in viewing and magnetic angles. Limits from CAST, ADMX and HAYSTAC are also shown. See Sec. 4.11 for further details.

A recent data release of multiple PTAs announced detection of signals consistent with a stochastic gravitational wave background (SGWB) sourced by supermassive black hole (SMBH) mergers [240]. This has prompted many authors to investigate PTA signatures of dark matter, including re-interpretation of the data in terms of primordial black holes [399, 400] (which is, however, in tension with the Hubble Space Telescope’s measurement of the luminosity function of galaxies [401]), a modification of the spectral index of the SGWB due to cosmic DM-induced dynamical friction [402], a modulation in the amplitude due to a DM spike surrounding the SMBHs [403], an inflationary blue-tilted tensor power spectrum in a setup thermally overproducing WIMPs [404], a soliton of ultralight DM enclosed by the SMBHs [405], an electroweak phase transition induced by a potential involving DM [406], an ultralight radion arising from a fifth space-time dimension [407], and dark photon DM produced by the decay of cosmic string loops that may have sourced the SGWB [408].

#### 4.10.2. Binary pulsar timing

Pulsar timing without the use of a pulsar array can also be a valuable tool to detect DM. The orbits of inspiraling binary pulsars may undergo seasonal modulation due to dynamical friction caused by DM, which may be used to set bounds on the density of DM in the environment [409]. Measurements of the orbital period and period decay of binary pulsars also help to set limits on ultralight scalars that could constitute DM via their radiation from NSs [410] and their coherent oscillations [411, 412, 413], and the rate of mass loss in NSs due to, *e.g.*, conversions of neutrons to dark baryons [303, 414, 313, 415], although these latter limits are superseded by considerations of NS heating via the Auger effect (Sec. 4.8) as detailed in Ref. [302].

#### 4.10.3. Pulsar spin-down

Milli-charged DM accreting onto NSs provides surplus charge that must be expelled from the polar caps to maintain charge neutrality. Thus an additional electric current (following open magnetic field lines) is induced, contributing to the NS  $B$  field, and therefore to the slowing down of its spin as per the discussion in Sec. 2.8. In this way milli-charged DM could explain the observation of pulsar braking indices  $n < 3$  [416, 417].

#### 4.11. Axion-like and very light dark matter, and neutron stars

The above sub-sections considered particulate DM confronting NS detectors. Now we will see that very light, wave-like dark matter can also be discovered with NSs. The poster child for such DM is the QCD axion and its extension, axion-like particles (ALPs). In this section we will focus on the utility of compact stars in discovering ALP DM, referring the reader to the review in Ref. [420] for a thorough treatment of generic ALPs interacting with compact objects.

ALPs of masses  $m_a$  in the range  $10^{-7}$ – $10^{-4}$  eV, when falling into NSs, convert to photons in their magnetospheres via the Primakoff effect [421], *i.e.* via the interaction

$$\mathcal{L} \supset \frac{g_{a\gamma}}{4} a F_{\mu\nu} \tilde{F}^{\mu\nu} \rightarrow -g_{a\gamma} a \mathbf{E} \cdot \mathbf{B}. \quad (65)$$

The conversion probability is enhanced by the large magnetic field, and resonantly so for ALP masses degenerate with the photon plasma mass [422, 423, 424, 425, 426, 427]. The result is radio emission observable as a monochromatic line signal at a frequency set by the ALP mass: the narrow bandwidth is set by the small dispersion in the speed of the ALP DM. Limits exploiting this signature on the ALP-photon coupling and ALP mass have been set using the Green Bank Telescope, the Very Large Array, and the Effelsberg 100-m Radio Telescope [418, 428, 429, 427, 419]. In the near future, observations can be made at the Parkes Observatory, the Sardinia Radio Telescope, MeerKAT, the Murchison Widefield Array, and the Hydrogen Epoch of Reionization Array [430]. Analogous limits have been placed on  $O(10^{-5})$  eV mass spin-1 DM converting to photons via kinetic mixing in the plasma of NSs and accreting WDs in the Galactic Center [431]. Time-domain data (as opposed to frequency-domain) of PSR J2144–3933 at MeerKAT have been used to set limits on ALP emission [432], taking advantage of time variation of the periodic signal due to pulsar rotation and magnetospheric plasma effects. Resonant conversion of ALP DM can also occur in the corona of a magnetic WD, which could prove more sensitive than NSs to sub-microeV ALPs [115]. In Fig. 17 we show recent NS-based constraints on the ALP-photon coupling versus ALP mass.

On the theoretical side, accounting for the semi-relativistic speeds of ALP DM infall and anisotropy of the magnetic field can potentially modify the ALP-photon conversion rate by orders of magnitude [433]. One can also consider enhanced radio emission from NSs in binary systems with intermediate mass ( $10^3$ – $10^5 M_\odot$ ) black holes, taking advantage of a possible spike in the DM density [434]. Ray-tracing simulations accounting for signal photon propagation in the NS gravitational potential are an important direction toward accurate determinations of the outgoing radio flux [435, 436, 437]. Some of the uncertainties addressed by these efforts relate to the absorption of radio waves in the plasma and their refraction and reflection in the magnetosphere, signal broadening due to photon-plasma interactions, and time-dependence of the signal.

As with particulate DM discussed in Sec. 2.4, ALP DM could also form substructure such as axion mini-clusters and axion stars. If large fractions of the DM mass are present in such substructure the sensitivities of laboratory searches for ALP DM may be diluted, and NSs as ALP probes grow in importance. Encounters of NSs with ALP substructure can produce distinct transient radio signals, including fast radio bursts [438, 227, 439, 440, 441, 442]. In the bottom right panel of Fig. 11, taken from Ref. [227], are shown for two different axion mini-cluster profiles the mean flux densities of the radio signal and the sensitivities of telescope arrays. These signal rates may be smaller for more conservative estimates of the NS magnetic fields that account for possible mechanisms of their decay [442].

ALPs that are not necessarily the cosmic DM may also be studied in NS systems. Produced with  $O(100)$  keV energies in the core via nucleon bremsstrahlung, ALPs could convert in the magnetosphere to photons that may be observed as x-ray and gamma-ray emissions. As these ALPs carry away energy they also provide an additional cooling mechanism for the NS. For further details and observation prospects of ALP emissions

from within NSs, see Ref. [430] and the references therein. ALPs could also overheat NSs by contributing to the NS magnetic energy via a dynamo mechanism generated by axio-electrodynamics [443].

As a reminder, other signatures of ALPs have already been discussed in this review: their modification of WD EoS (Sec. 3.4) and their considerable effects on pulsar timing measurements (Sec. 4.10).

## 5. Conclusions and perspective

In this review we have described how various authors have exploited the unique and extreme properties of compact stars to enable far-reaching searches for a vast assortment of dark matter scenarios<sup>10</sup>. We have, of course, chosen to focus on the commonly accepted and well-observed classes of compact stars: WDs and NSs. Several adjacent stellar entities may play a role in the discovery of dark matter, *e.g.*, black holes, proto-NSs, supernovae and their remnants, and Thorne-Żytkow objects; for accounts of some of these, we refer the reader to Ref. [430] and other literature.

Given the richness of physics involving both dark matter and compact stars, it is impossible to exhaust the progress that can be made hereupon. We mention a few possibilities.

- While research has gone into detecting wave-like, particulate, macroscopic and black hole dark matter with compact stars, what happens to DM in the form of topological defects (macroscopic monopoles, cosmic strings, and domain walls) [445, 446] in a compact star environment is as yet relatively unexplored, although for some initial work in this direction see Ref. [389]. This points to a property of WDs and NSs that could be further exploited – as sirens of dark matter well-distributed through the galaxy, they have special sensitivity to variations in dark matter properties across the halo and substructure [164].
- The physics of BEC and BCS states formed by dark matter in NSs, essential to understanding collapse to black holes, is yet to be worked out satisfactorily. Many of the computations have used coarse estimates.
- Detecting dark matter via thermonuclear explosions in WD cores and NS oceans requires knowledge of trigger lengths, which while numerically estimated in Ref. [84] with a large nuclear reaction network, is only available for a narrow range of densities and compositions. We believe that the significance of these computations for a scientific question as fundamental as dark matter warrants further exploration of the 31 year-old results of Ref. [84] by the nuclear astrophysics community.
- The impact of WD explosions on the evolution on galactic structure and star formation is yet to be scrutinized.

In closing, dark matter may first become manifest through some effect on compact stars detailed in this document. On the other hand, since compact stars have the distinction of being the densest objects composed of known particles, it may be that some variety of dark matter, hitherto unexpected, will first become evident through a surprising and as-yet-unforeseen interaction with them. In either case, we can look forward to the interplay between our burgeoning understanding of compact stars and the ebullient search for dark matter in the coming decades.

---

<sup>10</sup>Although there are some for which compact stars get in the way of discovering dark matter, *e.g.* searches via microlensing [444] and globular clusters [138]!

## Acknowledgments

For helpful interactions we thank Melissa Diamond, Michael Fedderke, Raghuveer Garani, Bradley Kavanagh, Ranjan Laha, and Camellia Sinensis. The work of J. B. is supported by the Natural Sciences and Engineering Research Council of Canada. N. R. acknowledges support from TRIUMF Inc. and the Arthur B. McDonald Canadian Astroparticle Physics Research Institute at Queen’s University during the course of this work. This research was undertaken thanks in part to funding from the Canada First Research Excellence Fund through the Arthur B. McDonald Canadian Astroparticle Research Institute. Research at Perimeter Institute is supported in part by the Government of Canada through the Department of Innovation, Science and Economic Development Canada and by the Province of Ontario through the Ministry of Colleges and Universities.

## References

- [1] R. H. Fowler, On dense matter, *Mon. Not. Roy. Astron. Soc.* 87 (1926) 114–122.
- [2] W. Anderson, Über die Grenzdichte der Materie und der Energie, *Zeitschrift für Physik* 56 (11-12) (1929) 851–856. doi:10.1007/BF01340146.
- [3] E. C. S. Ph.D., Lxxxvii. the equilibrium of dense stars, *The London, Edinburgh, and Dublin Philosophical Magazine and Journal of Science* 9 (60) (1930) 944–963. doi:10.1080/14786443008565066. URL <https://doi.org/10.1080/14786443008565066>
- [4] S. Chandrasekhar, The Maximum Mass of Ideal White Dwarfs, *APJ* 74 (1931) 81. doi:10.1086/143324.
- [5] W. Baade, F. Zwicky, On Super-Novae, *Proc. Nat. Acad. Sci.* 20 (5) (1934) 254–259. doi:10.1073/pnas.20.5.254.
- [6] D. G. Yakovlev, P. Haensel, G. Baym, C. Pethick, Lev Landau and the concept of neutron stars, *Physics Uspekhi* 56 (3) (2013) 289–295. arXiv:1210.0682, doi:10.3367/UFNe.0183.201303f.0307.
- [7] J. Isern, S. Torres, A. Rebassa-Mansergas, White Dwarfs as Physics Laboratories: Lights and Shadows, *Front. Astron. Space Sci.* 9 (2022) 815517. arXiv:2202.02052, doi:10.3389/fspas.2022.815517.
- [8] J. Näätä, J. J. E. Kajava, Fundamental physics with neutron stars (11 2022). arXiv:2211.15721, doi:10.1007/978-981-16-4544-0\_105-1.
- [9] W. H. Press, D. N. Spergel, Capture by the sun of a galactic population of weakly interacting massive particles, *Astrophys. J.* 296 (1985) 679–684. doi:10.1086/163485.
- [10] A. Gould, Resonant Enhancements in WIMP Capture by the Earth, *Astrophys. J.* 321 (1987) 571. doi:10.1086/165653.
- [11] I. Goldman, S. Nussinov, Weakly Interacting Massive Particles and Neutron Stars, *Phys. Rev. D* 40 (1989) 3221–3230. doi:10.1103/PhysRevD.40.3221.
- [12] G. Bertone, D. Hooper, J. Silk, Particle dark matter: Evidence, candidates and constraints, *Phys. Rept.* 405 (2005) 279–390. arXiv:hep-ph/0404175, doi:10.1016/j.physrep.2004.08.031.
- [13] D. Saumon, S. Blouin, P.-E. Tremblay, Current challenges in the physics of white dwarf stars, *Phys. Rept.* 988 (2022) 1–63. arXiv:2209.02846, doi:10.1016/j.physrep.2022.09.001.
- [14] J. M. Lattimer, M. Prakash, The Physics of Neutron Stars, *Science* 304 (5670) (2004) 536–542. arXiv:astro-ph/0405262, doi:10.1126/science.1090720.
- [15] A. G. Lyne, D. R. Lorimer, High birth velocities of radio pulsars, *Nature* 369 (1994) 127. doi:10.1038/369127a0.
- [16] L. Scheck, T. Plewa, H.-T. Janka, K. Kifonidis, E. Mueller, Pulsar recoil by large scale anisotropies in supernova explosions, *Phys. Rev. Lett.* 92 (2004) 011103. arXiv:astro-ph/0307352, doi:10.1103/PhysRevLett.92.011103.
- [17] L. Scheck, K. Kifonidis, H. T. Janka, E. Mueller, Multidimensional supernova simulations with approximative neutrino transport. 1. neutron star kicks and the anisotropy of neutrino-driven explosions in two spatial dimensions, *Astron. Astrophys.* 457 (2006) 963. arXiv:astro-ph/0601302, doi:10.1051/0004-6361:20064855.
- [18] C. Y. Ng, R. W. Romani, Birth Kick Distributions and the Spin-Kick Correlation of Young Pulsars, *Astrophys. J.* 660 (2007) 1357–1374. arXiv:astro-ph/0702180, doi:10.1086/513597.
- [19] J. Nordhaus, T. D. Brandt, A. Burrows, E. Livne, C. D. Ott, Theoretical Support for the Hydrodynamic Mechanism of Pulsar Kicks, *Phys. Rev. D* 82 (2010) 103016. arXiv:1010.0674, doi:10.1103/PhysRevD.82.103016.
- [20] A. Kusenko, G. Segre, Velocities of pulsars and neutrino oscillations, *Phys. Rev. Lett.* 77 (1996) 4872–4875. arXiv:hep-ph/9606428, doi:10.1103/PhysRevLett.77.4872.
- [21] A. Kusenko, G. Segre, Pulsar kicks from neutrino oscillations, *Phys. Rev. D* 59 (1999) 061302. arXiv:astro-ph/9811144, doi:10.1103/PhysRevD.59.061302.

- [22] M. Barkovich, J. C. D’Olivo, R. Montemayor, J. F. Zanella, Neutrino oscillation mechanism for pulsar kicks revisited, *Phys. Rev. D* 66 (2002) 123005. [arXiv:astro-ph/0206471](https://arxiv.org/abs/astro-ph/0206471), [doi:10.1103/PhysRevD.66.123005](https://doi.org/10.1103/PhysRevD.66.123005).
- [23] S. Chandrasekhar, *Xlviii. the density of white dwarf stars*, *The London, Edinburgh, and Dublin Philosophical Magazine and Journal of Science* 11 (70) (1931) 592–596. [arXiv:https://doi.org/10.1080/14786443109461710](https://arxiv.org/abs/https://doi.org/10.1080/14786443109461710), [doi:10.1080/14786443109461710](https://doi.org/10.1080/14786443109461710).  
URL <https://doi.org/10.1080/14786443109461710>
- [24] A. Burrows, J. P. Ostriker, The Astronomical Reach of Fundamental Physics, *Proc. Nat. Acad. Sci.* 111 (2014) 2409. [arXiv:1401.1814](https://arxiv.org/abs/1401.1814), [doi:10.1073/pnas.1318003111](https://doi.org/10.1073/pnas.1318003111).
- [25] R. R. Silbar, S. Reddy, Neutron stars for undergraduates, *Am. J. Phys.* 72 (2004) 892–905, [Erratum: *Am.J.Phys.* 73, 286 (2005)]. [arXiv:nucl-th/0309041](https://arxiv.org/abs/nucl-th/0309041), [doi:10.1119/1.1852544](https://doi.org/10.1119/1.1852544).
- [26] S. L. Shapiro, S. A. Teukolsky, *Black holes, white dwarfs, and neutron stars : the physics of compact objects*, 1983.
- [27] P. Haensel, J. L. Zdunik, F. Douchin, Equation of state of dense matter and the minimum mass of cold neutron stars, *Astron. Astrophys.* 385 (2002) 301. [arXiv:astro-ph/0201434](https://arxiv.org/abs/astro-ph/0201434), [doi:10.1051/0004-6361:20020131](https://doi.org/10.1051/0004-6361:20020131).
- [28] V. Doroshenko, V. Suleimanov, G. Pühlhofer, A. Santangelo, A strangely light neutron star within a supernova remnant, *Nature Astronomy* 6 (2022) 1444–1451. [doi:10.1038/s41550-022-01800-1](https://doi.org/10.1038/s41550-022-01800-1).
- [29] F. Di Clemente, A. Drago, G. Pagliara, Is the compact object associated with HESS J1731-347 a strange quark star? (11 2022). [arXiv:2211.07485](https://arxiv.org/abs/2211.07485).
- [30] V. Sagun, E. Giangrandi, T. Dietrich, O. Ivanytskyi, R. Negreiros, C. Providência, What is the nature of the HESS J1731-347 compact object? (6 2023). [arXiv:2306.12326](https://arxiv.org/abs/2306.12326).
- [31] Y. Suwa, T. Yoshida, M. Shibata, H. Umeda, K. Takahashi, On the minimum mass of neutron stars, *Mon. Not. Roy. Astron. Soc.* 481 (3) (2018) 3305–3312. [arXiv:1808.02328](https://arxiv.org/abs/1808.02328), [doi:10.1093/mnras/sty2460](https://doi.org/10.1093/mnras/sty2460).
- [32] J. M. Lattimer, M. Prakash, The physics of neutron stars, *Science* 304 (2004) 536–542. [arXiv:astro-ph/0405262](https://arxiv.org/abs/astro-ph/0405262), [doi:10.1126/science.1090720](https://doi.org/10.1126/science.1090720).
- [33] F. Özel, P. Freire, Masses, Radii, and the Equation of State of Neutron Stars, *Ann. Rev. Astron. Astrophys.* 54 (2016) 401–440. [arXiv:1603.02698](https://arxiv.org/abs/1603.02698), [doi:10.1146/annurev-astro-081915-023322](https://doi.org/10.1146/annurev-astro-081915-023322).
- [34] J. M. Lattimer, Neutron Stars and the Nuclear Matter Equation of State, *Ann. Rev. Nucl. Part. Sci.* 71 (2021) 433–464. [doi:10.1146/annurev-nucl-102419-124827](https://doi.org/10.1146/annurev-nucl-102419-124827).
- [35] M. Rotondo, J. A. Rueda, R. Ruffini, S.-S. Xue, The Relativistic Feynman-Metropolis-Teller theory for white dwarfs in general relativity, *Phys. Rev. D* 84 (2011) 084007. [arXiv:1012.0154](https://arxiv.org/abs/1012.0154), [doi:10.1103/PhysRevD.84.084007](https://doi.org/10.1103/PhysRevD.84.084007).
- [36] E. R. Most, L. R. Weih, L. Rezzolla, J. Schaffner-Bielich, New constraints on radii and tidal deformabilities of neutron stars from GW170817, *Phys. Rev. Lett.* 120 (26) (2018) 261103. [arXiv:1803.00549](https://arxiv.org/abs/1803.00549), [doi:10.1103/PhysRevLett.120.261103](https://doi.org/10.1103/PhysRevLett.120.261103).
- [37] B. P. Abbott, et al., GW170817: Measurements of neutron star radii and equation of state, *Phys. Rev. Lett.* 121 (16) (2018) 161101. [arXiv:1805.11581](https://arxiv.org/abs/1805.11581), [doi:10.1103/PhysRevLett.121.161101](https://doi.org/10.1103/PhysRevLett.121.161101).
- [38] C. Raithel, F. Özel, D. Psaltis, Tidal deformability from GW170817 as a direct probe of the neutron star radius, *Astrophys. J. Lett.* 857 (2) (2018) L23. [arXiv:1803.07687](https://arxiv.org/abs/1803.07687), [doi:10.3847/2041-8213/aabcbf](https://doi.org/10.3847/2041-8213/aabcbf).
- [39] H. T. Cromartie, et al., Relativistic Shapiro delay measurements of an extremely massive millisecond pulsar, *Nature Astron.* 4 (1) (2019) 72–76. [arXiv:1904.06759](https://arxiv.org/abs/1904.06759), [doi:10.1038/s41550-019-0880-2](https://doi.org/10.1038/s41550-019-0880-2).
- [40] J. W. T. Hessels, S. M. Ransom, I. H. Stairs, P. C. C. Freire, V. M. Kaspi, F. Camilo, A radio pulsar spinning at 716-hz, *Science* 311 (2006) 1901–1904. [arXiv:astro-ph/0601337](https://arxiv.org/abs/astro-ph/0601337), [doi:10.1126/science.1123430](https://doi.org/10.1126/science.1123430).
- [41] T. E. Riley, A. L. Watts, S. Bogdanov, P. S. Ray, R. M. Ludlam, S. Guillot, Z. Arzoumanian, C. L. Baker, A. V. Bilous, D. Chakrabarty, et al., A nicer view of psr j0030+ 0451: Millisecond pulsar parameter estimation, *The Astrophysical Journal Letters* 887 (1) (2019) L21.
- [42] T. E. Riley, A. L. Watts, P. S. Ray, S. Bogdanov, S. Guillot, S. M. Morsink, A. V. Bilous, Z. Arzoumanian, D. Choudhury, J. S. Deneva, et al., A nicer view of the massive pulsar psr j0740+ 6620 informed by radio timing and xmm-newton spectroscopy, *The Astrophysical Journal Letters* 918 (2) (2021) L27.
- [43] M. Miller, F. K. Lamb, A. Dittmann, S. Bogdanov, Z. Arzoumanian, K. C. Gendreau, S. Guillot, A. Harding, W. Ho, J. Lattimer, et al., Psr j0030+ 0451 mass and radius from nicer data and implications for the properties of neutron star matter, *The Astrophysical Journal Letters* 887 (1) (2019) L24.
- [44] M. Miller, F. K. Lamb, A. Dittmann, S. Bogdanov, Z. Arzoumanian, K. Gendreau, S. Guillot, W. Ho, J. Lattimer, M. Loewenstein, et al., The radius of psr j0740+ 6620 from nicer and xmm-newton data, *The Astrophysical Journal Letters* 918 (2) (2021) L28.
- [45] S. Chatterjee, R. Garani, R. K. Jain, B. Kanodia, M. S. N. Kumar, S. K. Vempati, Faint light of old neutron stars and detectability at the James Webb Space Telescope, *Phys. Rev. D* 108 (2) (2023) L021301. [arXiv:2205.05048](https://arxiv.org/abs/2205.05048), [doi:10.1103/PhysRevD.108.L021301](https://doi.org/10.1103/PhysRevD.108.L021301).
- [46] A. Reisenegger, F. S. Zepeda, Order-of-magnitude physics of neutron stars, *Eur. Phys. J. A* 52 (3) (2016) 52. [arXiv:](https://arxiv.org/abs/)



- 1511.08813, doi:10.1140/epja/i2016-16052-y.
- [47] M. A. Fedderke, P. W. Graham, S. Rajendran, White dwarf bounds on charged massive particles, *Phys. Rev. D* 101 (11) (2020) 115021. [arXiv:1911.08883](https://arxiv.org/abs/1911.08883), doi:10.1103/PhysRevD.101.115021.
- [48] J. F. Acevedo, J. Bramante, R. K. Leane, N. Raj, Warming Nuclear Pasta with Dark Matter: Kinetic and Annihilation Heating of Neutron Star Crusts, *JCAP* 03 (2020) 038. [arXiv:1911.06334](https://arxiv.org/abs/1911.06334), doi:10.1088/1475-7516/2020/03/038.
- [49] J. M. Pearson, N. Chamel, A. Y. Potekhin, A. F. Fantina, C. Ducoin, A. K. Dutta, S. Goriely, Unified equations of state for cold non-accreting neutron stars with Brussels-Montreal functionals: I. Role of symmetry energy, *Mon. Not. Roy. Astron. Soc.* 481 (3) (2018) 2994–3026, [Erratum: *Mon. Not. Roy. Astron. Soc.* 486, no. 1, 768 (2019)]. [arXiv:1903.04981](https://arxiv.org/abs/1903.04981), doi:10.1093/mnras/sty2413, 10.1093/mnras/stz800.
- [50] N. Chamel, P. Haensel, *Physics of neutron star crusts*, *Living Reviews in Relativity* 11 (1) (2008) 10. doi:10.12942/lrr-2008-10.  
URL <https://doi.org/10.12942/lrr-2008-10>
- [51] A. Y. Potekhin, A. F. Fantina, N. Chamel, J. M. Pearson, S. Goriely, Analytical representations of unified equations of state for neutron-star matter, *Astron. Astrophys.* 560 (2013) A48. [arXiv:1310.0049](https://arxiv.org/abs/1310.0049), doi:10.1051/0004-6361/201321697.
- [52] G. Baym, H. A. Bethe, C. J. Pethick, *Neutron star matter*, *Nuclear Physics A* 175 (2) (1971) 225 – 271. doi:[https://doi.org/10.1016/0375-9474\(71\)90281-8](https://doi.org/10.1016/0375-9474(71)90281-8).  
URL <http://www.sciencedirect.com/science/article/pii/0375947471902818>
- [53] J. Lattimer, C. Pethick, D. Ravenhall, D. Lamb, *Physical properties of hot, dense matter: The general case*, *Nuclear Physics A* 432 (3) (1985) 646 – 742. doi:[https://doi.org/10.1016/0375-9474\(85\)90006-5](https://doi.org/10.1016/0375-9474(85)90006-5).  
URL <http://www.sciencedirect.com/science/article/pii/0375947485900065>
- [54] D. G. Ravenhall, C. J. Pethick, J. R. Wilson, Structure of Matter Below Nuclear Saturation Density, *Phys. Rev. Lett.* 50 (1983) 2066–2069. doi:10.1103/PhysRevLett.50.2066.
- [55] M. Hashimoto, H. Seki, M. Yamada, *Shape of Nuclei in the Crust of Neutron Star*, *Progress of Theoretical Physics* 71 (2) (1984) 320–326. [arXiv:http://oup.prod.sis.lan/ptp/article-pdf/71/2/320/5459325/71-2-320.pdf](https://arxiv.org/abs/http://oup.prod.sis.lan/ptp/article-pdf/71/2/320/5459325/71-2-320.pdf), doi:10.1143/PTP.71.320.  
URL <https://doi.org/10.1143/PTP.71.320>
- [56] K. Oyamatsu, M. Hashimoto, M. Yamada, *Further Study of the Nuclear Shape in High-Density Matter*, *Progress of Theoretical Physics* 72 (2) (1984) 373–375. [arXiv:http://oup.prod.sis.lan/ptp/article-pdf/72/2/373/5179866/72-2-373.pdf](https://arxiv.org/abs/http://oup.prod.sis.lan/ptp/article-pdf/72/2/373/5179866/72-2-373.pdf), doi:10.1143/PTP.72.373.  
URL <https://doi.org/10.1143/PTP.72.373>
- [57] R. D. Williams, S. E. Koonin, Sub-saturation phases of nuclear matter, *Nucl. Phys.* A435 (1985) 844–858. doi:10.1016/0375-9474(85)90191-5.
- [58] C. P. Lorenz, D. G. Ravenhall, C. J. Pethick, Neutron star crusts, *Phys. Rev. Lett.* 70 (1993) 379–382. doi:10.1103/PhysRevLett.70.379.
- [59] K. Oyamatsu, Nuclear shapes in the inner crust of a neutron star, *Nucl. Phys.* A561 (1993) 431–452. doi:10.1016/0375-9474(93)90020-X.
- [60] J. B. Hartle, R. F. Sawyer, D. J. Scalapino, Pion condensed matter at high densities: equation of state and stellar models., *Astrophysical Journal* 199 (1975) 471–481. doi:10.1086/153713.
- [61] P. Haensel, M. Proszynski, Pion condensation in cold dense matter and neutron stars, *Astrophysical Journal* 258 (1982) 306–320. doi:10.1086/160080.
- [62] G. Brown, W. Weise, *Pion condensates*, *Physics Reports* 27 (1) (1976) 1 – 34. doi:[https://doi.org/10.1016/0370-1573\(76\)90008-9](https://doi.org/10.1016/0370-1573(76)90008-9).  
URL <http://www.sciencedirect.com/science/article/pii/0370157376900089>
- [63] D. Page, S. Reddy, Dense Matter in Compact Stars: Theoretical Developments and Observational Constraints, *Ann. Rev. Nucl. Part. Sci.* 56 (2006) 327–374. [arXiv:astro-ph/0608360](https://arxiv.org/abs/astro-ph/0608360), doi:10.1146/annurev.nucl.56.080805.140600.
- [64] B. Holdom, J. Ren, C. Zhang, Quark matter may not be strange, *Phys. Rev. Lett.* 120 (22) (2018) 222001. [arXiv:1707.06610](https://arxiv.org/abs/1707.06610), doi:10.1103/PhysRevLett.120.222001.
- [65] D. D. Ivanenko, D. F. Kurdgelaidze, *Hypothesis concerning quark stars*, *Astrophysics* 1 (4) (1965) 251–252. doi:10.1007/BF01042830.  
URL <https://doi.org/10.1007/BF01042830>
- [66] D. Ivanenko, D. F. Kurdgelaidze, *Remarks on quark stars*, *Lettere al Nuovo Cimento* (1969-1970) 2 (1) (1969) 13–16. doi:10.1007/BF02753988.  
URL <https://doi.org/10.1007/BF02753988>
- [67] J. C. Collins, M. J. Perry, Superdense Matter: Neutrons Or Asymptotically Free Quarks?, *Phys. Rev. Lett.* 34 (1975) 1353. doi:10.1103/PhysRevLett.34.1353.
- [68] F. Weber, Quark matter in neutron stars, *J. Phys.* G25 (1999) R195–R229. doi:10.1088/0954-3889/25/9/201.



- [69] R. Lastowiecki, D. Blaschke, T. Fischer, T. Klähn, [Quark matter in high-mass neutron stars?](#), *Physics of Particles and Nuclei* 46 (5) (2015) 843–845. doi:10.1134/S1063779615050159.  
URL <https://doi.org/10.1134/S1063779615050159>
- [70] D. Chatterjee, I. Vidaña, Do hyperons exist in the interior of neutron stars?, *Eur. Phys. J. A52* (2) (2016) 29. [arXiv:1510.06306](#), doi:10.1140/epja/i2016-16029-x.
- [71] B. C. Barrois, [Superconducting quark matter](#), *Nuclear Physics B* 129 (3) (1977) 390–396. doi:[https://doi.org/10.1016/0550-3213\(77\)90123-7](https://doi.org/10.1016/0550-3213(77)90123-7).  
URL <https://www.sciencedirect.com/science/article/pii/0550321377901237>
- [72] S. C. Frautschi, ASYMPTOTIC FREEDOM AND COLOR SUPERCONDUCTIVITY IN DENSE QUARK MATTER, in: *Workshop on Theoretical Physics: Hadronic Matter at Extreme Energy Density*, 1978.
- [73] M. G. Alford, A. Schmitt, K. Rajagopal, T. Schafer, Color superconductivity in dense quark matter, *Rev. Mod. Phys.* 80 (2008) 1455–1515. [arXiv:0709.4635](#), doi:10.1103/RevModPhys.80.1455.
- [74] R. Anglani, R. Casalbuoni, M. Ciminale, N. Ippolito, R. Gatto, M. Mannarelli, M. Ruggieri, [Crystalline color superconductors](#), *Reviews of Modern Physics* 86 (2) (2014) 509–561. doi:10.1103/revmodphys.86.509.  
URL <http://dx.doi.org/10.1103/RevModPhys.86.509>
- [75] M. G. Alford, K. Rajagopal, F. Wilczek, Color flavor locking and chiral symmetry breaking in high density QCD, *Nucl. Phys. B* 537 (1999) 443–458. [arXiv:hep-ph/9804403](#), doi:10.1016/S0550-3213(98)00668-3.
- [76] N. K. Glendenning, S. Pei, Crystalline structure of the mixed confined - deconfined phase in neutron stars, *Phys. Rev. C* 52 (1995) 2250–2253. doi:10.1103/PhysRevC.52.2250.
- [77] P. F. Bedaque, T. Schafer, High density quark matter under stress, *Nucl. Phys. A* 697 (2002) 802–822. [arXiv:hep-ph/0105150](#), doi:10.1016/S0375-9474(01)01272-6.
- [78] D. B. Kaplan, S. Reddy, Novel phases and transitions in color flavor locked matter, *Phys. Rev. D* 65 (2002) 054042. [arXiv:hep-ph/0107265](#), doi:10.1103/PhysRevD.65.054042.
- [79] D. Maoz, F. Mannucci, Type-Ia supernova rates and the progenitor problem, a review, *Publ. Astron. Soc. Austral.* 29 (2012) 447. [arXiv:1111.4492](#), doi:10.1071/AS11052.
- [80] A. Cumming, L. Bildsten, Carbon flashes in the heavy element ocean on accreting neutron stars, *Astrophys. J. Lett.* 559 (2001) L127. [arXiv:astro-ph/0107213](#), doi:10.1086/323937.
- [81] J. in 't Zand, [Understanding superbursts](#), 2017. [arXiv:1702.04899](#).
- [82] D. K. Galloway, J. in 't Zand, J. Chenevez, H. Wörfel, L. Keek, L. Ootes, A. L. Watts, L. Gisler, C. Sanchez-Fernandez, E. Kuulkers, The Multi-INstrument Burst ARchive (MINBAR), *Astrophys. J. Suppl.* 249 (2) (2020) 32. [arXiv:2003.00685](#), doi:10.3847/1538-4365/ab9f2e.
- [83] e. a. Alizai, K. [A catalogue of unusually long thermonuclear bursts on neutron stars](#), *Monthly Notices of the Royal Astronomical Society* 521 (3) (2023) 3608–3624. [arXiv:https://academic.oup.com/mnras/article-pdf/521/3/3608/49630407/stad374.pdf](#), doi:10.1093/mnras/stad374.  
URL <https://doi.org/10.1093/mnras/stad374>
- [84] F. X. Timmes, S. E. Woosley, The Conductive Propagation of Nuclear Flames. I. Degenerate C + O and O + NE + MG White Dwarfs, *APJ* 396 (1992) 649. doi:10.1086/171746.
- [85] J. Bramante, Dark matter ignition of type Ia supernovae, *Phys. Rev. Lett.* 115 (14) (2015) 141301. [arXiv:1505.07464](#), doi:10.1103/PhysRevLett.115.141301.
- [86] J. F. Acevedo, J. Bramante, R. K. Leane, N. Raj, [Cooking Pasta with Dark Matter: Kinetic and Annihilation Heating of Neutron Star Crusts](#) (2019). [arXiv:1911.06334](#).
- [87] L. G. Althaus, A. H. Corsico, J. Isern, E. García-Berro, Evolutionary and pulsational properties of white dwarf stars, *The Astronomy and Astrophysics Review* 18 (4) (2010) 471–566. doi:10.1007/s00159-010-0033-1.
- [88] A. Cumming, E. F. Brown, F. J. Fattoyev, C. J. Horowitz, D. Page, S. Reddy, A lower limit on the heat capacity of the neutron star core, *Phys. Rev. C* 95 (2) (2017) 025806. [arXiv:1608.07532](#), doi:10.1103/PhysRevC.95.025806.
- [89] D. Page, J. M. Lattimer, M. Prakash, A. W. Steiner, Minimal cooling of neutron stars: A New paradigm, *Astrophys. J. Suppl.* 155 (2004) 623–650. [arXiv:astro-ph/0403657](#), doi:10.1086/424844.
- [90] D. G. Yakovlev, C. J. Pethick, Neutron star cooling, *Ann. Rev. Astron. Astrophys.* 42 (2004) 169–210. [arXiv:astro-ph/0402143](#), doi:10.1146/annurev.astro.42.053102.134013.
- [91] J. A. Harvey, C. T. Hill, R. J. Hill, Anomaly mediated neutrino-photon interactions at finite baryon density, *Phys. Rev. Lett.* 99 (2007) 261601. [arXiv:0708.1281](#), doi:10.1103/PhysRevLett.99.261601.
- [92] S. Chakraborty, A. Gupta, M. Vanvlasselaer, Anomaly induced cooling of Neutron Stars: A Standard Model contribution (6 2023). [arXiv:2306.15872](#).
- [93] D. D. Ofengeim, M. Fortin, P. Haensel, D. G. Yakovlev, J. L. Zdunik, Neutrino luminosities and heat capacities of neutron stars in analytic form, *Phys. Rev. D* 96 (4) (2017) 043002. [arXiv:1708.08272](#), doi:10.1103/PhysRevD.96.043002.
- [94] A. Y. Potekhin, D. A. Zyuzin, D. G. Yakovlev, M. V. Beznogov, Y. A. Shibano, Thermal luminosities of cooling neutron

- stars, *Mon. Not. Roy. Astron. Soc.* 496 (4) (2020) 5052–5071. [arXiv:2006.15004](#), [doi:10.1093/mnras/staa1871](#).
- [95] E. H. Gudmundsson, C. J. Pethick, R. I. Epstein, Structure of neutron star envelopes, *apj* 272 (1983) 286–300. [doi:10.1086/161292](#).
- [96] M. V. Beznogov, A. Y. Potekhin, D. G. Yakovlev, Heat blanketing envelopes of neutron stars, *Phys. Rept.* 919 (2021) 1–68. [arXiv:2103.12422](#), [doi:10.1016/j.physrep.2021.03.004](#).
- [97] D. D. Ofengeim, D. G. Yakovlev, Analytic description of neutron star cooling, *Mon. Not. Roy. Astron. Soc.* 467 (3) (2017) 3598–3603. [doi:10.1093/mnras/stx366](#).
- [98] A. B. Migdal, Superfluidity and the moments of inertia of nuclei, *Nuclear Physics* 13 (5) (1959) 655–674. [doi:10.1016/0029-5582\(59\)90264-0](#).
- [99] D. G. Yakovlev, K. P. Levenfish, Y. A. Shibano, Cooling neutron stars and superfluidity in their interiors, *Phys. Usp.* 42 (1999) 737–778. [arXiv:astro-ph/9906456](#), [doi:10.1070/PU1999v042n08ABEH000556](#).
- [100] B. Haskell, A. Sedrakian, Superfluidity and Superconductivity in Neutron Stars, *Astrophys. Space Sci. Libr.* 457 (2018) 401–454. [arXiv:1709.10340](#), [doi:10.1007/978-3-319-97616-7-8](#).
- [101] M. G. Alford, K. Rajagopal, F. Wilczek, QCD at finite baryon density: Nucleon droplets and color superconductivity, *Phys. Lett. B* 422 (1998) 247–256. [arXiv:hep-ph/9711395](#), [doi:10.1016/S0370-2693\(98\)00051-3](#).
- [102] <https://www.cv.nrao.edu/~sransom/web/Ch6.html/>.
- [103] M. Caleb, et al., Discovery of a radio-emitting neutron star with an ultra-long spin period of 76 s, *Nature Astron.* 6 (7) (2022) 828–836. [arXiv:2206.01346](#), [doi:10.1038/s41550-022-01688-x](#).
- [104] A. Reisenegger, Stable magnetic equilibria and their evolution in the upper main sequence, white dwarfs, and neutron stars, *AAP* 499 (2) (2009) 557–566. [arXiv:0809.0361](#), [doi:10.1051/0004-6361/200810895](#).
- [105] D. A. H. Buckley, P. J. Meintjes, S. B. Potter, T. R. Marsh, B. T. Gänsicke, Polarimetric evidence of a white dwarf pulsar in the binary system AR Scorpii, *Nature Astron.* 1 (2017) 0029. [arXiv:1612.03185](#), [doi:10.1038/s41550-016-0029](#).
- [106] I. Pelisoli, et al., A 5.3-minute-period pulsing white dwarf in a binary detected from radio to X-rays (6 2023). [arXiv:2306.09272](#).
- [107] R. N. Manchester, G. B. Hobbs, A. Teoh, M. Hobbs, The Australia Telescope National Facility pulsar catalogue, *Astron. J.* 129 (2005) 1993. [arXiv:astro-ph/0412641](#), [doi:10.1086/428488](#).
- [108] T. M. Tauris, Spin-Down of Radio Millisecond Pulsars at Genesis, *Science* 335 (6068) (2012) 561. [arXiv:1202.0551](#), [doi:10.1126/science.1216355](#).
- [109] N. Aghanim, et al., Planck 2018 results. VI. Cosmological parameters, *Astron. Astrophys.* 641 (2020) A6, [Erratum: *Astron. Astrophys.* 652, C4 (2021)]. [arXiv:1807.06209](#), [doi:10.1051/0004-6361/201833910](#).
- [110] N. Tetzlaff, R. Neuhäuser, M. M. Hohle, G. Maciejewski, Identifying birth places of young isolated neutron stars, *MNRAS* 402 (4) (2010) 2369–2387. [arXiv:0911.4441](#), [doi:10.1111/j.1365-2966.2009.16093.x](#).
- [111] F. F. Kou, H. Tong, R. X. Xu, X. Zhou, Rotational Evolution of the Slowest Radio Pulsar, PSR J0250+5854, *APJ* 876 (2) (2019) 131. [arXiv:1901.00300](#), [doi:10.3847/1538-4357/ab17da](#).
- [112] M. Caleb, et al., Discovery of a radio-emitting neutron star with an ultra-long spin period of 76 s, *Nature Astron.* 6 (7) (2022) 828–836. [arXiv:2206.01346](#), [doi:10.1038/s41550-022-01688-x](#).
- [113] M. D. Young, R. N. Manchester, S. Johnston, A radio pulsar with an 8.5-second period that challenges emission models, *Nature* 400 (6747) (1999) 848–849. [doi:10.1038/23650](#).
- [114] F. F. Kou, H. Tong, [Rotational evolution of psr j2251-3711 \(the second slowest radio pulsar\)](#), *Research Notes of the AAS* 3 (11) (2019) 175. [doi:10.387/2515-5172/ab595f](#).  
URL <https://dx.doi.org/10.3847/2515-5172/ab595f>
- [115] J.-W. Wang, X.-J. Bi, R.-M. Yao, P.-F. Yin, Exploring axion dark matter through radio signals from magnetic white dwarf stars, *Phys. Rev. D* 103 (11) (2021) 115021. [arXiv:2101.02585](#), [doi:10.1103/PhysRevD.103.115021](#).
- [116] R. Garani, N. Raj, J. Reynoso-Cordova, Could compact stars in globular clusters constrain dark matter? (3 2023). [arXiv:2303.18009](#).
- [117] M. McCullough, M. Fairbairn, Capture of Inelastic Dark Matter in White Dwarves, *Phys. Rev. D* 81 (2010) 083520. [arXiv:1001.2737](#), [doi:10.1103/PhysRevD.81.083520](#).
- [118] G. Bertone, M. Fairbairn, Compact Stars as Dark Matter Probes, *Phys. Rev. D* 77 (2008) 043515. [arXiv:0709.1485](#), [doi:10.1103/PhysRevD.77.043515](#).
- [119] D. Hooper, D. Spolyar, A. Vallinotto, N. Y. Gnedin, Inelastic Dark Matter As An Efficient Fuel For Compact Stars, *Phys. Rev. D* 81 (2010) 103531. [arXiv:1002.0005](#), [doi:10.1103/PhysRevD.81.103531](#).
- [120] C. Horowitz, Nuclear and dark matter heating in massive white dwarf stars (8 2020). [arXiv:2008.03291](#).
- [121] J. Bramante, A. Delgado, A. Martin, Multiscatter stellar capture of dark matter, *Phys. Rev. D* 96 (6) (2017) 063002. [arXiv:1703.04043](#), [doi:10.1103/PhysRevD.96.063002](#).
- [122] C. Kouvaris, P. Tinyakov, Constraining Asymmetric Dark Matter through observations of compact stars, *Phys. Rev. D* 83 (2011) 083512. [arXiv:1012.2039](#), [doi:10.1103/PhysRevD.83.083512](#).

- [123] M. Cermeno, M. Perez-Garcia, Gamma rays from dark mediators in white dwarfs, *Phys. Rev. D* 98 (6) (2018) 063002. [arXiv:1807.03318](https://arxiv.org/abs/1807.03318), [doi:10.1103/PhysRevD.98.063002](https://doi.org/10.1103/PhysRevD.98.063002).
- [124] B. Dasgupta, A. Gupta, A. Ray, Dark matter capture in celestial objects: Improved treatment of multiple scattering and updated constraints from white dwarfs, *JCAP* 08 (2019) 018. [arXiv:1906.04204](https://arxiv.org/abs/1906.04204), [doi:10.1088/1475-7516/2019/08/018](https://doi.org/10.1088/1475-7516/2019/08/018).
- [125] G. Panotopoulos, I. Lopes, Constraints on light dark matter particles using white dwarf stars, *International Journal of Modern Physics D* 29 (08) (2020) 2050058. [doi:10.1142/s0218271820500583](https://doi.org/10.1142/s0218271820500583).
- [126] R. K. Leane, T. Linden, P. Mukhopadhyay, N. Toro, Celestial-Body Focused Dark Matter Annihilation Throughout the Galaxy, *Phys. Rev. D* 103 (7) (2021) 075030. [arXiv:2101.12213](https://arxiv.org/abs/2101.12213), [doi:10.1103/PhysRevD.103.075030](https://doi.org/10.1103/PhysRevD.103.075030).
- [127] N. F. Bell, G. Busoni, M. E. Ramirez-Quezada, S. Robles, M. Virgato, Improved treatment of dark matter capture in white dwarfs, *JCAP* 10 (2021) 083. [arXiv:2104.14367](https://arxiv.org/abs/2104.14367), [doi:10.1088/1475-7516/2021/10/083](https://doi.org/10.1088/1475-7516/2021/10/083).
- [128] A. Biswas, A. Kar, H. Kim, S. Scopel, L. Velasco-Sevilla, Improved white dwarves constraints on inelastic dark matter and left-right symmetric models, *Phys. Rev. D* 106 (8) (2022) 083012. [arXiv:2206.06667](https://arxiv.org/abs/2206.06667), [doi:10.1103/PhysRevD.106.083012](https://doi.org/10.1103/PhysRevD.106.083012).
- [129] M. E. Ramirez-Quezada, Constraining dark matter interactions mediated by a light scalar with white dwarfs (12 2022). [arXiv:2212.09785](https://arxiv.org/abs/2212.09785).
- [130] L. Searle, R. Zinn, Composition of halo clusters and the formation of the galactic halo., *apj* 225 (1978) 357–379. [doi:10.1086/156499](https://doi.org/10.1086/156499).
- [131] P. J. E. Peebles, Dark matter and the origin of galaxies and globular star clusters, *apj* 277 (1984) 470–477. [doi:10.1086/161714](https://doi.org/10.1086/161714).
- [132] J. Diemand, P. Madau, B. Moore, The distribution and kinematics of early high- $\sigma$  peaks in present-day haloes: implications for rare objects and old stellar populations, *MNRAS* 364 (2) (2005) 367–383. [arXiv:astro-ph/0506615](https://arxiv.org/abs/astro-ph/0506615), [doi:10.1111/j.1365-2966.2005.09604.x](https://doi.org/10.1111/j.1365-2966.2005.09604.x).
- [133] A. V. Kravtsov, O. Y. Gnedin, Formation of globular clusters in hierarchical cosmology, *Astrophys. J.* 623 (2005) 650–665. [arXiv:astro-ph/0305199](https://arxiv.org/abs/astro-ph/0305199), [doi:10.1086/428636](https://doi.org/10.1086/428636).
- [134] I. Claydon, M. Gieles, A. L. Varri, D. C. Heggie, A. Zocchi, Spherical models of star clusters with potential escapers, *Monthly Notices of the Royal Astronomical Society* 487 (1) (2019) 147–160. [doi:10.1093/mnras/stz1109](https://doi.org/10.1093/mnras/stz1109).
- [135] K. M. Ashman, S. E. Zepf, Some constraints on the formation of globular clusters, *The Astronomical Journal* 122 (4) (2001) 1888–1895. [doi:10.1086/323133](https://doi.org/10.1086/323133).
- [136] S. van den Bergh, How did globular clusters form?, *The Astrophysical Journal* 559 (2) (2001) L113–L114. [doi:10.1086/323754](https://doi.org/10.1086/323754).
- [137] B. Willman, J. Strader, 'Galaxy,' Defined, *Astron. J.* 144 (2012) 76. [arXiv:1203.2608](https://arxiv.org/abs/1203.2608), [doi:10.1088/0004-6256/144/3/76](https://doi.org/10.1088/0004-6256/144/3/76).
- [138] A. J. Evans, L. E. Strigari, P. Zivick, Dark and luminous mass components of Omega Centauri from stellar kinematics, *Mon. Not. Roy. Astron. Soc.* 511 (3) (2022) 4251–4264. [arXiv:2109.10998](https://arxiv.org/abs/2109.10998), [doi:10.1093/mnras/stac261](https://doi.org/10.1093/mnras/stac261).
- [139] R. Ibata, C. Nipoti, A. Sollima, M. Bellazzini, S. C. Chapman, E. Dalessandro, Do globular clusters possess dark matter haloes? a case study in NGC 2419, *Monthly Notices of the Royal Astronomical Society* 428 (4) (2012) 3648–3659. [doi:10.1093/mnras/sts302](https://doi.org/10.1093/mnras/sts302).  
URL <https://doi.org/10.1093/mnras/sts302>
- [140] R. Krall, M. Reece, Last Electroweak WIMP Standing: Pseudo-Dirac Higgsino Status and Compact Stars as Future Probes, *Chin. Phys. C* 42 (4) (2018) 043105. [arXiv:1705.04843](https://arxiv.org/abs/1705.04843), [doi:10.1088/1674-1137/42/4/043105](https://doi.org/10.1088/1674-1137/42/4/043105).
- [141] R. Janish, V. Narayan, P. Riggins, Type Ia supernovae from dark matter core collapse, *Phys. Rev. D* 100 (3) (2019) 035008. [arXiv:1905.00395](https://arxiv.org/abs/1905.00395), [doi:10.1103/PhysRevD.100.035008](https://doi.org/10.1103/PhysRevD.100.035008).
- [142] K. Petraki, R. R. Volkas, Review of asymmetric dark matter, *Int. J. Mod. Phys. A* 28 (2013) 1330028. [arXiv:1305.4939](https://arxiv.org/abs/1305.4939), [doi:10.1142/S0217751X13300287](https://doi.org/10.1142/S0217751X13300287).
- [143] J. F. Acevedo, J. Bramante, A. Goodman, J. Kopp, T. Opferkuch, Dark Matter, Destroyer of Worlds: Neutrino, Thermal, and Existential Signatures from Black Holes in the Sun and Earth, *JCAP* 04 (2021) 026. [arXiv:2012.09176](https://arxiv.org/abs/2012.09176), [doi:10.1088/1475-7516/2021/04/026](https://doi.org/10.1088/1475-7516/2021/04/026).
- [144] S. A. R. Ellis, Premature black hole death of Population III stars by dark matter, *JCAP* 05 (05) (2022) 025. [arXiv:2111.02414](https://arxiv.org/abs/2111.02414), [doi:10.1088/1475-7516/2022/05/025](https://doi.org/10.1088/1475-7516/2022/05/025).
- [145] M. D. Diamond, D. E. Kaplan, Constraints on relic magnetic black holes, *JHEP* 03 (2022) 157. [arXiv:2103.01850](https://arxiv.org/abs/2103.01850), [doi:10.1007/JHEP03\(2022\)157](https://doi.org/10.1007/JHEP03(2022)157).
- [146] P. W. Graham, S. Rajendran, J. Varela, Dark Matter Triggers of Supernovae, *Phys. Rev. D* 92 (6) (2015) 063007. [arXiv:1505.04444](https://arxiv.org/abs/1505.04444), [doi:10.1103/PhysRevD.92.063007](https://doi.org/10.1103/PhysRevD.92.063007).
- [147] S. C. Leung, M. C. Chu, L. M. Lin, K. W. Wong, Dark-matter admixed white dwarfs, *Phys. Rev. D* 87 (12) (2013) 123506. [arXiv:1305.6142](https://arxiv.org/abs/1305.6142), [doi:10.1103/PhysRevD.87.123506](https://doi.org/10.1103/PhysRevD.87.123506).

- [148] J. F. Acevedo, J. Bramante, Supernovae Sparked By Dark Matter in White Dwarfs, *Phys. Rev. D* 100 (4) (2019) 043020. [arXiv:1904.11993](#), [doi:10.1103/PhysRevD.100.043020](#).
- [149] P. W. Graham, R. Janish, V. Narayan, S. Rajendran, P. Riggins, White Dwarfs as Dark Matter Detectors, *Phys. Rev. D* 98 (11) (2018) 115027. [arXiv:1805.07381](#), [doi:10.1103/PhysRevD.98.115027](#).
- [150] J. F. Acevedo, J. Bramante, A. Goodman, Nuclear fusion inside dark matter, *Phys. Rev. D* 103 (12) (2021) 123022. [arXiv:2012.10998](#), [doi:10.1103/PhysRevD.103.123022](#).
- [151] P. Montero-Camacho, X. Fang, G. Vasquez, M. Silva, C. M. Hirata, Revisiting constraints on asteroid-mass primordial black holes as dark matter candidates, *JCAP* 08 (2019) 031. [arXiv:1906.05950](#), [doi:10.1088/1475-7516/2019/08/031](#).
- [152] J. S. Sidhu, G. D. Starkman, Reconsidering astrophysical constraints on macroscopic dark matter, *Physical Review D* 101 (8) (apr 2020). [doi:10.1103/physrevd.101.083503](#).
- [153] N. Raj, Supernovae and superbursts by dark matter clumps (6 2023). [arXiv:2306.14981](#).
- [154] A. Das, S. A. R. Ellis, P. C. Schuster, K. Zhou, Stellar Shocks From Dark Matter (6 2021). [arXiv:2106.09033](#).
- [155] H. Steigerwald, E. Tejeda, Bondi-Hoyle-Lyttleton Accretion in a Reactive Medium: Detonation Ignition and a Mechanism for Type Ia Supernovae, *Phys. Rev. Lett.* 127 (1) (2021) 011101. [arXiv:2104.07066](#), [doi:10.1103/PhysRevLett.127.011101](#).
- [156] H. Steigerwald, V. Marra, S. Profumo, Revisiting constraints on asymmetric dark matter from collapse in white dwarf stars, *Phys. Rev. D* 105 (8) (2022) 083507. [arXiv:2203.09054](#), [doi:10.1103/PhysRevD.105.083507](#).
- [157] R. A. Scalzo, A. J. Ruiten, S. A. Sim, The ejected mass distribution of type Ia supernovae: A significant rate of non-Chandrasekhar-mass progenitors, *Mon. Not. Roy. Astron. Soc.* 445 (3) (2014) 2535–2544. [arXiv:1408.6601](#), [doi:10.1093/mnras/stu1808](#).
- [158] Y. C. Pan, et al., The Host Galaxies of Type Ia Supernovae Discovered by the Palomar Transient Factory, *Mon. Not. Roy. Astron. Soc.* 438 (2) (2014) 1391–1416. [arXiv:1311.6344](#), [doi:10.1093/mnras/stt2287](#).
- [159] M. M. Kasliwal, et al., Calcium-rich gap transients in the remote outskirts of galaxies, *Astrophys. J.* 755 (2012) 161. [arXiv:1111.6109](#), [doi:10.1088/0004-637X/755/2/161](#).
- [160] H. Steigerwald, D. Rodrigues, S. Profumo, V. Marra, Type Ia supernova magnitude step from the local dark matter environment, *Mon. Not. Roy. Astron. Soc.* 510 (4) (2022) 4779–4795. [arXiv:2112.09739](#), [doi:10.1093/mnras/stab3747](#).
- [161] J. Smirnov, A. Goobar, T. Linden, E. Mörtzell, White Dwarfs in Dwarf Spheroidal Galaxies: A New Class of Compact-Dark-Matter Detectors (10 2022). [arXiv:2211.00013](#).
- [162] S.-C. Leung, S. Zha, M.-C. Chu, L.-M. Lin, K. Nomoto, Accretion-Induced Collapse of Dark Matter Admixed White Dwarfs – I: Formation of Low-mass Neutron Stars, *Astrophys. J.* 884 (2019) 9. [arXiv:1908.05102](#), [doi:10.3847/1538-4357/ab3b5e](#).
- [163] S. Zha, M.-C. Chu, S.-C. Leung, L.-M. Lin, Accretion-Induced Collapse of Dark Matter Admixed White Dwarfs – II: Rotation and Gravitational-wave Signals (8 2019). [arXiv:1908.05150](#), [doi:10.3847/1538-4357/ab3640](#).
- [164] J. Bramante, B. J. Kavanagh, N. Raj, Scattering Searches for Dark Matter in Subhalos: Neutron Stars, Cosmic Rays, and Old Rocks, *Phys. Rev. Lett.* 128 (23) (2022) 231801. [arXiv:2109.04582](#), [doi:10.1103/PhysRevLett.128.231801](#).
- [165] R. Balkin, J. Serra, K. Springmann, S. Stelzl, A. Weiler, White dwarfs as a probe of light QCD axions (11 2022). [arXiv:2211.02661](#).
- [166] A. Joglekar, N. Raj, P. Tanedo, H.-B. Yu, Kinetic Heating from Contact Interactions with Relativistic Targets: Electrons Capture Dark Matter in Neutron Stars (4 2020). [arXiv:2004.09539](#).
- [167] R. Garani, Y. Genolini, T. Hambye, New Analysis of Neutron Star Constraints on Asymmetric Dark Matter, *JCAP* 1905 (05) (2019) 035. [arXiv:1812.08773](#), [doi:10.1088/1475-7516/2019/05/035](#).
- [168] F. Anzuini, N. F. Bell, G. Busoni, T. F. Motta, S. Robles, A. W. Thomas, M. Virgato, Improved Treatment of Dark Matter Capture in Neutron Stars III: Nucleon and Exotic Targets (8 2021). [arXiv:2108.02525](#).
- [169] N. F. Bell, G. Busoni, S. Robles, M. Virgato, Improved Treatment of Dark Matter Capture in Neutron Stars (4 2020). [arXiv:2004.14888](#).
- [170] N. F. Bell, G. Busoni, T. F. Motta, S. Robles, A. W. Thomas, M. Virgato, Nucleon Structure and Strong Interactions in Dark Matter Capture in Neutron Stars (12 2020). [arXiv:2012.08918](#).
- [171] W. DeRocco, M. Galanis, R. Lasenby, Dark matter scattering in astrophysical media: collective effects, *JCAP* 05 (05) (2022) 015. [arXiv:2201.05167](#), [doi:10.1088/1475-7516/2022/05/015](#).
- [172] B. Dasgupta, A. Gupta, A. Ray, Dark matter capture in celestial objects: light mediators, self-interactions, and complementarity with direct detection, *JCAP* 10 (2020) 023. [arXiv:2006.10773](#), [doi:10.1088/1475-7516/2020/10/023](#).
- [173] D. Bose, S. Sarkar, Impact of galactic distributions in celestial capture of dark matter, *Phys. Rev. D* 107 (6) (2023) 063010. [arXiv:2211.16982](#), [doi:10.1103/PhysRevD.107.063010](#).
- [174] M. Baryakhtar, J. Bramante, S. W. Li, T. Linden, N. Raj, Dark Kinetic Heating of Neutron Stars and An Infrared Window On WIMPs, SIMPs, and Pure Higgsinos, *Phys. Rev. Lett.* 119 (13) (2017) 131801. [arXiv:1704.01577](#), [doi:10.1103/PhysRevLett.119.131801](#).



- [175] W. Skidmore, et al., Thirty Meter Telescope Detailed Science Case: 2015, Res. Astron. Astrophys. 15 (12) (2015) 1945–2140. [arXiv:1505.01195](#), [doi:10.1088/1674-4527/15/12/001](#).
- [176] B. Neichel, D. Mouillet, E. Gendron, C. Correia, J. F. Sauvage, T. Fusco, Overview of the european extremely large telescope and its instrument suite (2018). [arXiv:1812.06639](#).
- [177] J. P. Gardner, et al., The James Webb Space Telescope, Space Sci. Rev. 123 (2006) 485. [arXiv:astro-ph/0606175](#), [doi:10.1007/s11214-006-8315-7](#).
- [178] R. Nan, D. Li, C. Jin, Q. Wang, L. Zhu, W. Zhu, H. Zhang, Y. Yue, L. Qian, [The five-hundred-meter aperture spherical radio telescope \(fast\) project](#), International Journal of Modern Physics D 20 (06) (2011) 989–1024. [doi:10.1142/S0218271811019335](#).  
URL <http://dx.doi.org/10.1142/S0218271811019335>
- [179] M. Amiri, K. M. Bandura, P. J. Boyle, C. Brar, J.-F. Cliche, K. Crowter, D. Cubranic, P. B. Demorest, N. T. Denman, M. Dobbs, et al., [The chime pulsar project: System overview](#), The Astrophysical Journal Supplement Series 255 (1) (2021) 5. [doi:10.3847/1538-4365/abfdcb](#).  
URL <http://dx.doi.org/10.3847/1538-4365/abfdcb>
- [180] C. L. Carilli, S. Rawlings, Science with the Square Kilometer Array: Motivation, key science projects, standards and assumptions, New Astron. Rev. 48 (2004) 979. [arXiv:astro-ph/0409274](#), [doi:10.1016/j.newar.2004.09.001](#).
- [181] A.-C. Eilers, D. W. Hogg, H.-W. Rix, M. K. Ness, [The circular velocity curve of the milky way from 5 to 25 kpc](#), The Astrophysical Journal 871 (1) (2019) 120. [doi:10.3847/1538-4357/aaf648](#).  
URL <http://dx.doi.org/10.3847/1538-4357/aaf648>
- [182] L. Brayer, P. Tinyakov, Enhancement of dark matter capture by neutron stars in binary systems, Phys. Rev. Lett. 109 (2012) 061301. [arXiv:1111.3205](#), [doi:10.1103/PhysRevLett.109.061301](#).
- [183] R. Garani, S. Palomares-Ruiz, Evaporation of dark matter from celestial bodies, JCAP 05 (05) (2022) 042. [arXiv:2104.12757](#), [doi:10.1088/1475-7516/2022/05/042](#).
- [184] C. Kouvaris, WIMP Annihilation and Cooling of Neutron Stars, Phys. Rev. D 77 (2008) 023006. [arXiv:0708.2362](#), [doi:10.1103/PhysRevD.77.023006](#).
- [185] C.-S. Chen, Y.-H. Lin, Reheating neutron stars with the annihilation of self-interacting dark matter, JHEP 08 (2018) 069. [arXiv:1804.03409](#), [doi:10.1007/JHEP08\(2018\)069](#).
- [186] N. Raj, P. Tanedo, H.-B. Yu, Neutron stars at the dark matter direct detection frontier, Phys. Rev. D 97 (4) (2018) 043006. [arXiv:1707.09442](#), [doi:10.1103/PhysRevD.97.043006](#).
- [187] E. O. Ofek, Space and Velocity Distributions of Galactic Isolated Old Neutron Stars, *pasp* 121 (882) (2009) 814. [arXiv:0910.3684](#), [doi:10.1086/605389](#).
- [188] N. Sartore, E. Ripamonti, A. Treves, R. Turolla, [Galactic neutron stars](#), Astronomy and Astrophysics 510 (2010) A23. [doi:10.1051/0004-6361/200912222](#).  
URL <http://dx.doi.org/10.1051/0004-6361/200912222>
- [189] B. Bertoni, A. E. Nelson, S. Reddy, Dark Matter Thermalization in Neutron Stars, Phys. Rev. D 88 (2013) 123505. [arXiv:1309.1721](#), [doi:10.1103/PhysRevD.88.123505](#).
- [190] N. F. Bell, G. Busoni, S. Robles, Capture of Leptophilic Dark Matter in Neutron Stars, JCAP 1906 (06) (2019) 054. [arXiv:1904.09803](#), [doi:10.1088/1475-7516/2019/06/054](#).
- [191] R. Garani, J. Heeck, Dark matter interactions with muons in neutron stars, Phys. Rev. D 100 (3) (2019) 035039. [arXiv:1906.10145](#), [doi:10.1103/PhysRevD.100.035039](#).
- [192] A. Joglekar, N. Raj, P. Tanedo, H.-B. Yu, Relativistic capture of dark matter by electrons in neutron stars (11 2019). [arXiv:1911.13293](#).
- [193] N. F. Bell, G. Busoni, S. Robles, M. Virgato, Improved Treatment of Dark Matter Capture in Neutron Stars II: Leptonic Targets, JCAP 03 (2021) 086. [arXiv:2010.13257](#), [doi:10.1088/1475-7516/2021/03/086](#).
- [194] R. Garani, A. Gupta, N. Raj, Observing the thermalization of dark matter in neutron stars, Phys. Rev. D 103 (4) (2021) 043019. [arXiv:2009.10728](#), [doi:10.1103/PhysRevD.103.043019](#).
- [195] J. Coffey, D. McKeen, D. E. Morrissey, N. Raj, Neutron star observations of pseudoscalar-mediated dark matter, Phys. Rev. D 106 (11) (2022) 115019. [arXiv:2207.02221](#), [doi:10.1103/PhysRevD.106.115019](#).
- [196] N. F. Bell, G. Busoni, S. Robles, Heating up Neutron Stars with Inelastic Dark Matter, JCAP 1809 (09) (2018) 018. [arXiv:1807.02840](#), [doi:10.1088/1475-7516/2018/09/018](#).
- [197] G. Alvarez, A. Joglekar, M. Phoroutan-Mehr, H.-B. Yu, Heating Neutron Stars with Inelastic Dark Matter and Relativistic Targets (1 2023). [arXiv:2301.08767](#).
- [198] J. Bramante, A. Delgado, A. Martin, Multiscatter stellar capture of dark matter, Phys. Rev. D 96 (6) (2017) 063002. [arXiv:1703.04043](#), [doi:10.1103/PhysRevD.96.063002](#).
- [199] C. Ilie, J. Pilawa, S. Zhang, Comment on “Multiscatter stellar capture of dark matter”, Phys. Rev. D 102 (4) (2020) 048301. [arXiv:2005.05946](#), [doi:10.1103/PhysRevD.102.048301](#).

- [200] A. de Lavallaz, M. Fairbairn, Neutron Stars as Dark Matter Probes, *Phys. Rev. D* 81 (2010) 123521. [arXiv:1004.0629](#), [doi:10.1103/PhysRevD.81.123521](#).
- [201] S. Reddy, M. Prakash, J. M. Lattimer, Neutrino interactions in hot and dense matter, *Phys. Rev. D* 58 (1998) 013009. [arXiv:astro-ph/9710115](#), [doi:10.1103/PhysRevD.58.013009](#).
- [202] D. Bose, T. N. Maity, T. S. Ray, Neutrinos from captured dark matter annihilation in a galactic population of neutron stars, *JCAP* 05 (05) (2022) 001. [arXiv:2108.12420](#), [doi:10.1088/1475-7516/2022/05/001](#).
- [203] T. T. Q. Nguyen, T. M. P. Tait, Bounds on Long-lived Dark Matter Mediators from Neutron Stars (12 2022). [arXiv:2212.12547](#).
- [204] H. Davoudiasl, D. E. Morrissey, K. Sigurdson, S. Tulin, Hylogenesis: A Unified Origin for Baryonic Visible Matter and Antibaryonic Dark Matter, *Phys. Rev. Lett.* 105 (2010) 211304. [arXiv:1008.2399](#), [doi:10.1103/PhysRevLett.105.211304](#).
- [205] H. Davoudiasl, D. E. Morrissey, K. Sigurdson, S. Tulin, Baryon Destruction by Asymmetric Dark Matter, *Phys. Rev. D* 84 (2011) 096008. [arXiv:1106.4320](#), [doi:10.1103/PhysRevD.84.096008](#).
- [206] M. Jin, Y. Gao, Nucleon - Light Dark Matter Annihilation through Baryon Number Violation, *Phys. Rev. D* 98 (7) (2018) 075026. [arXiv:1808.10644](#), [doi:10.1103/PhysRevD.98.075026](#).
- [207] W.-Y. Keung, D. Marfatia, P.-Y. Tseng, Heating neutron stars with GeV dark matter, *JHEP* 07 (2020) 181. [arXiv:2001.09140](#), [doi:10.1007/JHEP07\(2020\)181](#).
- [208] Y. Bai, J. Berger, M. Korwar, N. Orlofsky, Phenomenology of magnetic black holes with electroweak-symmetric coronas, *JHEP* 10 (2020) 210. [arXiv:2007.03703](#), [doi:10.1007/JHEP10\(2020\)210](#).
- [209] A. Herrero, M. A. Pérez-García, J. Silk, C. Albertus, Dark matter and bubble nucleation in old neutron stars, *Phys. Rev. D* 100 (10) (2019) 103019. [arXiv:1905.00893](#), [doi:10.1103/PhysRevD.100.103019](#).
- [210] E. W. Kolb, S. A. Colgate, J. A. Harvey, Monopole Catalysis of Nucleon Decay in Neutron Stars, *Phys. Rev. Lett.* 49 (1982) 1373. [doi:10.1103/PhysRevLett.49.1373](#).
- [211] S. Dimopoulos, J. Preskill, F. Wilczek, Catalyzed Nucleon Decay in Neutron Stars, *Phys. Lett. B* 119 (1982) 320. [doi:10.1016/0370-2693\(82\)90679-7](#).
- [212] R. Garani, J. Heeck, Dark Matter Interactions with Muons in Neutron Stars, *Phys. Rev. D* 100 (3) (2019) 035039. [arXiv:1906.10145](#), [doi:10.1103/PhysRevD.100.035039](#).
- [213] M. Fujiwara, K. Hamaguchi, N. Nagata, J. Zheng, Capture of Electroweak Multiplet Dark Matter in Neutron Stars (4 2022). [arXiv:2204.02238](#).
- [214] D. A. Camargo, F. S. Queiroz, R. Sturani, Detecting Dark Matter with Neutron Star Spectroscopy, *JCAP* 1909 (09) (2019) 051. [arXiv:1901.05474](#), [doi:10.1088/1475-7516/2019/09/051](#).
- [215] T. N. Maity, F. S. Queiroz, Detecting bosonic dark matter with neutron stars (2021). [arXiv:2104.02700](#).
- [216] G.-L. Lin, Y.-H. Lin, Exploring dark sector parameters in light of neutron star temperatures, *Phys. Rev. D* 104 (6) (2021) 063021. [arXiv:2102.11151](#), [doi:10.1103/PhysRevD.104.063021](#).
- [217] Y.-P. Zeng, X. Xiao, W. Wang, Constraints on Pseudo-Nambu-Goldstone dark matter from direct detection experiment and neutron star reheating temperature, *Phys. Lett. B* 824 (2022) 136822. [arXiv:2108.11381](#), [doi:10.1016/j.physletb.2021.136822](#).
- [218] K. Hamaguchi, N. Nagata, M. E. Ramirez-Quezada, Neutron Star Heating in Dark Matter Models for the Muon  $g - 2$  Discrepancy (4 2022). [arXiv:2204.02413](#).
- [219] A. Treves, R. Turolla, S. Zane, M. Colpi, Isolated neutron stars: accretors and coolers, *Publ. Astron. Soc. Pac.* 112 (2000) 297. [arXiv:astro-ph/9911430](#), [doi:10.1086/316529](#).
- [220] E. B. Jenkins, A unified representation of gas-phase element depletions in the interstellar medium\*, *The Astrophysical Journal* 700 (2) (2009) 1299. [doi:10.1088/0004-637X/700/2/1299](#). URL <https://dx.doi.org/10.1088/0004-637X/700/2/1299>
- [221] K. Hamaguchi, N. Nagata, K. Yanagi, Dark Matter Heating vs. Rotochemical Heating in Old Neutron Stars, *Phys. Lett. B* 795 (2019) 484–489. [arXiv:1905.02991](#), [doi:10.1016/j.physletb.2019.06.060](#).
- [222] K. Yanagi, N. Nagata, K. Hamaguchi, Cooling Theory Faced with Old Warm Neutron Stars: Role of Non-Equilibrium Processes with Proton and Neutron Gaps, *Mon. Not. Roy. Astron. Soc.* 492 (4) (2020) 5508–5523. [arXiv:1904.04667](#), [doi:10.1093/mnras/staa076](#).
- [223] D. Gonzalez, A. Reisenegger, Internal heating of old neutron stars: contrasting different mechanisms, *AAP* 522 (2010) A16. [arXiv:1005.5699](#), [doi:10.1051/0004-6361/201015084](#).
- [224] F. Köpp, J. E. Horvath, D. Hadjimichef, C. A. Z. Vasconcellos, P. O. Hess, Internal heating mechanisms in neutron stars (8 2022). [arXiv:2208.07770](#).
- [225] T. Prinz, W. Becker, A Search for X-ray Counterparts of Radio Pulsars (11 2015). [arXiv:1511.07713](#).
- [226] J. A. Pons, J. A. Miralles, U. Geppert, Magneto–thermal evolution of neutron stars, *Astron. Astrophys.* 496 (2009) 207–216. [arXiv:0812.3018](#), [doi:10.1051/0004-6361:200811229](#).



- [227] T. D. P. Edwards, B. J. Kavanagh, L. Visinelli, C. Weniger, Transient Radio Signatures from Neutron Star Encounters with QCD Axion Miniclusters (11 2020). [arXiv:2011.05378](#).
- [228] A. L. Erickcek, K. Sigurdson, [Reheating effects in the matter power spectrum and implications for substructure](#), Phys. Rev. D 84 (2011) 083503. [doi:10.1103/PhysRevD.84.083503](#).  
URL <https://link.aps.org/doi/10.1103/PhysRevD.84.083503>
- [229] G. Barenboim, J. Rasero, Structure Formation during an early period of matter domination, JHEP 04 (2014) 138. [arXiv:1311.4034](#), [doi:10.1007/JHEP04\(2014\)138](#).
- [230] J. Fan, O. Özsoy, S. Watson, [Nonthermal histories and implications for structure formation](#), Phys. Rev. D 90 (2014) 043536. [doi:10.1103/PhysRevD.90.043536](#).  
URL <https://link.aps.org/doi/10.1103/PhysRevD.90.043536>
- [231] J. A. Dror, E. Kuflik, B. Melcher, S. Watson, [Concentrated dark matter: Enhanced small-scale structure from codecaying dark matter](#), Phys. Rev. D 97 (2018) 063524. [doi:10.1103/PhysRevD.97.063524](#).  
URL <https://link.aps.org/doi/10.1103/PhysRevD.97.063524>
- [232] P. W. Graham, J. Mardon, S. Rajendran, [Vector dark matter from inflationary fluctuations](#), Phys. Rev. D 93 (2016) 103520. [doi:10.1103/PhysRevD.93.103520](#).  
URL <https://link.aps.org/doi/10.1103/PhysRevD.93.103520>
- [233] M. R. Buckley, A. DiFranzo, Collapsed Dark Matter Structures, Phys. Rev. Lett. 120 (5) (2018) 051102. [arXiv:1707.03829](#), [doi:10.1103/PhysRevLett.120.051102](#).
- [234] S. Nussinov, Y. Zhang, Dark Matter Clusters and Time Correlations in Direct Detection Experiments, JHEP 03 (2020) 133. [arXiv:1807.00846](#), [doi:10.1007/JHEP03\(2020\)133](#).
- [235] G. Barenboim, N. Blinov, A. Stebbins, Smallest Remnants of Early Matter Domination (7 2021). [arXiv:2107.10293](#).
- [236] S. Guillot, G. G. Pavlov, C. Reyes, A. Reisenegger, L. Rodriguez, B. Rangelov, O. Kargaltsev, Hubble Space Telescope Nondetection of PSR J2144–3933: The Coldest Known Neutron Star, Astrophys. J. 874 (2) (2019) 175. [arXiv:1901.07998](#), [doi:10.3847/1538-4357/ab0f38](#).
- [237] H. Bondi, F. Hoyle, On the mechanism of accretion by stars, Mon. Not. Roy. Astron. Soc. 104 (1944) 273. [doi:10.1093/mnras/104.5.273](#).
- [238] H. Bondi, On spherically symmetrical accretion, Mon. Not. Roy. Astron. Soc. 112 (1952) 195. [doi:10.1093/mnras/112.2.195](#).
- [239] M. C. Begelman, Nearly collisionless spherical accretion., Mon. Not. Roy. Astron. Soc. 181 (1977) 347–363. [doi:10.1093/mnras/181.2.347](#).
- [240] A. Afzal, et al., The NANOGrav 15 yr Data Set: Search for Signals from New Physics, Astrophys. J. Lett. 951 (1) (2023) L11. [arXiv:2306.16219](#), [doi:10.3847/2041-8213/acdc91](#).
- [241] M. I. Gresham, V. S. H. Lee, K. M. Zurek, Astrophysical observations of a dark matter-Baryon fifth force, JCAP 02 (2023) 048. [arXiv:2209.03963](#), [doi:10.1088/1475-7516/2023/02/048](#).
- [242] A. Gould, B. T. Draine, R. W. Romani, S. Nussinov, Neutron Stars: Graveyard of Charged Dark Matter, Phys. Lett. B238 (1990) 337–343. [doi:10.1016/0370-2693\(90\)91745-W](#).
- [243] C. Kouvaris, P. Tinyakov, Can Neutron stars constrain Dark Matter?, Phys. Rev. D82 (2010) 063531. [arXiv:1004.0586](#), [doi:10.1103/PhysRevD.82.063531](#).
- [244] S. D. McDermott, H.-B. Yu, K. M. Zurek, Constraints on Scalar Asymmetric Dark Matter from Black Hole Formation in Neutron Stars, Phys. Rev. D85 (2012) 023519. [arXiv:1103.5472](#), [doi:10.1103/PhysRevD.85.023519](#).
- [245] C. Kouvaris, P. Tinyakov, Excluding Light Asymmetric Bosonic Dark Matter, Phys. Rev. Lett. 107 (2011) 091301. [arXiv:1104.0382](#), [doi:10.1103/PhysRevLett.107.091301](#).
- [246] C. Kouvaris, Limits on Self-Interacting Dark Matter, Phys. Rev. Lett. 108 (2012) 191301. [arXiv:1111.4364](#), [doi:10.1103/PhysRevLett.108.191301](#).
- [247] J. Bramante, K. Fukushima, J. Kumar, Constraints on bosonic dark matter from observation of old neutron stars, Phys. Rev. D87 (5) (2013) 055012. [arXiv:1301.0036](#), [doi:10.1103/PhysRevD.87.055012](#).
- [248] N. F. Bell, A. Melatos, K. Petraki, Realistic neutron star constraints on bosonic asymmetric dark matter, Phys. Rev. D87 (12) (2013) 123507. [arXiv:1301.6811](#), [doi:10.1103/PhysRevD.87.123507](#).
- [249] J. Bramante, T. Linden, Detecting Dark Matter with Imploding Pulsars in the Galactic Center, Phys. Rev. Lett. 113 (19) (2014) 191301. [arXiv:1405.1031](#), [doi:10.1103/PhysRevLett.113.191301](#).
- [250] J. Bramante, T. Linden, On the  $r$ -Process Enrichment of Dwarf Spheroidal Galaxies, Astrophys. J. 826 (1) (2016) 57. [arXiv:1601.06784](#), [doi:10.3847/0004-637X/826/1/57](#).
- [251] J. Bramante, T. Linden, Y.-D. Tsai, Searching for dark matter with neutron star mergers and quiet kilonovae, Phys. Rev. D 97 (5) (2018) 055016. [arXiv:1706.00001](#), [doi:10.1103/PhysRevD.97.055016](#).
- [252] R. Garani, Y. Genolini, T. Hambye, New Analysis of Neutron Star Constraints on Asymmetric Dark Matter, JCAP 1905 (05) (2019) 035. [arXiv:1812.08773](#), [doi:10.1088/1475-7516/2019/05/035](#).

- [253] C. Kouvaris, P. Tinyakov, M. H. Tytgat, NonPrimordial Solar Mass Black Holes, *Phys. Rev. Lett.* 121 (22) (2018) 221102. [arXiv:1804.06740](#), [doi:10.1103/PhysRevLett.121.221102](#).
- [254] J. Kopp, R. Laha, T. Opferkuch, W. Shepherd, Cuckoo’s eggs in neutron stars: can LIGO hear chirps from the dark sector?, *JHEP* 11 (2018) 096. [arXiv:1807.02527](#), [doi:10.1007/JHEP11\(2018\)096](#).
- [255] W. E. East, L. Lehner, Fate of a neutron star with an endoparasitic black hole and implications for dark matter, *Phys. Rev. D* 100 (12) (2019) 124026. [arXiv:1909.07968](#), [doi:10.1103/PhysRevD.100.124026](#).
- [256] Y.-D. Tsai, A. Palmese, S. Profumo, T. Jeltema, Is GW170817 a Multimessenger Neutron Star-Primordial Black Hole Merger?, *JCAP* 10 (2021) 019. [arXiv:2007.03686](#), [doi:10.1088/1475-7516/2021/10/019](#).
- [257] V. Takhistov, G. M. Fuller, A. Kusenko, Test for the Origin of Solar Mass Black Holes, *Phys. Rev. Lett.* 126 (7) (2021) 071101. [arXiv:2008.12780](#), [doi:10.1103/PhysRevLett.126.071101](#).
- [258] B. Dasgupta, R. Laha, A. Ray, Low Mass Black Holes from Dark Core Collapse (9 2020). [arXiv:2009.01825](#).
- [259] R. Garani, D. Levkov, P. Tinyakov, Solar mass black holes from neutron stars and bosonic dark matter, *Phys. Rev. D* 105 (6) (2022) 063019. [arXiv:2112.09716](#), [doi:10.1103/PhysRevD.105.063019](#).
- [260] P. Giffin, J. Lloyd, S. D. McDermott, S. Profumo, Neutron star quantum death by small black holes, *Phys. Rev. D* 105 (12) (2022) 123030. [arXiv:2105.06504](#), [doi:10.1103/PhysRevD.105.123030](#).
- [261] A. Ray, Celestial objects as strongly-interacting nonannihilating dark matter detectors, *Phys. Rev. D* 107 (8) (2023) 083012. [arXiv:2301.03625](#), [doi:10.1103/PhysRevD.107.083012](#).
- [262] J. Fuller, C. Ott, Dark Matter-induced Collapse of Neutron Stars: A Possible Link Between Fast Radio Bursts and the Missing Pulsar Problem, *Mon. Not. Roy. Astron. Soc.* 450 (1) (2015) L71–L75. [arXiv:1412.6119](#), [doi:10.1093/mnrasl/slv049](#).
- [263] K. M. Zurek, Asymmetric Dark Matter: Theories, Signatures, and Constraints, *Phys. Rept.* 537 (2014) 91–121. [arXiv:1308.0338](#), [doi:10.1016/j.physrep.2013.12.001](#).
- [264] J. Kumar, Asymmetric Dark Matter, *AIP Conf. Proc.* 1604 (1) (2015) 389–396. [arXiv:1308.4513](#), [doi:10.1063/1.4883455](#).
- [265] J. Bramante, K. Fukushima, J. Kumar, E. Stopnitzky, Bounds on self-interacting fermion dark matter from observations of old neutron stars, *Phys. Rev. D* 89 (1) (2014) 015010. [arXiv:1310.3509](#), [doi:10.1103/PhysRevD.89.015010](#).
- [266] A. M. Green, B. J. Kavanagh, Primordial Black Holes as a dark matter candidate, *J. Phys. G* 48 (4) (2021) 043001. [arXiv:2007.10722](#), [doi:10.1088/1361-6471/abc534](#).
- [267] B. Carr, F. Kuhnel, M. Sandstad, Primordial Black Holes as Dark Matter, *Phys. Rev. D* 94 (8) (2016) 083504. [arXiv:1607.06077](#), [doi:10.1103/PhysRevD.94.083504](#).
- [268] F. Capela, M. Pshirkov, P. Tinyakov, Constraints on Primordial Black Holes as Dark Matter Candidates from Star Formation, *Phys. Rev. D* 87 (2) (2013) 023507. [arXiv:1209.6021](#), [doi:10.1103/PhysRevD.87.023507](#).
- [269] F. Capela, M. Pshirkov, P. Tinyakov, Constraints on primordial black holes as dark matter candidates from capture by neutron stars, *Phys. Rev. D* 87 (12) (2013) 123524. [arXiv:1301.4984](#), [doi:10.1103/PhysRevD.87.123524](#).
- [270] P. Pani, A. Loeb, Tidal capture of a primordial black hole by a neutron star: implications for constraints on dark matter, *JCAP* 06 (2014) 026. [arXiv:1401.3025](#), [doi:10.1088/1475-7516/2014/06/026](#).
- [271] Y. Kurita, H. Nakano, Gravitational waves from dark matter collapse in a star, *Phys. Rev. D* 93 (2) (2016) 023508. [arXiv:1510.00893](#), [doi:10.1103/PhysRevD.93.023508](#).
- [272] M. A. Abramowicz, M. Bejger, M. Wielgus, Collisions of neutron stars with primordial black holes as fast radio bursts engines, *Astrophys. J.* 868 (1) (2018) 17. [arXiv:1704.05931](#), [doi:10.3847/1538-4357/aae64a](#).
- [273] V. Takhistov, Positrons from Primordial Black Hole Microquasars and Gamma-ray Bursts, *Phys. Lett. B* 789 (2019) 538–544. [arXiv:1710.09458](#), [doi:10.1016/j.physletb.2018.12.043](#).
- [274] V. Takhistov, Transmuted Gravity Wave Signals from Primordial Black Holes, *Phys. Lett. B* 782 (2018) 77–82. [arXiv:1707.05849](#), [doi:10.1016/j.physletb.2018.05.026](#).
- [275] Y. Genolini, P. Serpico, P. Tinyakov, Revisiting primordial black hole capture into neutron stars, *Phys. Rev. D* 102 (8) (2020) 083004. [arXiv:2006.16975](#), [doi:10.1103/PhysRevD.102.083004](#).
- [276] T. W. Baumgarte, S. L. Shapiro, Neutron Stars Harboring a Primordial Black Hole: Maximum Survival Time, *Phys. Rev. D* 103 (8) (2021) L081303. [arXiv:2101.12220](#), [doi:10.1103/PhysRevD.103.L081303](#).
- [277] J. Estes, M. Kavic, S. L. Liebling, M. Lippert, J. H. Simonetti, Stability and observability of magnetic primordial black hole-neutron star collisions, *JCAP* 06 (2023) 017. [arXiv:2209.06060](#), [doi:10.1088/1475-7516/2023/06/017](#).
- [278] Y. Zenati, C. Albertus, M. A. Pérez-García, J. Silk, Neutrino signals from Neutron Star implosions to Black Holes (4 2023). [arXiv:2304.06746](#).
- [279] J. Bramante, F. Elahi, Higgs portals to pulsar collapse, *Phys. Rev. D* 91 (11) (2015) 115001. [arXiv:1504.04019](#), [doi:10.1103/PhysRevD.91.115001](#).
- [280] M. I. Gresham, K. M. Zurek, Asymmetric Dark Stars and Neutron Star Stability, *Phys. Rev. D* 99 (8) (2019) 083008. [arXiv:1809.08254](#), [doi:10.1103/PhysRevD.99.083008](#).

- [281] C. Kouvaris, P. Tinyakov, (Not)-constraining heavy asymmetric bosonic dark matter, *Phys. Rev. D* 87 (12) (2013) 123537. [arXiv:1212.4075](#), [doi:10.1103/PhysRevD.87.123537](#).
- [282] R. Garani, M. H. G. Tytgat, J. Vandecasteele, Condensed dark matter with a Yukawa interaction, *Phys. Rev. D* 106 (11) (2022) 116003. [arXiv:2207.06928](#), [doi:10.1103/PhysRevD.106.116003](#).
- [283] C. Kouvaris, P. Tinyakov, Growth of Black Holes in the interior of Rotating Neutron Stars, *Phys. Rev. D* 90 (4) (2014) 043512. [arXiv:1312.3764](#), [doi:10.1103/PhysRevD.90.043512](#).
- [284] M. Autzen, C. Kouvaris, Blocking the Hawking Radiation, *Phys. Rev. D* 89 (12) (2014) 123519. [arXiv:1403.1072](#), [doi:10.1103/PhysRevD.89.123519](#).
- [285] D. Liang, L. Shao, Improved bounds on the bosonic dark matter with pulsars in the Milky Way (3 2023). [arXiv:2303.05107](#).
- [286] J. Dexter, R. M. O’Leary, The Peculiar Pulsar Population of the Central Parsec, *Astrophys. J. Lett.* 783 (2014) L7. [arXiv:1310.7022](#), [doi:10.1088/2041-8205/783/1/L7](#).
- [287] A. Suresh, J. M. Cordes, S. Chatterjee, V. Gajjar, K. I. Perez, A. P. V. Siemion, M. Lebofsky, D. H. E. MacMahon, C. Ng, 4–8 GHz Fourier-domain Searches for Galactic Center Pulsars, *Astrophys. J.* 933 (2) (2022) 121. [arXiv:2203.00036](#), [doi:10.3847/1538-4357/ac74c0](#).
- [288] G. M. Fuller, A. Kusenko, V. Takhistov, Primordial Black Holes and r-Process Nucleosynthesis, *Phys. Rev. Lett.* 119 (6) (2017) 061101. [arXiv:1704.01129](#), [doi:10.1103/PhysRevLett.119.061101](#).
- [289] C. B. Richards, T. W. Baumgarte, S. L. Shapiro, Accretion onto a small black hole at the center of a neutron star, *Phys. Rev. D* 103 (10) (2021) 104009. [arXiv:2102.09574](#), [doi:10.1103/PhysRevD.103.104009](#).
- [290] Y. Zenati, C. Albertus, M. A. Pérez-García, J. Silk, Neutrino signals from Neutron Star implosions to Black Holes (4 2023). [arXiv:2304.06746](#).
- [291] S. Bhattacharya, B. Dasgupta, R. Laha, A. Ray, Can LIGO Detect Asymmetric Dark Matter? (2 2023). [arXiv:2302.07898](#).
- [292] H. Yang, W. E. East, L. Lehner, Can we distinguish low mass black holes in neutron star binaries?, *Astrophys. J.* 856 (2) (2018) 110, [Erratum: *Astrophys. J.* 870, 139 (2019)]. [arXiv:1710.05891](#), [doi:10.3847/1538-4357/aab2b0](#).
- [293] F. Capela, M. Pshirkov, P. Tinyakov, Constraints on primordial black holes as dark matter candidates from capture by neutron stars, *Phys. Rev. D* 87 (12) (2013) 123524. [arXiv:1301.4984](#), [doi:10.1103/PhysRevD.87.123524](#).
- [294] P. Pani, A. Loeb, Tidal capture of a primordial black hole by a neutron star: implications for constraints on dark matter, *JCAP* 06 (2014) 026. [arXiv:1401.3025](#), [doi:10.1088/1475-7516/2014/06/026](#).
- [295] G. Defillon, E. Granet, P. Tinyakov, M. H. G. Tytgat, Tidal capture of primordial black holes by neutron stars, *Phys. Rev. D* 90 (10) (2014) 103522. [arXiv:1409.0469](#), [doi:10.1103/PhysRevD.90.103522](#).
- [296] C. B. Richards, T. W. Baumgarte, S. L. Shapiro, Accretion onto a small black hole at the center of a neutron star, *Phys. Rev. D* 103 (10) (2021) 104009. [arXiv:2102.09574](#), [doi:10.1103/PhysRevD.103.104009](#).
- [297] T. W. Baumgarte, S. L. Shapiro, Neutron Stars Harboring a Primordial Black Hole: Maximum Survival Time, *Phys. Rev. D* 103 (8) (2021) L081303. [arXiv:2101.12220](#), [doi:10.1103/PhysRevD.103.L081303](#).
- [298] K. Kainulainen, S. Nurmi, E. D. Schiappacasse, T. T. Yanagida, Can primordial black holes as all dark matter explain fast radio bursts?, *Phys. Rev. D* 104 (12) (2021) 123033. [arXiv:2108.08717](#), [doi:10.1103/PhysRevD.104.123033](#).
- [299] D. McKeen, A. E. Nelson, S. Reddy, D. Zhou, Neutron stars exclude light dark baryons, *Phys. Rev. Lett.* 121 (6) (2018) 061802. [arXiv:1802.08244](#), [doi:10.1103/PhysRevLett.121.061802](#).
- [300] R. W. Romani, D. Kandel, A. V. Filippenko, T. G. Brink, W. Zheng, PSR J0952–0607: The Fastest and Heaviest Known Galactic Neutron Star, *Astrophys. J. Lett.* 934 (2) (2022) L17. [arXiv:2207.05124](#), [doi:10.3847/2041-8213/ac8007](#).
- [301] S. D. McDermott, S. Reddy, S. Sen, Deeply bound dibaryon is incompatible with neutron stars and supernovae, *Phys. Rev. D* 99 (3) (2019) 035013. [arXiv:1809.06765](#), [doi:10.1103/PhysRevD.99.035013](#).
- [302] D. McKeen, M. Pospelov, N. Raj, Neutron Star Internal Heating Constraints on Mirror Matter, *Phys. Rev. Lett.* 127 (6) (2021) 061805. [arXiv:2105.09951](#), [doi:10.1103/PhysRevLett.127.061805](#).
- [303] I. Goldman, R. N. Mohapatra, S. Nussinov, Bounds on neutron-mirror neutron mixing from pulsar timing, *Phys. Rev. D* 100 (12) (2019) 123021. [arXiv:1901.07077](#), [doi:10.1103/PhysRevD.100.123021](#).
- [304] B. Fornal, B. Grinstein, Dark Matter Interpretation of the Neutron Decay Anomaly, *Phys. Rev. Lett.* 120 (19) (2018) 191801, [Erratum: *Phys.Rev.Lett.* 124, 219901 (2020)]. [arXiv:1801.01124](#), [doi:10.1103/PhysRevLett.120.191801](#).
- [305] D. McKeen, A. E. Nelson, CP Violating Baryon Oscillations, *Phys. Rev. D* 94 (7) (2016) 076002. [arXiv:1512.05359](#), [doi:10.1103/PhysRevD.94.076002](#).
- [306] G. Alonso-Álvarez, G. Elor, M. Escudero, B. Fornal, B. Grinstein, J. M. Camalich, The Strange Physics of Dark Baryons (11 2021). [arXiv:2111.12712](#).
- [307] Z. Berezhiani, Neutron lifetime puzzle and neutron–mirror neutron oscillation, *Eur. Phys. J. C* 79 (6) (2019) 484. [arXiv:1807.07906](#), [doi:10.1140/epjc/s10052-019-6995-x](#).
- [308] G. Baym, D. Beck, P. Geltenbort, J. Shelton, Testing dark decays of baryons in neutron stars, *Phys. Rev. Lett.* 121 (6) (2018) 061801. [arXiv:1802.08282](#), [doi:10.1103/PhysRevLett.121.061801](#).

- [309] T. Motta, P. Guichon, A. Thomas, Implications of Neutron Star Properties for the Existence of Light Dark Matter, *J. Phys. G* 45 (5) (2018) 05LT01. [arXiv:1802.08427](#), [doi:10.1088/1361-6471/aab689](#).
- [310] O. Ivanytskyi, V. Sagun, I. Lopes, Neutron stars: New constraints on asymmetric dark matter, *Phys. Rev. D* 102 (6) (2020) 063028. [arXiv:1910.09925](#), [doi:10.1103/PhysRevD.102.063028](#).
- [311] J. Ellis, G. Hütsi, K. Kannike, L. Marzola, M. Raidal, V. Vaskonen, Dark Matter Effects On Neutron Star Properties, *Phys. Rev. D* 97 (12) (2018) 123007. [arXiv:1804.01418](#), [doi:10.1103/PhysRevD.97.123007](#).
- [312] E. Giangrandi, V. Sagun, O. Ivanytskyi, C. Providência, T. Dietrich, The Effects of Self-interacting Bosonic Dark Matter on Neutron Star Properties, *Astrophys. J.* 953 (1) (2023) 115. [arXiv:2209.10905](#), [doi:10.3847/1538-4357/ace104](#).
- [313] J. M. Berryman, S. Gardner, M. Zakeri, Neutron Stars with Baryon Number Violation, Probing Dark Sectors, *Symmetry* 14 (3) (2022) 518. [arXiv:2201.02637](#), [doi:10.3390/sym14030518](#).
- [314] N. Rutherford, G. Raaijmakers, C. Prescod-Weinstein, A. Watts, Constraining bosonic asymmetric dark matter with neutron star mass-radius measurements, *Phys. Rev. D* 107 (10) (2023) 103051. [arXiv:2208.03282](#), [doi:10.1103/PhysRevD.107.103051](#).
- [315] I. Lopes, G. Panotopoulos, Dark matter admixed strange quark stars in the Starobinsky model, *Phys. Rev. D* 97 (2) (2018) 024030. [arXiv:1801.05031](#), [doi:10.1103/PhysRevD.97.024030](#).
- [316] G. Panotopoulos, I. Lopes, Millisecond pulsars modeled as strange quark stars admixed with condensed dark matter, *Int. J. Mod. Phys. D* 27 (09) (2018) 1850093. [arXiv:1804.05023](#), [doi:10.1142/S0218271818500931](#).
- [317] G. Panotopoulos, I. Lopes, Radial oscillations of strange quark stars admixed with fermionic dark matter, *Phys. Rev. D* 98 (8) (2018) 083001. [doi:10.1103/PhysRevD.98.083001](#).
- [318] A. Strumia, Dark Matter interpretation of the neutron decay anomaly, *JHEP* 02 (2022) 067. [arXiv:2112.09111](#), [doi:10.1007/JHEP02\(2022\)067](#).
- [319] G. Narain, J. Schaffner-Bielich, I. N. Mishustin, Compact stars made of fermionic dark matter, *Phys. Rev. D* 74 (2006) 063003. [arXiv:astro-ph/0605724](#), [doi:10.1103/PhysRevD.74.063003](#).
- [320] J. M. Cline, J. M. Cornell, Dark decay of the neutron, *JHEP* 07 (2018) 081. [arXiv:1803.04961](#), [doi:10.1007/JHEP07\(2018\)081](#).
- [321] M. Hippert, E. Dillingham, H. Tan, D. Curtin, J. Noronha-Hostler, N. Yunes, Dark Matter or Regular Matter in Neutron Stars? How to tell the difference from the coalescence of compact objects (11 2022). [arXiv:2211.08590](#).
- [322] M. Collier, D. Croon, R. K. Leane, Tidal Love numbers of novel and admixed celestial objects, *Phys. Rev. D* 106 (12) (2022) 123027. [arXiv:2205.15337](#), [doi:10.1103/PhysRevD.106.123027](#).
- [323] D. R. Karkevadani, S. Shakeri, V. Sagun, O. Ivanytskyi, Bosonic dark matter in neutron stars and its effect on gravitational wave signal, *Phys. Rev. D* 105 (2) (2022) 023001. [arXiv:2109.03801](#), [doi:10.1103/PhysRevD.105.023001](#).
- [324] Y. Dengler, J. Schaffner-Bielich, L. Tolos, Second Love number of dark compact planets and neutron stars with dark matter, *Phys. Rev. D* 105 (4) (2022) 043013. [arXiv:2111.06197](#), [doi:10.1103/PhysRevD.105.043013](#).
- [325] S. Shakeri, D. R. Karkevadani, Bosonic Dark Matter in Light of the NICER Precise Mass-Radius Measurements (10 2022). [arXiv:2210.17308](#).
- [326] G. R. Farrar, Stable Sexaquark (8 2017). [arXiv:1708.08951](#).
- [327] G. R. Farrar, A precision test of the nature of Dark Matter and a probe of the QCD phase transition (5 2018). [arXiv:1805.03723](#).
- [328] E. W. Kolb, M. S. Turner, Dibaryons cannot be the dark matter, *Phys. Rev. D* 99 (6) (2019) 063519. [arXiv:1809.06003](#), [doi:10.1103/PhysRevD.99.063519](#).
- [329] M. Shahrabaf, D. Blaschke, S. Typel, G. R. Farrar, D. E. Alvarez-Castillo, Sexaquark dilemma in neutron stars and its solution by quark deconfinement, *Phys. Rev. D* 105 (10) (2022) 103005. [arXiv:2202.00652](#), [doi:10.1103/PhysRevD.105.103005](#).
- [330] R. Foot, Mirror matter-type dark matter, *Int. J. Mod. Phys. D* 13 (2004) 2161–2192. [arXiv:astro-ph/0407623](#), [doi:10.1142/S0218271804006449](#).
- [331] J. Fan, A. Katz, L. Randall, M. Reece, Double-Disk Dark Matter, *Phys. Dark Univ.* 2 (2013) 139–156. [arXiv:1303.1521](#), [doi:10.1016/j.dark.2013.07.001](#).
- [332] M. Ángeles Pérez-García, H. Grigorian, C. Albertus, D. Barba, J. Silk, Cooling of Neutron Stars admixed with light dark matter: A case study, *Phys. Lett. B* 827 (2022) 136937. [arXiv:2202.00702](#), [doi:10.1016/j.physletb.2022.136937](#).
- [333] M. Hippert, J. Setford, H. Tan, D. Curtin, J. Noronha-Hostler, N. Yunes, Mirror neutron stars, *Phys. Rev. D* 106 (3) (2022) 035025. [arXiv:2103.01965](#), [doi:10.1103/PhysRevD.106.035025](#).
- [334] M. Ryan, D. Radice, Exotic compact objects: The dark white dwarf, *Phys. Rev. D* 105 (11) (2022) 115034. [arXiv:2201.05626](#), [doi:10.1103/PhysRevD.105.115034](#).
- [335] A. Howe, J. Setford, D. Curtin, C. D. Matzner, How to search for mirror stars with Gaia, *JHEP* 07 (2022) 059. [arXiv:2112.05766](#), [doi:10.1007/JHEP07\(2022\)059](#).
- [336] Z. Berezhiani, Antistars or Antimatter Cores in Mirror Neutron Stars?, *Universe* 8 (6) (2022) 313. [arXiv:2106.11203](#),



[doi:10.3390/universe8060313](https://doi.org/10.3390/universe8060313).

- [337] C. Kouvaris, N. G. Nielsen, Asymmetric Dark Matter Stars, *Phys. Rev. D* 92 (6) (2015) 063526. [arXiv:1507.00959](https://arxiv.org/abs/1507.00959), [doi:10.1103/PhysRevD.92.063526](https://doi.org/10.1103/PhysRevD.92.063526).
- [338] B. B. Kamenetskaia, A. Brenner, A. Ibarra, C. Kouvaris, Proton Capture in Compact Dark Stars and Observable Implications (11 2022). [arXiv:2211.05845](https://arxiv.org/abs/2211.05845).
- [339] V. Cardoso, P. Pani, Testing the nature of dark compact objects: a status report, *Living Rev. Rel.* 22 (1) (2019) 4. [arXiv:1904.05363](https://arxiv.org/abs/1904.05363), [doi:10.1007/s41114-019-0020-4](https://doi.org/10.1007/s41114-019-0020-4).
- [340] D. Croon, D. McKeen, N. Raj, Gravitational microlensing by dark matter in extended structures, *Phys. Rev. D* 101 (8) (2020) 083013. [arXiv:2002.08962](https://arxiv.org/abs/2002.08962), [doi:10.1103/PhysRevD.101.083013](https://doi.org/10.1103/PhysRevD.101.083013).
- [341] D. Croon, D. McKeen, N. Raj, Z. Wang, Subaru-HSC through a different lens: Microlensing by extended dark matter structures, *Phys. Rev. D* 102 (8) (2020) 083021. [arXiv:2007.12697](https://arxiv.org/abs/2007.12697), [doi:10.1103/PhysRevD.102.083021](https://doi.org/10.1103/PhysRevD.102.083021).
- [342] Y. Bai, A. J. Long, S. Lu, Tests of Dark MACHOs: Lensing, Accretion, and Glow, *JCAP* 09 (2020) 044. [arXiv:2003.13182](https://arxiv.org/abs/2003.13182), [doi:10.1088/1475-7516/2020/09/044](https://doi.org/10.1088/1475-7516/2020/09/044).
- [343] E. Witten, Cosmic Separation of Phases, *Phys. Rev. D* 30 (1984) 272–285. [doi:10.1103/PhysRevD.30.272](https://doi.org/10.1103/PhysRevD.30.272).
- [344] Y. Bai, A. J. Long, S. Lu, Dark Quark Nuggets, *Phys. Rev. D* 99 (5) (2019) 055047. [arXiv:1810.04360](https://arxiv.org/abs/1810.04360), [doi:10.1103/PhysRevD.99.055047](https://doi.org/10.1103/PhysRevD.99.055047).
- [345] C. Gross, G. Landini, A. Strumia, D. Teresi, Dark Matter as dark dwarfs and other macroscopic objects: multiverse relics?, *JHEP* 09 (2021) 033. [arXiv:2105.02840](https://arxiv.org/abs/2105.02840), [doi:10.1007/JHEP09\(2021\)033](https://doi.org/10.1007/JHEP09(2021)033).
- [346] D. McKeen, M. Pospelov, N. Raj, Cosmological and astrophysical probes of dark baryons, *Phys. Rev. D* 103 (11) (2021) 115002. [arXiv:2012.09865](https://arxiv.org/abs/2012.09865), [doi:10.1103/PhysRevD.103.115002](https://doi.org/10.1103/PhysRevD.103.115002).
- [347] T. L. Team, The luvoir mission concept study final report (2019). [arXiv:1912.06219](https://arxiv.org/abs/1912.06219).
- [348] J. R. Peterson, [Dark energy studies with lsst image simulations, final report](https://arxiv.org/abs/2007.12697) (7 2016). [doi:10.2172/1272167](https://doi.org/10.2172/1272167). URL <https://www.osti.gov/biblio/1272167>
- [349] v. Ivezić, et al., LSST: from Science Drivers to Reference Design and Anticipated Data Products, *Astrophys. J.* 873 (2) (2019) 111. [arXiv:0805.2366](https://arxiv.org/abs/0805.2366), [doi:10.3847/1538-4357/ab042c](https://doi.org/10.3847/1538-4357/ab042c).
- [350] H. T. Diehl, et al., The Dark Energy Survey and Operations: Year 6 – The Finale (10 2019). [doi:10.2172/1596042](https://doi.org/10.2172/1596042).
- [351] J. Green, P. Schechter, C. Baltay, R. Bean, D. Bennett, R. Brown, C. Conselice, M. Donahue, X. Fan, B. S. Gaudi, C. Hirata, J. Kalirai, T. Lauer, B. Nichol, N. Padmanabhan, S. Perlmutter, B. Rauscher, J. Rhodes, T. Roellig, D. Stern, T. Sumi, A. Tanner, Y. Wang, D. Weinberg, E. Wright, N. Gehrels, R. Sambruna, W. Traub, J. Anderson, K. Cook, P. Garnavich, L. Hillenbrand, Z. Ivezić, E. Kerins, J. Lunine, P. McDonald, M. Penny, M. Phillips, G. Rieke, A. Riess, R. van der Marel, R. K. Barry, E. Cheng, D. Content, R. Cutri, R. Goullioud, K. Grady, G. Helou, C. Jackson, J. Krug, M. Melton, C. Peddie, N. Rioux, M. Seiffert, Wide-field infrared survey telescope (wfirst) final report (2012). [arXiv:1208.4012](https://arxiv.org/abs/1208.4012).
- [352] I. Goldman, R. N. Mohapatra, S. Nussinov, Y. Zhang, Neutron-Mirror-Neutron Oscillation and Neutron Star Cooling, *Phys. Rev. Lett.* 129 (6) (2022) 061103. [arXiv:2208.03771](https://arxiv.org/abs/2208.03771), [doi:10.1103/PhysRevLett.129.061103](https://doi.org/10.1103/PhysRevLett.129.061103).
- [353] H. Davoudiasl, Stellar Signals of a Baryon-Number-Violating Long-Range Force (4 2023). [arXiv:2304.06071](https://arxiv.org/abs/2304.06071).
- [354] <https://cajohare.github.io/AxionLimits/docs/fa.html>.
- [355] D. Croon, A. E. Nelson, C. Sun, D. G. E. Walker, Z.-Z. Xianyu, Hidden-Sector Spectroscopy with Gravitational Waves from Binary Neutron Stars, *Astrophys. J. Lett.* 858 (1) (2018) L2. [arXiv:1711.02096](https://arxiv.org/abs/1711.02096), [doi:10.3847/2041-8213/aabe76](https://doi.org/10.3847/2041-8213/aabe76).
- [356] S. Alexander, E. McDonough, R. Sims, N. Yunes, Hidden-Sector Modifications to Gravitational Waves From Binary Inspirals, *Class. Quant. Grav.* 35 (23) (2018) 235012. [arXiv:1808.05286](https://arxiv.org/abs/1808.05286), [doi:10.1088/1361-6382/aab5c](https://doi.org/10.1088/1361-6382/aab5c).
- [357] J. Ellis, A. Hektor, G. Hutsi, K. Kannike, L. Marzola, M. Raidal, V. Vaskonen, [Search for dark matter effects on gravitational signals from neutron star mergers](https://arxiv.org/abs/1808.05286), *Physics Letters B* 781 (2018) 607?610. [doi:10.1016/j.physletb.2018.04.048](https://doi.org/10.1016/j.physletb.2018.04.048). URL <http://dx.doi.org/10.1016/j.physletb.2018.04.048>
- [358] M. Emma, F. Schianchi, F. Pannarale, V. Sagun, T. Dietrich, Numerical Simulations of Dark Matter Admixed Neutron Star Binaries, *Particles* 5 (3) (2022) 273–286. [arXiv:2206.10887](https://arxiv.org/abs/2206.10887), [doi:10.3390/particles5030024](https://doi.org/10.3390/particles5030024).
- [359] H. R. Rüter, V. Sagun, W. Tichy, T. Dietrich, Quasi-equilibrium configurations of binary systems of dark matter admixed neutron stars (1 2023). [arXiv:2301.03568](https://arxiv.org/abs/2301.03568).
- [360] A. Bauswein, G. Guo, J.-H. Lien, Y.-H. Lin, M.-R. Wu, Compact dark objects in neutron star mergers, *Phys. Rev. D* 107 (8) (2023) 083002. [arXiv:2012.11908](https://arxiv.org/abs/2012.11908), [doi:10.1103/PhysRevD.107.083002](https://doi.org/10.1103/PhysRevD.107.083002).
- [361] M. Fabbrichesi, A. Urbano, Charged neutron stars and observational tests of a dark force weaker than gravity, *JCAP* 06 (2020) 007. [arXiv:1902.07914](https://arxiv.org/abs/1902.07914), [doi:10.1088/1475-7516/2020/06/007](https://doi.org/10.1088/1475-7516/2020/06/007).
- [362] J. A. Dror, R. Laha, T. Opferkuch, Probing muonic forces with neutron star binaries, *Phys. Rev. D* 102 (2) (2020) 023005. [arXiv:1909.12845](https://arxiv.org/abs/1909.12845), [doi:10.1103/PhysRevD.102.023005](https://doi.org/10.1103/PhysRevD.102.023005).
- [363] A. Hook, J. Huang, Probing axions with neutron star inspirals and other stellar processes, *JHEP* 06 (2018) 036. [arXiv:1708.08464](https://arxiv.org/abs/1708.08464), [doi:10.1007/JHEP06\(2018\)036](https://doi.org/10.1007/JHEP06(2018)036).
- [364] H. G. Choi, S. Jung, New probe of dark matter-induced fifth force with neutron star inspirals, *Phys. Rev. D* 99 (1) (2019)

015013. [arXiv:1810.01421](#), [doi:10.1103/PhysRevD.99.015013](#).
- [365] G. Lambiase, T. K. Poddar, Pulsar kicks in ultralight dark matter background induced by neutrino oscillation (7 2023). [arXiv:2307.05229](#).
- [366] M. D. Diamond, G. Marques-Tavares, Gamma-Ray Flashes from Dark Photons in Neutron Star Mergers, *Phys. Rev. Lett.* 128 (21) (2022) 211101. [arXiv:2106.03879](#), [doi:10.1103/PhysRevLett.128.211101](#).
- [367] M. Diamond, D. F. G. Fiorillo, G. Marques-Tavares, I. Tamborra, E. Vitagliano, Multimessenger Constraints on Radiatively Decaying Axions from GW170817 (5 2023). [arXiv:2305.10327](#).
- [368] G. Hobbs, S. Dai, Gravitational wave research using pulsar timing arrays, *Natl. Sci. Rev.* 4 (5) (2017) 707–717. [arXiv:1707.01615](#), [doi:10.1093/nsr/nwx126](#).
- [369] P. K. Dahal, Review of pulsar timing array for gravitational wave research, *Journal of Astrophysics and Astronomy* 41 (1) (2020) 8. [arXiv:2002.01954](#), [doi:10.1007/s12036-020-9625-y](#).
- [370] N. Seto, A. Cooray, Searching for primordial black hole dark matter with pulsar timing arrays, *Astrophys. J. Lett.* 659 (2007) L33–L36. [arXiv:astro-ph/0702586](#), [doi:10.1086/516570](#).
- [371] E. R. Siegel, M. P. Hertzberg, J. N. Fry, Probing Dark Matter Substructure with Pulsar Timing, *Mon. Not. Roy. Astron. Soc.* 382 (2007) 879. [arXiv:astro-ph/0702546](#), [doi:10.1111/j.1365-2966.2007.12435.x](#).
- [372] S. Baghran, N. Afshordi, K. M. Zurek, Prospects for Detecting Dark Matter Halo Substructure with Pulsar Timing, *Phys. Rev. D* 84 (2011) 043511. [arXiv:1101.5487](#), [doi:10.1103/PhysRevD.84.043511](#).
- [373] K. Kashiyama, N. Seto, Enhanced exploration for primordial black holes using pulsar timing arrays, *MNRAS* 426 (2) (2012) 1369–1373. [arXiv:1208.4101](#), [doi:10.1111/j.1365-2966.2012.21935.x](#).
- [374] K. Kashiyama, M. Oguri, Detectability of Small-Scale Dark Matter Clumps with Pulsar Timing Arrays (1 2018). [arXiv:1801.07847](#).
- [375] H. A. Clark, G. F. Lewis, P. Scott, Investigating dark matter substructure with pulsar timing – I. Constraints on ultracompact minihaloes, *Mon. Not. Roy. Astron. Soc.* 456 (2) (2016) 1394–1401, [Erratum: *Mon. Not. Roy. Astron. Soc.* 464, 2468 (2017)]. [arXiv:1509.02938](#), [doi:10.1093/mnras/stv2743](#).
- [376] H. A. Clark, G. F. Lewis, P. Scott, Investigating dark matter substructure with pulsar timing – II. Improved limits on small-scale cosmology, *Mon. Not. Roy. Astron. Soc.* 456 (2) (2016) 1402–1409, [Erratum: *Mon. Not. Roy. Astron. Soc.* 464, 955–956 (2017)]. [arXiv:1509.02941](#), [doi:10.1093/mnras/stv2529](#).
- [377] K. Schutz, A. Liu, Pulsar timing can constrain primordial black holes in the LIGO mass window, *Phys. Rev. D* 95 (2) (2017) 023002. [arXiv:1610.04234](#), [doi:10.1103/PhysRevD.95.023002](#).
- [378] J. A. Dror, H. Ramani, T. Trickle, K. M. Zurek, Pulsar Timing Probes of Primordial Black Holes and Subhalos, *Phys. Rev. D* 100 (2) (2019) 023003. [arXiv:1901.04490](#), [doi:10.1103/PhysRevD.100.023003](#).
- [379] H. Ramani, T. Trickle, K. M. Zurek, Observability of Dark Matter Substructure with Pulsar Timing Correlations, *JCAP* 12 (2020) 033. [arXiv:2005.03030](#), [doi:10.1088/1475-7516/2020/12/033](#).
- [380] V. S. H. Lee, S. R. Taylor, T. Trickle, K. M. Zurek, Bayesian Forecasts for Dark Matter Substructure Searches with Mock Pulsar Timing Data, *JCAP* 08 (2021) 025. [arXiv:2104.05717](#), [doi:10.1088/1475-7516/2021/08/025](#).
- [381] V. S. H. Lee, A. Mitridate, T. Trickle, K. M. Zurek, Probing Small-Scale Power Spectra with Pulsar Timing Arrays, *JHEP* 06 (2021) 028. [arXiv:2012.09857](#), [doi:10.1007/JHEP06\(2021\)028](#).
- [382] Z. Arzoumanian, et al., The NANOGrav 11-year Data Set: High-precision timing of 45 Millisecond Pulsars, *Astrophys. J. Suppl.* 235 (2) (2018) 37. [arXiv:1801.01837](#), [doi:10.3847/1538-4365/aab5b0](#).
- [383] Z. Arzoumanian, et al., The NANOGrav 11-year Data Set: Pulsar-timing Constraints On The Stochastic Gravitational-wave Background, *Astrophys. J.* 859 (1) (2018) 47. [arXiv:1801.02617](#), [doi:10.3847/1538-4357/aabd3b](#).
- [384] A. Khmelnitsky, V. Rubakov, Pulsar timing signal from ultralight scalar dark matter, *JCAP* 02 (2014) 019. [arXiv:1309.5888](#), [doi:10.1088/1475-7516/2014/02/019](#).
- [385] J. M. Armaleo, D. López Nacir, F. R. Urban, Pulsar timing array constraints on spin-2 ULDM, *JCAP* 09 (2020) 031. [arXiv:2005.03731](#), [doi:10.1088/1475-7516/2020/09/031](#).
- [386] N. K. Porayko, K. A. Postnov, Constraints on ultralight scalar dark matter from pulsar timing, *Phys. Rev. D* 90 (6) (2014) 062008. [arXiv:1408.4670](#), [doi:10.1103/PhysRevD.90.062008](#).
- [387] N. K. Porayko, et al., Parkes Pulsar Timing Array constraints on ultralight scalar-field dark matter, *Phys. Rev. D* 98 (10) (2018) 102002. [arXiv:1810.03227](#), [doi:10.1103/PhysRevD.98.102002](#).
- [388] C. Smarra, et al., The second data release from the European Pulsar Timing Array: VI. Challenging the ultralight dark matter paradigm (6 2023). [arXiv:2306.16228](#).
- [389] Y. V. Stadnik, V. V. Flambaum, Searches for topological defect dark matter via nongravitational signatures, *Phys. Rev. Lett.* 113 (15) (2014) 151301. [arXiv:1405.5337](#), [doi:10.1103/PhysRevLett.113.151301](#).
- [390] G. Desvignes, et al., High-precision timing of 42 millisecond pulsars with the European Pulsar Timing Array, *Mon. Not. Roy. Astron. Soc.* 458 (3) (2016) 3341–3380. [arXiv:1602.08511](#), [doi:10.1093/mnras/stw483](#).
- [391] R. N. Manchester, G. Hobbs, M. Bailes, W. A. Coles, W. van Straten, M. J. Keith, R. M. Shannon, N. D. R. Bhat, A. Brown,



- S. G. Burke-Spolaor, D. J. Champion, A. Chaudhary, R. T. Edwards, G. Hampson, A. W. Hotan, A. Jameson, F. A. Jenet, M. J. Kesteven, J. Khoo, J. Kocz, K. Maciesiak, S. Osłowski, V. Ravi, J. R. Reynolds, J. M. Sarkissian, J. P. W. Verbiest, Z. L. Wen, W. E. Wilson, D. Yardley, W. M. Yan, X. P. You, The Parkes Pulsar Timing Array Project, PASA 30 (2013) e017. [arXiv:1210.6130](#), [doi:10.1017/pasa.2012.017](#).
- [392] A. Brazier, et al., The NANOGrav Program for Gravitational Waves and Fundamental Physics (8 2019). [arXiv:1908.05356](#).
- [393] P. Tarafdar, et al., The Indian Pulsar Timing Array: First data release, Publ. Astron. Soc. Austral. 39 (2022) e053. [arXiv:2206.09289](#), [doi:10.1017/pasa.2022.46](#).
- [394] B. B. P. Perera, et al., The International Pulsar Timing Array: Second data release, Mon. Not. Roy. Astron. Soc. 490 (4) (2019) 4666–4687. [arXiv:1909.04534](#), [doi:10.1093/mnras/stz2857](#).
- [395] M. Bailes, et al., MeerTime - the MeerKAT Key Science Program on Pulsar Timing, PoS MeerKAT2016 (2018) 011. [arXiv:1803.07424](#), [doi:10.22323/1.277.0011](#).
- [396] G. Hobbs, S. Dai, R. N. Manchester, R. M. Shannon, M. Kerr, K. J. Lee, R. Xu, The Role of FAST in Pulsar Timing Arrays, Res. Astron. Astrophys. 19 (2) (2019) 020. [arXiv:1407.0435](#), [doi:10.1088/1674-4527/19/2/20](#).
- [397] R. Smits, M. Kramer, B. Stappers, D. R. Lorimer, J. Cordes, A. Faulkner, Pulsar searches and timing with the square kilometre array, AAP 493 (3) (2009) 1161–1170. [arXiv:0811.0211](#), [doi:10.1051/0004-6361:200810383](#).
- [398] P. A. Rosado, A. Sesana, J. Gair, Expected properties of the first gravitational wave signal detected with pulsar timing arrays, Mon. Not. Roy. Astron. Soc. 451 (3) (2015) 2417–2433. [arXiv:1503.04803](#), [doi:10.1093/mnras/stv1098](#).
- [399] P. F. Depta, K. Schmidt-Hoberg, C. Tasillo, Do pulsar timing arrays observe merging primordial black holes? (6 2023). [arXiv:2306.17836](#).
- [400] K. Inomata, K. Kohri, T. Terada, The Detected Stochastic Gravitational Waves and Sub-Solar Primordial Black Holes (6 2023). [arXiv:2306.17834](#).
- [401] Y. Gouttenoire, S. Trifinopoulos, G. Valogiannis, M. Vanvlasselaer, Scrutinizing the Primordial Black Holes Interpretation of PTA Gravitational Waves and JWST Early Galaxies (7 2023). [arXiv:2307.01457](#).
- [402] A. Ghoshal, A. Strumia, Probing the Dark Matter density with gravitational waves from super-massive binary black holes (6 2023). [arXiv:2306.17158](#).
- [403] Z.-Q. Shen, G.-W. Yuan, Y.-Y. Wang, Y.-Z. Wang, Dark Matter Spike surrounding Supermassive Black Holes Binary and the nanohertz Stochastic Gravitational Wave Background (6 2023). [arXiv:2306.17143](#).
- [404] D. Borah, S. Jyoti Das, R. Samanta, Inflationary origin of gravitational waves with  $\text{textit{Miracle-less}}$  WIMP dark matter in the light of recent PTA results (7 2023). [arXiv:2307.00537](#).
- [405] T. Broadhurst, C. Chen, T. Liu, K.-F. Zheng, Binary Supermassive Black Holes Orbiting Dark Matter Solitons: From the Dual AGN in UGC4211 to NanoHertz Gravitational Waves (6 2023). [arXiv:2306.17821](#).
- [406] Y. Xiao, J. M. Yang, Y. Zhang, Implications of Nano-Hertz Gravitational Waves on Electroweak Phase Transition in the Singlet Dark Matter Model (7 2023). [arXiv:2307.01072](#).
- [407] L. A. Anchordoqui, I. Antoniadis, D. Lust, Fuzzy Dark Matter, the Dark Dimension, and the Pulsar Timing Array Signal (7 2023). [arXiv:2307.01100](#).
- [408] N. Kitajima, K. Nakayama, Nanohertz gravitational waves from cosmic strings and dark photon dark matter (6 2023). [arXiv:2306.17390](#).
- [409] P. Pani, Binary pulsars as dark-matter probes, Phys. Rev. D 92 (12) (2015) 123530. [arXiv:1512.01236](#), [doi:10.1103/PhysRevD.92.123530](#).
- [410] T. Kumar Poddar, S. Mohanty, S. Jana, Constraints on ultralight axions from compact binary systems, Phys. Rev. D 101 (8) (2020) 083007. [arXiv:1906.00666](#), [doi:10.1103/PhysRevD.101.083007](#).
- [411] D. Blas, D. L. Nacir, S. Sibiryakov, Ultralight Dark Matter Resonates with Binary Pulsars, Phys. Rev. Lett. 118 (26) (2017) 261102. [arXiv:1612.06789](#), [doi:10.1103/PhysRevLett.118.261102](#).
- [412] D. Blas, D. López Nacir, S. Sibiryakov, Secular effects of ultralight dark matter on binary pulsars, Phys. Rev. D 101 (6) (2020) 063016. [arXiv:1910.08544](#), [doi:10.1103/PhysRevD.101.063016](#).
- [413] L. Di Luzio, B. Gavela, P. Quilez, A. Ringwald, An even lighter QCD axion, JHEP 05 (2021) 184. [arXiv:2102.00012](#), [doi:10.1007/JHEP05\(2021\)184](#).
- [414] Z. Berezhiani, R. Biondi, M. Mannarelli, F. Tonelli, Neutron-mirror neutron mixing and neutron stars, Eur. Phys. J. C 81 (11) (2021) 1036. [arXiv:2012.15233](#), [doi:10.1140/epjc/s10052-021-09806-1](#).
- [415] J. M. Berryman, S. Gardner, M. Zakeri, How Macroscopic Limits on Neutron Star Baryon Loss Yield Microscopic Limits on Non-Standard-Model Baryon Decay (5 2023). [arXiv:2305.13377](#).
- [416] C. Kouvaris, M. A. Perez-Garcia, Can Dark Matter explain the Braking Index of Neutron Stars?, Phys. Rev. D 89 (10) (2014) 103539. [arXiv:1401.3644](#), [doi:10.1103/PhysRevD.89.103539](#).
- [417] X. Huang, X.-P. Zheng, W.-H. Wang, S.-Z. Li, Constraints on millicharged particles by neutron stars, Phys. Rev. D 91 (12) (2015) 123513. [arXiv:1509.07620](#), [doi:10.1103/PhysRevD.91.123513](#).

- [418] J. W. Foster, Y. Kahn, O. Macias, Z. Sun, R. P. Eatough, V. I. Kondratiev, W. M. Peters, C. Weniger, B. R. Safdi, Green Bank and Effelsberg Radio Telescope Searches for Axion Dark Matter Conversion in Neutron Star Magnetospheres, *Phys. Rev. Lett.* 125 (17) (2020) 171301. [arXiv:2004.00011](#), [doi:10.1103/PhysRevLett.125.171301](#).
- [419] R. A. Battye, J. Darling, J. I. McDonald, S. Srinivasan, Towards robust constraints on axion dark matter using PSR J1745-2900, *Phys. Rev. D* 105 (2) (2022) L021305. [arXiv:2107.01225](#), [doi:10.1103/PhysRevD.105.L021305](#).
- [420] P. Tinyakov, M. Pshirkov, S. Popov, Astroparticle Physics with Compact Objects, *Universe* 7 (11) (2021) 401. [arXiv:2110.12298](#), [doi:10.3390/universe7110401](#).
- [421] D. Lai, J. Heyl, Probing Axions with Radiation from Magnetic Stars, *Phys. Rev. D* 74 (2006) 123003. [arXiv:astro-ph/0609775](#), [doi:10.1103/PhysRevD.74.123003](#).
- [422] M. S. Pshirkov, S. B. Popov, Conversion of Dark matter axions to photons in magnetospheres of neutron stars, *J. Exp. Theor. Phys.* 108 (2009) 384–388. [arXiv:0711.1264](#), [doi:10.1134/S1063776109030030](#).
- [423] A. Hook, Y. Kahn, B. R. Safdi, Z. Sun, Radio Signals from Axion Dark Matter Conversion in Neutron Star Magnetospheres, *Phys. Rev. Lett.* 121 (24) (2018) 241102. [arXiv:1804.03145](#), [doi:10.1103/PhysRevLett.121.241102](#).
- [424] F. P. Huang, K. Kadota, T. Sekiguchi, H. Tashiro, Radio telescope search for the resonant conversion of cold dark matter axions from the magnetized astrophysical sources, *Phys. Rev. D* 97 (12) (2018) 123001. [arXiv:1803.08230](#), [doi:10.1103/PhysRevD.97.123001](#).
- [425] B. R. Safdi, Z. Sun, A. Y. Chen, Detecting Axion Dark Matter with Radio Lines from Neutron Star Populations, *Phys. Rev. D* 99 (12) (2019) 123021. [arXiv:1811.01020](#), [doi:10.1103/PhysRevD.99.123021](#).
- [426] R. A. Battye, B. Garbrecht, J. I. McDonald, F. Pace, S. Srinivasan, Dark matter axion detection in the radio/mm-waveband, *Phys. Rev. D* 102 (2) (2020) 023504. [arXiv:1910.11907](#), [doi:10.1103/PhysRevD.102.023504](#).
- [427] J. W. Foster, S. J. Witte, M. Lawson, T. Linden, V. Gajjar, C. Weniger, B. R. Safdi, Extraterrestrial Axion Search with the Breakthrough Listen Galactic Center Survey (2 2022). [arXiv:2202.08274](#).
- [428] J. Darling, Search for Axionic Dark Matter Using the Magnetar PSR J1745-2900, *Phys. Rev. Lett.* 125 (12) (2020) 121103. [arXiv:2008.01877](#), [doi:10.1103/PhysRevLett.125.121103](#).
- [429] J. Darling, New Limits on Axionic Dark Matter from the Magnetar PSR J1745-2900, *Astrophys. J. Lett.* 900 (2) (2020) L28. [arXiv:2008.11188](#), [doi:10.3847/2041-8213/abb23f](#).
- [430] M. Baryakhtar, et al., Dark Matter In Extreme Astrophysical Environments, in: 2022 Snowmass Summer Study, 2022. [arXiv:2203.07984](#).
- [431] E. Hardy, N. Song, Listening for Dark Photon Radio from the Galactic Centre (12 2022). [arXiv:2212.09756](#).
- [432] R. A. Battye, M. J. Keith, J. I. McDonald, S. Srinivasan, B. W. Stappers, P. Weltevrede, Searching for Time-Dependent Axion Dark Matter Signals in Pulsars (3 2023). [arXiv:2303.11792](#).
- [433] A. J. Millar, S. Baum, M. Lawson, M. C. D. Marsh, Axion-photon conversion in strongly magnetised plasmas, *JCAP* 11 (2021) 013. [arXiv:2107.07399](#), [doi:10.1088/1475-7516/2021/11/013](#).
- [434] T. D. P. Edwards, M. Chianese, B. J. Kavanagh, S. M. Nissanke, C. Weniger, Unique Multimessenger Signal of QCD Axion Dark Matter, *Phys. Rev. Lett.* 124 (16) (2020) 161101. [arXiv:1905.04686](#), [doi:10.1103/PhysRevLett.124.161101](#).
- [435] M. Leroy, M. Chianese, T. D. P. Edwards, C. Weniger, Radio Signal of Axion-Photon Conversion in Neutron Stars: A Ray Tracing Analysis, *Phys. Rev. D* 101 (12) (2020) 123003. [arXiv:1912.08815](#), [doi:10.1103/PhysRevD.101.123003](#).
- [436] S. J. Witte, D. Noordhuis, T. D. P. Edwards, C. Weniger, Axion-photon conversion in neutron star magnetospheres: The role of the plasma in the Goldreich-Julian model, *Phys. Rev. D* 104 (10) (2021) 103030. [arXiv:2104.07670](#), [doi:10.1103/PhysRevD.104.103030](#).
- [437] R. A. Battye, B. Garbrecht, J. I. McDonald, S. Srinivasan, Radio line properties of axion dark matter conversion in neutron stars, *JHEP* 09 (2021) 105. [arXiv:2104.08290](#), [doi:10.1007/JHEP09\(2021\)105](#).
- [438] B. J. Kavanagh, T. D. P. Edwards, L. Visinelli, C. Weniger, Stellar Disruption of Axion Miniclusters in the Milky Way (11 2020). [arXiv:2011.05377](#).
- [439] J. H. Buckley, P. S. B. Dev, F. Ferrer, F. P. Huang, Fast radio bursts from axion stars moving through pulsar magnetospheres, *Phys. Rev. D* 103 (4) (2021) 043015. [arXiv:2004.06486](#), [doi:10.1103/PhysRevD.103.043015](#).
- [440] S. Nurmi, E. D. Schiappacasse, T. T. Yanagida, Radio signatures from encounters between neutron stars and QCD-axion minihalos around primordial black holes, *JCAP* 09 (2021) 004. [arXiv:2102.05680](#), [doi:10.1088/1475-7516/2021/09/004](#).
- [441] Y. Bai, X. Du, Y. Hamada, Diluted axion star collisions with neutron stars, *JCAP* 01 (01) (2022) 041. [arXiv:2109.01222](#), [doi:10.1088/1475-7516/2022/01/041](#).
- [442] S. J. Witte, S. Baum, M. Lawson, M. C. D. Marsh, A. J. Millar, G. Salinas, Transient Radio Lines from Axion Miniclusters and Axion Stars (12 2022). [arXiv:2212.08079](#).
- [443] F. Anzuini, J. A. Pons, A. Gómez-Bañón, P. D. Lasky, F. Bianchini, A. Melatos, Magnetic dynamo caused by axions in neutron stars (11 2022). [arXiv:2211.10863](#).
- [444] H. Niikura, M. Takada, S. Yokoyama, T. Sumi, S. Masaki, Constraints on Earth-mass primordial black holes from OGLE

- 5-year microlensing events, Phys. Rev. D 99 (8) (2019) 083503. [arXiv:1901.07120](#), [doi:10.1103/PhysRevD.99.083503](#).
- [445] H. Murayama, J. Shu, Topological Dark Matter, Phys. Lett. B 686 (2010) 162–165. [arXiv:0905.1720](#), [doi:10.1016/j.physletb.2010.02.037](#).
- [446] A. Derevianko, M. Pospelov, Hunting for topological dark matter with atomic clocks, Nature Phys. 10 (2014) 933. [arXiv:1311.1244](#), [doi:10.1038/nphys3137](#).